The Development of a Lightweight Electric Vehicle Chassis and Investigation into the Suitability of TiAl for Automotive Applications

A thesis submitted in partial fulfilment
of the requirements for the degree of
Masters of Engineering
in Mechanical Engineering

By

Ryan Lovatt

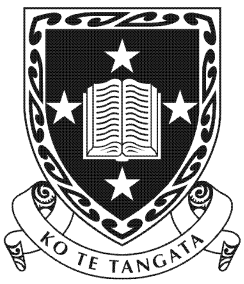

The University of Waikato
Te Whare Wānanga o Waikato

Hamilton, New Zealand

March 2008

Abstract

A lightweight chassis for a battery electric vehicle being developed at the University of Waikato was required. The chassis was designed around a predetermined body shape and suspension setup. A chassis, built from 20mm thick aluminium honeycomb sandwich panel, was designed and built to LVVTA standards allowing the car to be driven on public roads. The chassis weighs a little over a third the mass of a mass production car chassis. The car has been driven over 1800km with only one minor problem, indicating the chassis is reliable and well suited to its purpose.

Titanium aluminide properties were researched to identify where titanium aluminides could be used in an automobile. Titanium aluminides have a specific strength and stiffness near to steel yet only half the density making it an ideal replacement for steel components. Automotive applications identified that could benefit from the use of TiAl include valves, brake rotors and inside ‘in-wheel’ electric motors.

Acknowledgements

I would like to thank;

Page Macrae Engineering for undertaking the TIF and providing funding to undertake this project and associated research.

Dr. Mike Duke for his leadership and inspiration

Norm Stannard for sharing his experience and help in making the car a reality

Ian Macrae for having the foresight and belief in new technology and wanting to get hands during the WSC

Travis de Fluiter for being a great friend and someone to bounce ideas off for the last two years

Matthew Greaves, Ben Guymer and Bernie Walsh from *Hybrid*Auto, Australia and the previous **Ultra**commuter team for what they achieved

Nigel Burgess from South Bank University, England

Colin Ayres from Ayres Composite panels for their guidance in the use of aluminium honeycomb

The University of Waikato **Ultra**commuter team through which many lessons were learnt and great times had

The University of Waikato staff for their support

Finally, I would like to thank my family and friends for their help and support.

Table of Contents

List of Figures

List of Tables

Glossary

ABS	-Antilock Braking System
At%	-Atomic percentage
BEV	-Battery Electric Vehicle
CAD	-Computer Aided Drawing
CAE	-Computer Aided Engineering
CNC	-Computer Numerical Control
FEA	-Finite Element Analysis
'In-wheel' motors	-An electric drive completely contained within a wheel
Li-ion batteries	-Lithium ion batteries
LVVTA	-Low Volume Vehicle Technical Association
NNS	-Near Net Shape
NVH	-Noise Vibration and Harshness
NZeco	-2006 University of Waikato BEV group
PM	-Powder Metallurgy
PPM	-Parts Per Million
RP	-Rapid Prototyping
TiAl	-Titanium aluminide
Ultracommuter	-2007 University of Waikato BEV group
Vol.%	-volume percentage
WSC	-World Solar Challenge 2007
γ	-Gamma (from the Greek alphabet)
α	-Alpha (from the Greek alphabet)

Chapter 1 Introduction

1.1 Lightweight components in modern day cars

Over the last 25-30 years there has been an increasing requirement to lower vehicle mass. This has been driven by two factors; increasing petrol prices due to shortages in supply of crude oil and an increasing awareness of the environment and the need to reduce exhaust emissions.

Lowering the mass leads to less energy being required from the motor to accelerate and drive an automobile. These lower energy requirements mean emissions and petrol usage from a lighter vehicle will be less than for a heavier comparable car. A recent newspaper article has claimed every 100kg of weight saved in a car can save 0.2-0.4 litres of fuel per 100km, depending on the type of engine (Gupta, 2006).

The automobile industry's drive for lower vehicle emissions and energy consumption has led to the development of alternative means of propulsion, in particular Battery Electric Vehicles (BEV) and Fuel cells. For the above reasons a BEV has been developed at the University of Waikato. BEV's have become feasible due to improvements in battery technologies. The improvements have increased battery energy density which allows substantial improvements to driving range. Increasing range allows electric vehicles to be driven like conventional internal combustion engine vehicles.

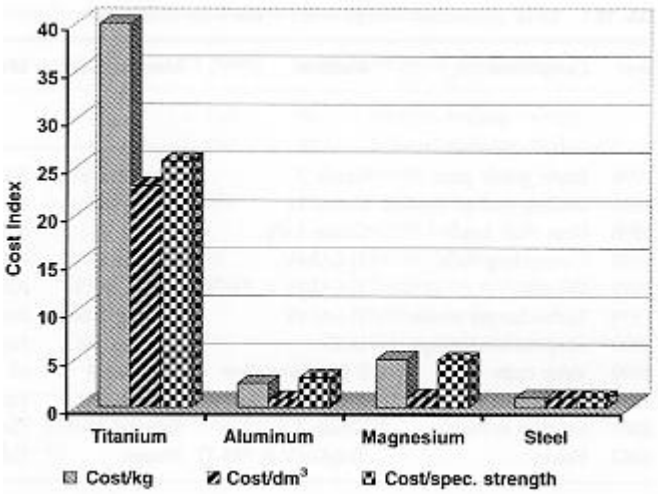

Figure 1.1 Comparison of lightweight metals cost (Leyens & Peters, 2006).

Reducing weight is a key factor to reducing energy consumption. Various lightweight materials being considered for use in vehicles include aluminium, magnesium, titanium, fibre reinforced plastics and metal matrix composites (MMC). Two drawbacks of these materials for their integration into vehicle production are differing mechanical and physical properties compared to the conventional vehicle material steel, and high material costs (Figure 1.1).

1.2 Reducing vehicle mass

The majority of automobiles are constructed from steel. Although in the past decade there have been improvements to the strength of steel, it still has a high density when compared to other lightweight metals (Figure 1.2).

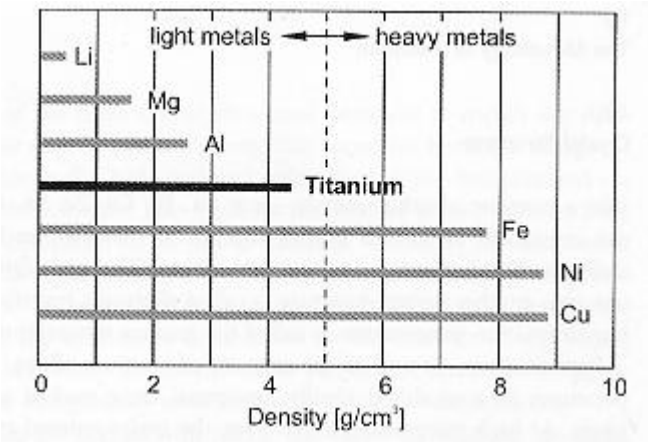

Figure 1.2 Density of some metals (Leyens & Peters, 2006)

Alternative lightweight metals such as aluminium, titanium and magnesium are being used in automobiles, but the material and development costs are currently too high for many car manufacturers. Much research currently focuses on new manufacturing processes as a way to reduce this influence of high material costs. Lightweight materials can replace steel components if the component's design is optimised to better suit the lightweight material. Component shapes can be optimised by using 3D Computer Aided Drawing (CAD) and Finite Element Analysis. An example of this can be seen in Figure 1.3 where a complex aluminium casting is used for mounting front suspension. This complex design allows the casting to be light weight yet very strong.

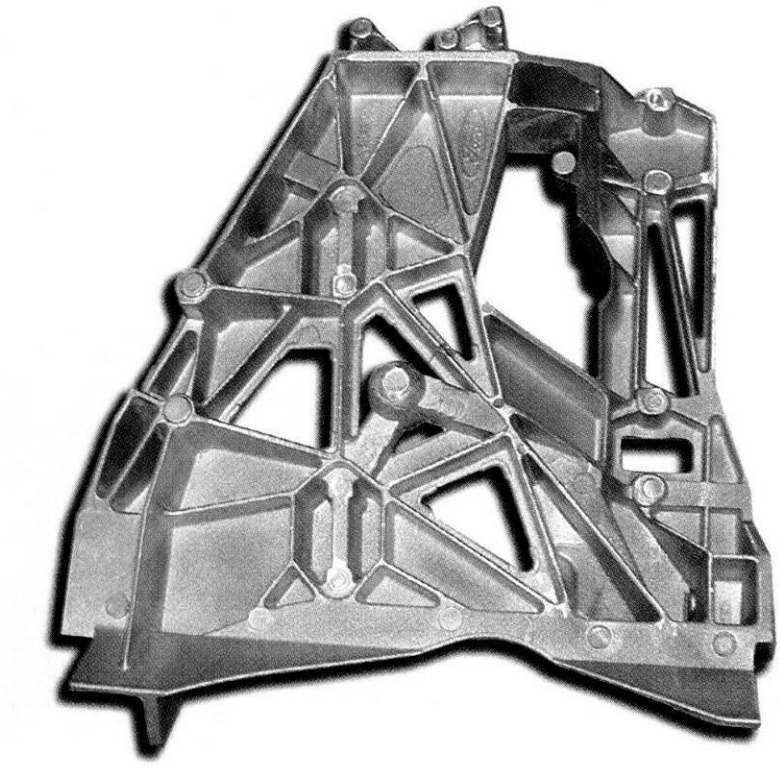

Figure 1.3 The front casting for the Ford GT (Ramsden, 2006)

Lightweight composite materials include reinforced plastics, MMC's and sandwich panels. These materials are beginning to appear in structural areas in premium vehicles. The addition of composite materials can bring about a significant cost increase due to their increased materials, processing and manufacturing costs.

1.3 Titanium aluminide

Titanium aluminides have been the subject of much research, particularly in Germany (Leyens & Peters, 2006) with the majority of research focused on developing materials for use inside jet engines as replacements for more dense nickel materials. More recent research has investigated automotive applications. The main drive for this research is due to their low density and strength at high temperatures. Titanium aluminides have begun to be used for automotive components, including race car engine valves and turbocharger rotors.

1.4 Research objective

This research was undertaken as a project to design and construct a lightweight chassis for a BEV to demonstrate the feasibility of a two seat high performance BEV in the 2007 Panasonic World Solar Challenge. Research would also be conducted into the properties of titanium aluminides for potential uses within the automotive industry.

Chapter 2 Literature review

2.1 Introduction

This review covers the function of a chassis, the different types of chassis and the different materials used for chassis's. From the review, a chassis suitable for a BEV will be designed and manufactured.

The properties of titanium aluminide (TiAl) for use in automotive applications are also investigated with the intention to design and manufacture a TiAl automotive component.

2.2 Automotive Chassis

The chassis is the main structural frame of an automobile. It connects all key vehicle components including suspension and drive train. There are five main functions of an automotive chassis; to provide an area for occupants and luggage, offer safety to the occupants and outside parties, provide points for mounting of suspension and drive train, provide a stiff framework linking all mounting points and to dampen Noise, Harshness and Vibration (NHV).

The vehicle chassis provides an area within or above where occupants can be seated. This area can allow up to three occupants to sit adjacent to each other in up to four rows. Space for luggage is generally provided near the occupant area. Figure 2.1 provides an example of a vehicle chassis.

A vehicle chassis provides safety to occupants of the vehicle and outside parties. It provides a means of absorbing energy from frontal, side and rollover impacts. The greater the energy absorbed by the chassis on impact the lower the energy levels transmitted to a vehicles occupants and surroundings, lowering the chances of injury.

Vehicles that are newly registered in New Zealand after 2002 and manufactured in high volume (greater than 200 vehicles per year) must pass frontal impact laws to prove occupant safety and meet the Land Transport Safety Authority's approved vehicle standards. Low volume vehicle manufacturers (less than 200 vehicles per year) are required to meet the Low Volume Vehicle Technical Association's (LVVTA) low volume vehicle code. The Low volume vehicle code does not require manufacturers to meet the frontal impact laws due to the high costs incurred with such testing but must prove to the LVVTA the vehicle is safe for occupants and other road users (Land Transport Safety Authority of NZ, 2001).

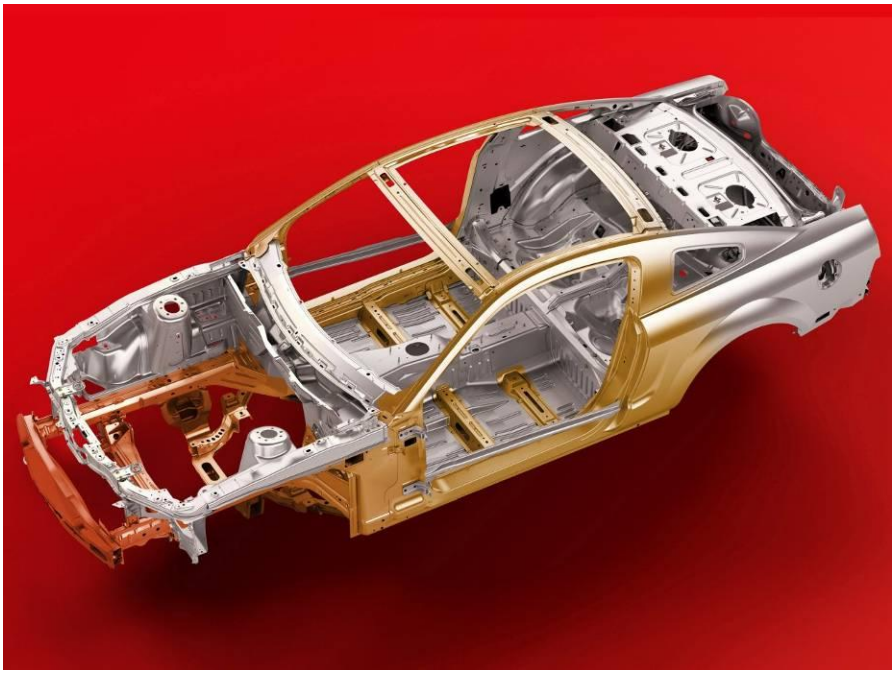

Figure 2.1 A Ford Mustang monocoque chassis (Ford Motor, 2005)

Major vehicle components are attached to the chassis as the chassis is the structural frame of the vehicle. Suspension, drivetrain, body (if not integral with the chassis) and steering are some of these components. The mounting of components must be such that they are rigid as large movements may cause components to interfere and thus not function as intended. Durability of all mountings to the chassis is required as the design life of the chassis is typically eight years. For example Toyota hybrid vehicles have a design life of eight years or 160,000km (Toyota, 2007).

A stiff chassis tends to produce superior handling and bends or twists less under extreme loading. Bending or twisting a chassis changes the relative distances between suspension mounting points, creating imprecise suspension geometry. Imprecise suspension geometry creates unsatisfactory camber and castor, leading to poor load distribution and surface area contact with the road, resulting in decreased levels of grip (Figure 2.2). Correct suspension setup is easier to achieve with a stiff chassis as a weak chassis can act like an unknown spring/damper system consequently affecting suspension properties. A common method for measuring chassis stiffness is torsional rigidity. Torsional rigidity is the degree one end of the chassis twists under an applied load if the opposing end of the chassis is restrained. A high performance topless sports car, e.g. Lotus Elise, has a torsional rigidity of 11,000Nm/deg, about the same as a modern salon car (Wan, 1998-2000).

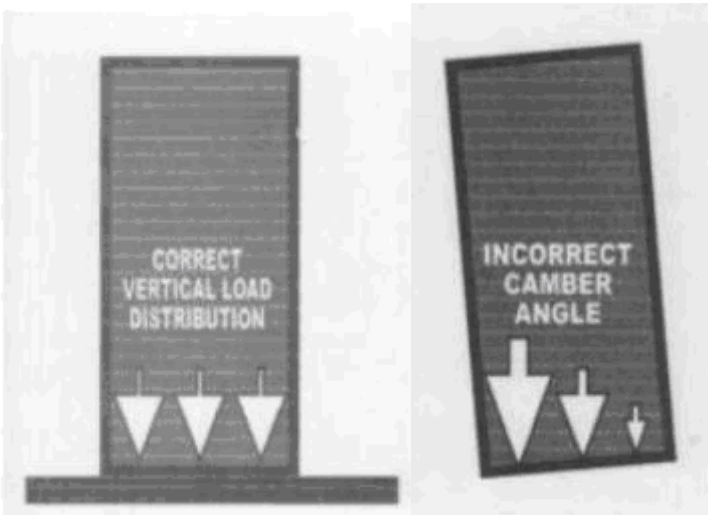

Figure 2.2 Demonstration of how changing the tyre camber can alter the forces and contact area of a tyre against the road (Alexander, October 2007).

There are five different scenarios where forces are acting on the chassis; cornering, braking, accelerating, occupant/luggage and aerodynamics. Increasing chassis stiffness means the forces are transferred across the chassis more directly and less force is absorbed by chassis deformation. Direct load transfer also creates improved handling due to the loads travelling along the intended load paths. Chassis stiffness is of importance in vehicles because the chassis locates the doors,

boot and bonnet. If the chassis twisted, they would no longer align and therefore would not function correctly.

A chassis is designed to reduce Noise, Vibration and Harshness (NVH). Sources of NVH are engine, driveline, tyres, road surface, and wind. NVH is designed to be minimised in the occupant cabin to improve the occupants driving experience. Over the last 10 years interior noise levels at constant speed on Germany's autobahn have been lowered nearly 50% (Braess & Seiffert, 2005).

2.3 Types of chassis

What follows is a brief overview of the different types of chassis and their advantages and disadvantages.

Much research was conducted into the design and construction methods of a variety of vehicles chassis and the latest advancements (Asnafi, Langstedt, Anderson, Ostergren, & Hakansson, 2000; Bak, Bartlett, & Hars, 1995; Brylawski & Lovins, 1999; Cole & Sherman, 1995; Corum, Battiste, Ruggles, & Ren, 2001; Cramer, Taggart, & Inc, 2002; Feraboli & Masini, 2004; GSV, 2005; Inagaki & Tanaka, 2002; Miller, 1996; Saito, Iwatsuki, Yasunaga, & Andoh, 2000; Tamaki, 1999; Yokota et al., 2002).

2.3.1 Ladder frame

Early car chassis design began as ladder frame due to its simplicity, versatility, durability and low development costs. The ladder frame was very common for passenger vehicles until the 1960's and are still used for many Sport Utility Vehicles (SUV's) and trucks (Wan, 1998-2000).

The ladder frame consists of two longitudinal beams with multiple cross members joining the two beams. An example of a Dodge RAM ladder frame chassis can be seen in (Figure 2.3). The ladder frame chassis is versatile as it allows virtually any body shape to be placed atop the chassis. This is beneficial because it allows a vehicle manufacturer to produce many different types of vehicle with the same chassis and driveline, lowering development costs. The ladder frame chassis is

very durable due to its simplicity. If damage were to occur to a ladder frame chassis it is much easier to repair than other types of chassis. The Longitudinal beams are very stiff under bending through the use of closed section beams with a high second moment of area. The high bending stiffness makes the ladder frame chassis well suited for carrying large weights. Due to its simplicity, durability and strength, ladder frame chassis' are still used today for heavy duty vehicles (Happian-Smith, 2001).

Many midsized SUV's are manufactured with the ladder frame chassis as it offers improved ride quality. The separate body atop a chassis can be very effectively isolated from the chassis, lowering NVH levels significantly.

The ladder frame chassis weaknesses are: it is weak in torsion, it generally has a higher centre of mass (COM), it can be heavy, a crumple zone is not able to be integrated and they usually have higher production costs.

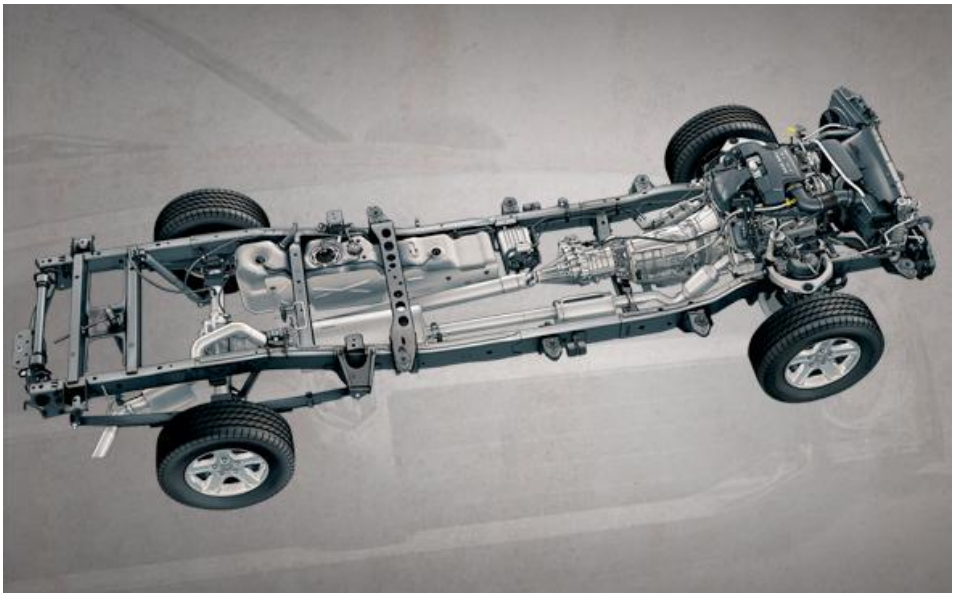

Figure 2.3 A Dodge Ram 2500 ladder frame chassis (Chrysler, 2007).

The ladder frame chassis is stiff in bending but its two dimensional design has low torsional rigidity (Wan, 1998-2000). The use of a cruciform (diagonal bracing) increases the torsional rigidity of a ladder frame chassis (Figure 2.4). The cruciform is unique in design in that no member is subject to torsion. Generally a

higher COM is attained due to the body being mounted above the chassis, and not being integral as in a unibody chassis. The Ladder frame chassis utilises more material than a unibody due to the body being entirely separate to the chassis. The result is increased mass and increased fuel consumption. A crumple zone is unable to be incorporated into the ladder frame chassis and must therefore be incorporated as a separate unit (Wan, 2000).

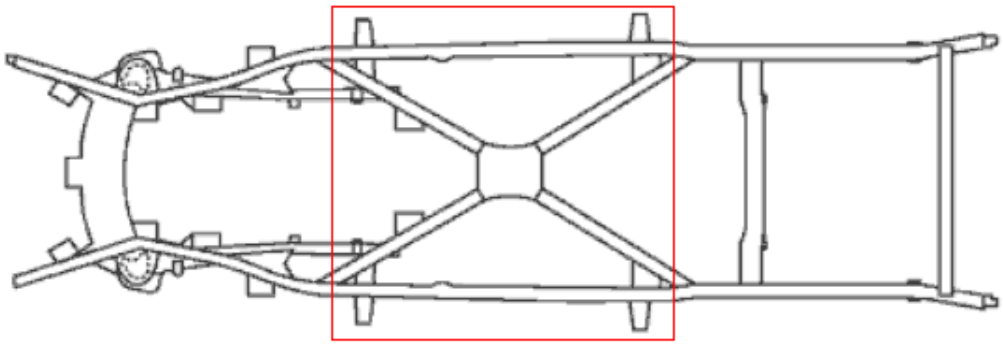

Figure 2.4 A cruciform attached to a ladder frame chassis to increase torsional stiffness (Happian-Smith, 2001)

2.3.2 Backbone (Torque Tube) chassis

An alternative to the ladder frame chassis is the backbone chassis. The backbone chassis design consists of a single, large, longitudinal structural beam running down the centre of the vehicle with lateral beams connecting the suspension. The suspension and motor lateral beams are mounted off the backbone (Figure 2.5). The strength and stiffness of the backbone chassis comes from the large closed section of the central beam. This chassis is stiffer than the ladder chassis but not stiff enough for high performance cars due to their higher torsion and strength demands (Wan, 1998-2000). Also, the body is mounted above the chassis as for the ladder frame (Happian-Smith, 2001).

Figure 2.5 The Lotus Elan Backbone chassis (Wan, 1998-2000)

The backbone chassis offers no side impact protection for occupants and thus occupant protection must be incorporated into the body.

2.3.3 Space frame

Space frames consist of many tubes joined together to create a complex, light and very stiff structure (Figure 2.6).

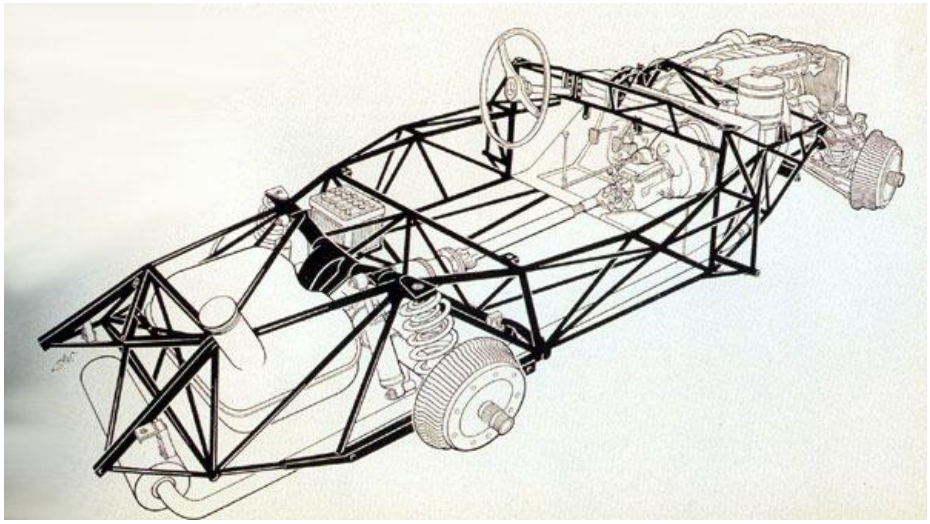

Figure 2.6 Mercedes Benz 300SL space frame chassis (restorations, 2007).

The complex design creates a very rigid frame. To the detriment of the space frame design there is difficulty in automating the assembly process due to the complex nature. The design usually incorporates raised door sills to increase the bending strength and stiffness. The high door sills can be seen in the Mercedes Benz 300sl (Figure 2.6). The raised door sills hinder occupant entry and exit. To overcome this, gull wing or butterfly doors are used as they allow easier occupant

access through larger door openings. The space frame chassis is light due to the minimal amount of structural material that is necessary. The required amount of material is minimal because of the triangulated design which keeps all beams under tension or compression, not torsion. With the beams not under torsion, the cross sectional area of the beams can be reduced. An increase in stiffness compared to the ladder frame and backbone chassis originates from the three dimensional shape adding height (depth) to the design.

Figure 2.7 Audi A8 ASF® (s.r.o., 2007)

Aluminium space frames have been designed to decrease chassis weight further. The first production aluminium space frame was the Audi A8 (Figure 2.7) which utilised an Aluminium Space Frame (ASF) ®. The Lotus Elise chassis (Figure 2.8), while technically not a space frame, is a low volume chassis design that utilises extrusions, castings and sheet aluminium.

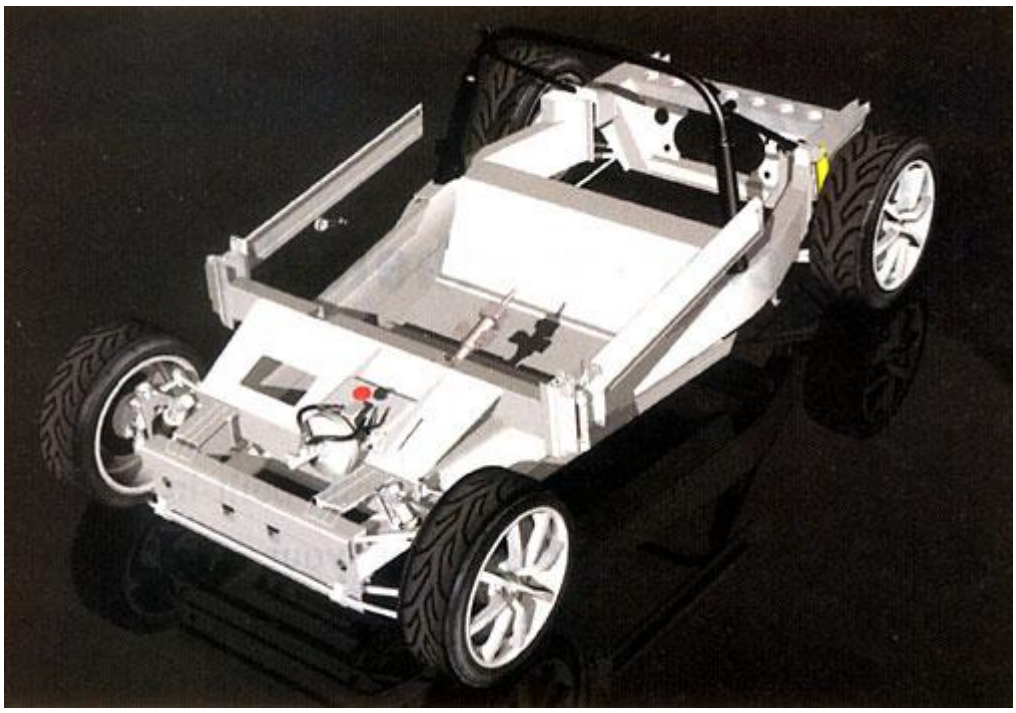

Figure 2.8 A CAD model of the Lotus Elise chassis (Jost, October 2004)

2.3.4 Monocoque/ Uni-body

A monocoque or uni-body chassis is a chassis that is integral with the body. The monocoque chassis is the chassis of choice for all major car manufacturers, equating to 99% of modern vehicles (Wan, 1998-2000). The monocoque chassis is very complex yet cheap to produce, has large spaces and is very safe but has rigidity to weight ratio similar to a ladder frame chassis.

The monocoque chassis is very complex. The complexity of the chassis is due to the integration with the body shell. The integration makes set up costs large as development of the chassis requires considerable time and money. The large set up costs restricts the monocoque to high volume manufacture of vehicles. The ease of manufacture is owing to the use of spot welds which is a very fast and efficient joining method. The monocoque, while being cost effective is also efficient at saving space due to the chassis being part of the body shell as there can then be large component free areas within the chassis. With elements of the body shell part of the structural chassis, reducing weight is difficult. The monocoque chassis has a low rigidity to weight ratio (Wan, 1998-2000) due to the

large amount of material used but the monocoque has high bending and torsional stiffness (Happian-Smith, 2001). This is attributed to the chassis design placing more emphasis on space efficiency than strength. Monocoque chassis can be seen in Figure 2.1 and Figure 2.9. The large amount of material in a steel monocoque chassis is beneficial for crash protection as the use of large amounts of material is offset by the material absorbing more energy through crumple zones in the event of an impact. (Happian-Smith, 2001; Wan, 1998-2000)

(a) **(b)**

Figure 2.9 Toyotas Funcargo, (a) monocoque chassis with right hand side doors and (b) The complete car (J. Yamaguchi & online, 2007).

Carbon fibre monocoque chassis designs are similar to metallic monocoque but they utilise carbon fibre to create the stiffest and is the most expensive chassis available. Due to the price of carbon fibre the carbon fibre monocoque chassis is used primarily for high performance sports cars. The carbon fibre monocoque is known for its superior torsional rigidity and is exceptionally lightweight. An example of the carbon fibre monocoque is the McLaren F1 in Figure 2.10 and the Koenigsegg CCX in Figure 2.11.

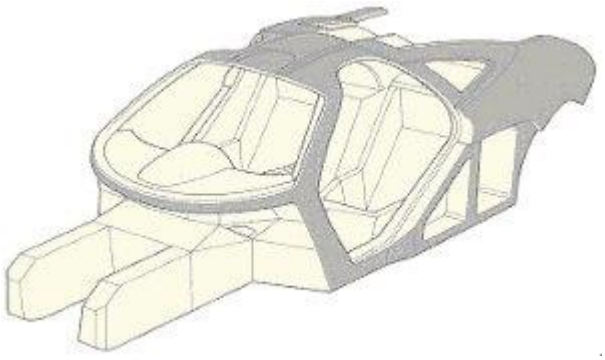

Figure 2.10 McLaren F1 composite chassis (Wan, 1998-2000)

Figure 2.11 Koenigsegg CCX carbon fibre chassis (Koenigsegg, 2007)

2.4 Chassis materials

As legislation demands lower fuel emissions and consumers call for lower fuel consumption as fuel prices rise, automotive manufacturers look towards lighter materials to lower vehicle mass. Many car manufacturers are now utilising lightweight materials (mainly aluminium and magnesium) for structural components. The replacement of steel parts with lightweight materials is not straightforward as the materials have differing physical and mechanical properties. The different material properties require different machining, heat treating and

joining techniques while creating new fabrication techniques that can better optimise component layout and shape.

Early in the development of automobiles slow moving steam powered vehicles were able to use wooden chassis but increasing speeds and motor vibrations caused durability problems. Steel has since been used for the majority of vehicle chassis. Aluminium chassis' have begun to be used by some high volume automotive manufacturers over the last 20 years as a way to reduce vehicle weight. Composites are also gaining more widespread use. Future chassis construction could lead to complete composite structures designed to optimise weight loss and mechanical properties, similar to the McLaren and Koenigsegg.

While many of these new materials are reducing the weight of the vehicle, the large range of materials used is becoming a challenge for the automotive repair industry. Correctly identifying the correct repair technique and material grade becomes a challenge.

Steel

With the need to dramatically reduce vehicle weight, many vehicle manufacturers are undertaking research into alternative materials. The 7,850kg/m^3 density of steel is high when compared to other materials used in automobiles. By comparison aluminium has a density of 2,700kg/m^3.

The steel industry, through the Ultra Light Steel Auto Body (ULSAB) consortium, launched research into the use of high strength steels and alternative fabrication techniques for manufacture of an automotive body. The aim of the consortium was to determine if a substantially lighter steel automotive body could be constructed. The results from the ULSAB consortium were a 25% mass reduction from the benchmark figure, 80% and 52% increase in bending and torsional rigidity respectively while exceeding all impact requirements. The techniques used for the ULSAB have since been used by car manufacturers in the 3-series BMW and Opel Astra. (Birch, 2000)

An advantage of steel over other structural materials is the majority of tooling and machinery used by the automotive industry is designed for steel construction. Steel has been used extensively within the automotive industry so its properties are very well known and therefore has been thoroughly researched.

Tailor welded blanks have been used since 1985 for reducing body structure mass. Tailor welded blanks involve designing parts with differing material thicknesses. Sheets are cut to shape and the different thickness sheets are welded together (Figure 2.12), usually with laser welding. The sheet is then placed into a die and formed to shape (Figure 2.13).Tailor welded blanks have many advantages such as mass reduction, ability to place optimal grades and thickness where needed, elimination of reinforcements, reduction of parts, improved energy transfer across joints making frame stiffer and better corrosion resistance because there are no overlapped joints. (Engineering, 2007; Porsche Engineering Services, 1998; Team, 1995)

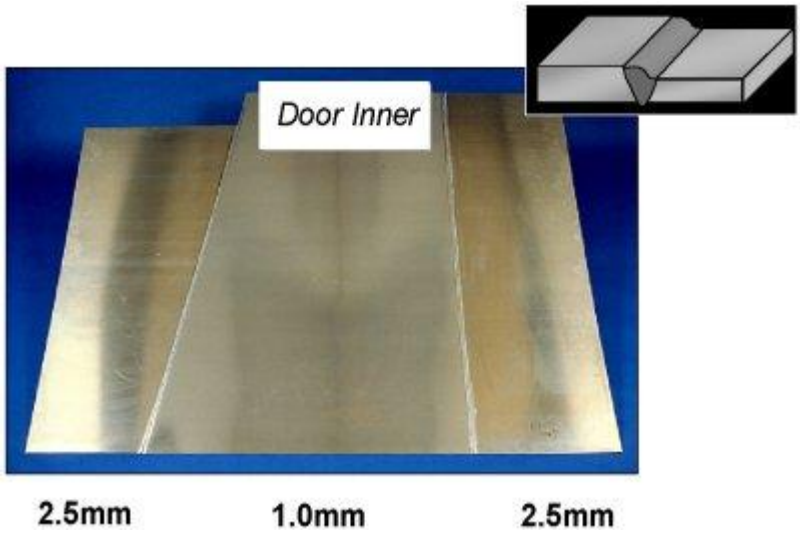

Figure 2.12 A tailor welded door inner ready for forming (Reynolds Metals Company and Ogihara America Corporation, 2007)

Figure 2.13 The tailor welded blank after forming (Reynolds Metals Company and Ogihara America Corporation, 2007)

Aluminium

Significant weight savings can be achieved through the replacement of a steel chassis with an aluminium chassis as aluminium has one third the density of steel. Cast aluminium components used in the Ford GT are required to meet the minimum Ultimate Tensile Strength of 180MPa and 5% elongation (Ramsden, 2006). Manufacturers are investigating the use of aluminium for structural components and a small number have started production. Current vehicle manufacturers and cars with aluminium chassis include the Audi range (A2, A4, A8, TT and R8), the Jaguar XJ (Figure 2.14), the Ford GT, the Chevrolet Corvette (Figure 2.17) and Lotus Elise. Due to aluminium's different mechanical properties, to replace a steel chassis with aluminium requires a complete redesign of the chassis. Different forming processes are able to be used with aluminium when compared to steel. Extrusions, sheet and castings are generally used, as well as some forged components. The Audi R8's ASF uses 70% extrusions, 22% panels and 8% vacuum die cast (Audi, 22 January 2007).

Due to aluminium's reactive oxide layer, components are laser welded or bonded and riveted using self piercing rivets. The aluminium oxide layer prevents the use of spot welding, the main joining technique of a steel chassis.

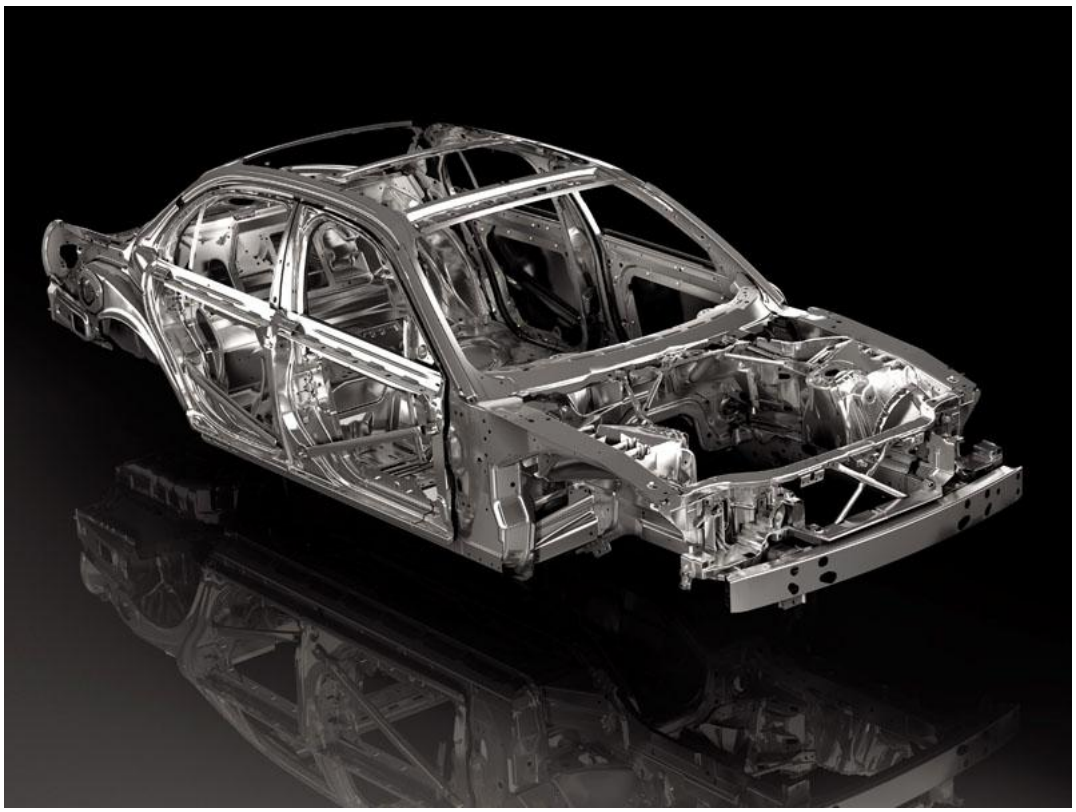

Figure 2.14 The Aluminium Jaguar XJ monocoque chassis (Jaguar, 2007)

The use of aluminium allows the reduction in the number of chassis parts. Casting and extruding allow many different shapes to be produced in a single component, whereas accomplishing the same from steel sheet would require the assembly of many pressed steel components. Audi's third generation ASF has only 267 parts whereas the previous ASF chassis had 334. Lower part counts lead to fewer joints which create increased stiffness and improved crashworthiness. (Audi, 2003)

The major obstacle to the widespread use of aluminium is the cost. An example of this is the cost of producing a bonnet (Hood). Porsche Engineering found that to produce an aluminium bonnet it would cost 104% more than a high strength steel equivalent, although the steel hood would weigh nearly twice as much (13.5kg vs. 26.3kg) (Porsche Engineering, 2005). Extensive use of lightweight materials within a vehicle to create a lightweight vehicle could lead to greater fuel savings. With fuel savings for the life of the vehicle, there is potential for the price difference to be reimbursed through lower fuel consumption and reduced greenhouse gas emissions.

The first Audi A8 that came out with an ASF chassis is claimed to have a 430kg weight reduction compared to the average luxury car. This weight savings translate into fuel consumption reduced by 1.9L/100km. Over the 160,000km lifetime of the vehicle, this equates to a 3,140 Litre savings (or $5,495 with 95 octane at $1.75/L). The reduced fuel consumption eliminates 6,800kg of carbon dioxide. (Schlendorf, 2002)

The Audi TT (similar to Figure 2.15) is a mass produced aluminium space frame vehicle. The chassis design is similar to the original steel monocoque but the Aluminium Space Frame (ASF) weighs only 52% of the steel monocoque and has an increase of 50% and 128% for torsional stiffness for the coupe and Roadster respectively (Audi, 8 December 2006). A photo of an aluminium space frame can be seen in Figure 2.16.

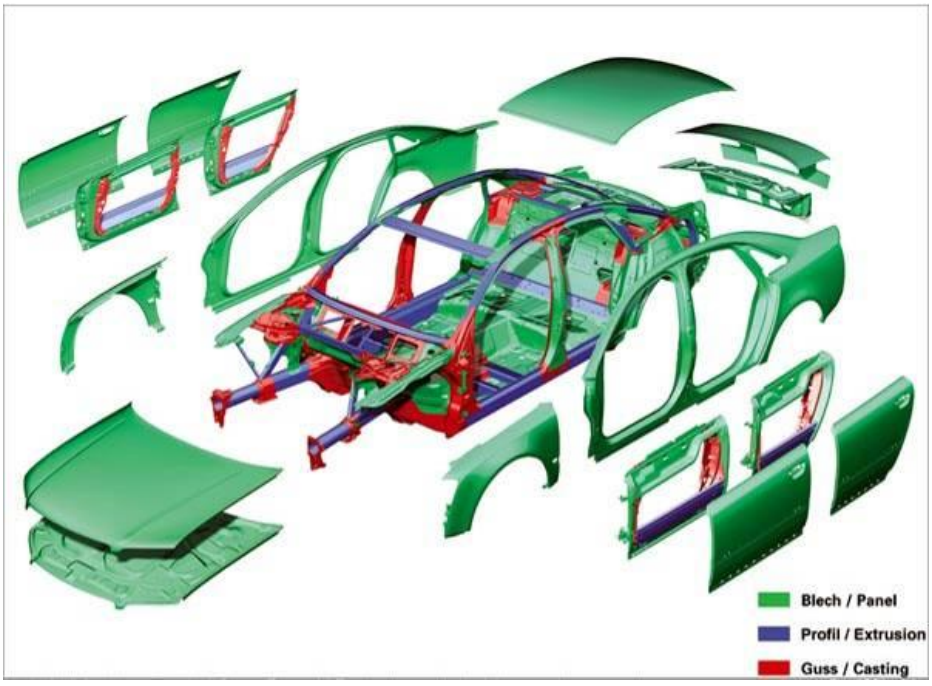

Figure 2.15 The Audi A8 Aluminium Space Frame (ASF) showing the makeup of the different chassis components (Audi AG, 2002)

Figure 2.16 Audi R8 Cutaway (Bryant, 2006)

Figure 2.17 The 2008 Corvette ZR1 aluminium space frame chassis (Bryant, 2008)

Aluminium is a difficult material to use for tailor welded blanks because of porosity, cracking and lowering of strength at the weld zone. The high reflectivity of aluminium also creates difficulties in coupling of the two materials. Examples of tailor welded blanks in use can be seen in Figure 2.18 (Engineering, 2007; Kinsey, Viswanathan, & Cao, 2001; Stasik & Wagoner, 1997)

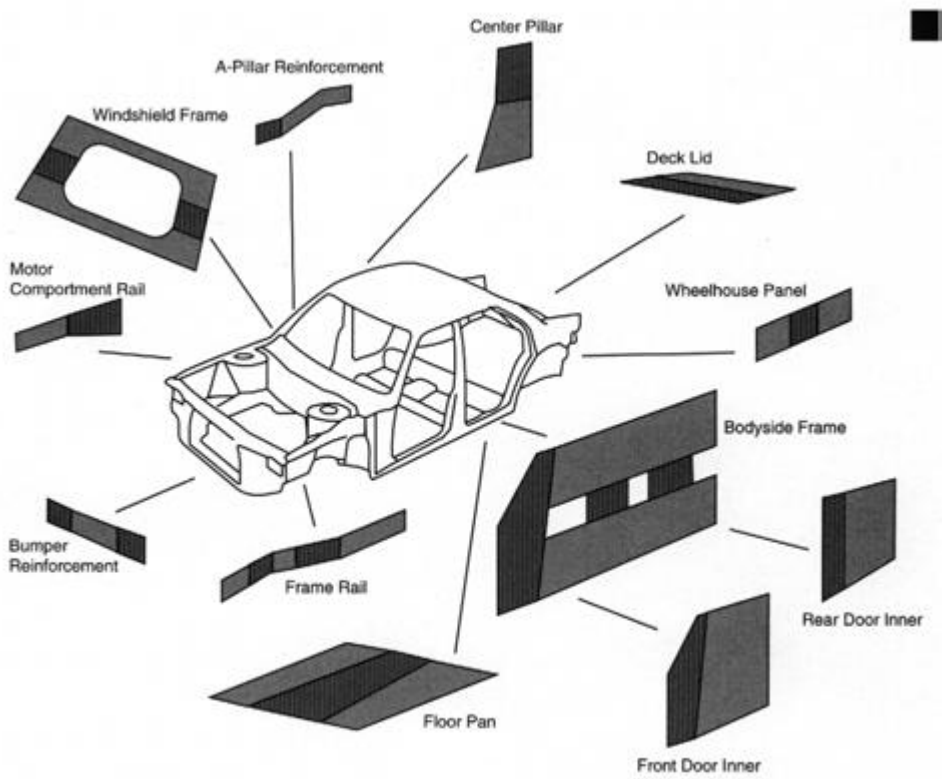

Figure 2.18 Body panels made using tailor welded blanks (Kinsey, Viswanathan, & Cao, 2001).

Composites

Composites are not widely used for chassis due to their high costs, their isotropic mechanical properties and their sometimes unpredictable failure modes. Examples of composite materials include: sandwich materials, reinforced plastics and Metal Matrix Composites (MMC). This review will predominantly cover reinforced plastics and sandwich materials.

Sandwich panels have been used in vehicles in many different forms. One of the first Ford GT40 race cars (1966) used aluminium honeycomb for its chassis. This created an exceptionally light stiff structure weighting 136kg lighter than the Mark II. The ford GT40 used one inch thick aluminium honeycomb sandwich panel for the front and rear bulkheads, and half inch thick aluminium honeycomb sandwich panel elsewhere. The aluminium honeycomb sandwich panel had 0.016inch (0.41mm) thick facings (Koganti, 2005; Spain, 2003). Aluminium honeycomb is used in many Formula cars, including Formula 1. A more recent vehicle to use sandwich material is the Strathcarron. The Strathcarron chassis can be seen in Figure 2.19. The Strathcarron car consisted of an aluminium honeycomb sandwich panel cockpit with space frames front and rear to attach the suspension and motor. Originally the front of the car was also made from the same sandwich panel as the cockpit, but it was found to be too strong in crash test modelling, so a deformable space frame was designed instead. The Strathcarron is no longer produced due to escalating development costs and emissions legislation (Pistonheads, 2001).

Figure 2.19 A Strathcarron chassis after construction. The front and rear subframes attach to this (Pistonheads, 2001).

Reinforced plastics are highly desirable to construct a chassis, particularly carbon fibre reinforced. The disadvantage of reinforced plastics is their increased cost and their difficulty to manufacture. For these reasons they are particularly suited for low volume production vehicles. In many situations they also form the outer skin of a sandwich panel structure. Carbon fibre reinforced plastic structures are highly desirable because they create very stiff structures at very low weight.

A carbon fibre car body involving many partners, including Lotus Engineering and the Cranfield University centre for Lightweight composites, is being designed and built that will have a bodyweight of 125kg. This is dramatically less than the 320kg in an average conventional steel car. The chassis itself weighs 92kg. This is exceptionally lightweight. The construction techniques used are designed for production of up to 20,000 vehicles a year, with the main time constraint the resin impregnation and curing times. The new process results in reduced material wastage and has the potential to be automated. Typical carbon fibre composite

chassis such as the McLaren F1 can take well over 1,000 man hours to mould the composite components. (Mills, 2002; Wilton, 2002)

Metal Matrix Composites (MMC's) are similar to reinforced plastics, but the matrix phase is metal as opposed to plastic. MMC's are still expensive so their use has been restricted to drive shafts, engine components (for their wear resistance) and forged suspension and transmission components. (Callister, 2003)

Examples of current cars utilising composite components include the McLaren F1 (Figure 2.10) and the Koenigsegg (Figure 2.20, Figure 2.21). These are high performance super cars and therefore the weight gains from using expensive composites can be justified.

Figure 2.20 Koenigsegg composite chassis (Koenigsegg, 2006).

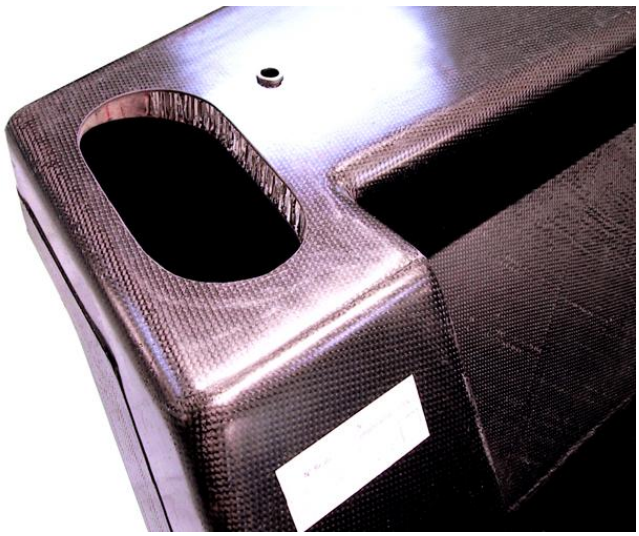

Figure 2.21 Close up of aluminium honeycomb under carbon fibre facings in the Koenigsegg chassis (Koenigsegg, 2006).

2.5 Titanium aluminides

Titanium aluminides are a material that has been widely investigated for aerospace use due to it reduced density, high temperature strength and oxidation resistance. Titanium use in the automotive industry has been limited due to its significantly increased material and processing costs compared to steel.

2.5.1 Introduction

Titanium aluminides (TiAl) are a class of titanium alloys containing 48-54% (Donachie, 2000) or 45-48% (Leyens & Peters, 2006) aluminium and having slightly lower densities to that of titanium. They can be characterised by the fact they generally form a TiO_2 oxide layer instead of Al_2O_3. The titanium aluminides are valued for their lower density than steel and nickel based superalloys, high strength retention at elevated temperatures and high modulus although they have limited ductility and poor fracture toughness. Titanium aluminides poor ductility and fracture toughness can lead to processing difficulties.

There are three classes of titanium aluminides alpha-2 (Ti_3Al), Gamma (TiAl) and Ti_2AlNb orthorhombic. Most Literature has been focused on the alpha-2 and gamma titanium aluminides. This research has been focused primarily within the

aerospace industry as aeroplanes have great benefit from reducing weight even at higher cost. Figure 2.22 shows how the weight savings for automobiles compared to aircraft. This figure indicates a saving of 1kg must only add an extra €0.01 to the automobile cost, whereas with a large aircraft, a weight saving of 1kg can add €1.00 to the aircraft cost. This is because there can be long term savings in less fuel used, larger payloads within the aeroplane and less maintenance.

	T€ / kg	T€ / wt.-%
Automobile	0.01	0.1
Regional aircraft	0.5	100
Large aircraft	1	1000
Space	10	10 000

Figure 2.22 Tolerable extra costs for weight reduction of 1kg or 1% of the structural weight. (Peters, Kumpfert, Ward, & Leyens, 2003)

Automotive use of titanium began in 1992 with the Honda Acura NSX using it for connecting rods. The titanium alloy used was Ti-3Al-2V-rare earth. The titanium connecting rods weighed 30% less and permitted a 700RPM higher rev limit primarily due to the reduced rotating mass (Honda). Several other components have been manufactured since but the limiting factor is the cost of titanium metal and its processing.

While titanium has weaknesses these hurdles can be overcome to produce components, in a similar fashion to the rust proofing of steel for chassis use enables it to last significantly longer than if it were uncoated.

2.5.2 Titanium

Titanium is the ninth most abundant element and fourth most abundant structural element on the earth. It was first discovered in 1791 by Rev. William Gregor in England and later isolated in impure form in 1880. Pure titanium was not isolated until 1910 titanium, when Matthew Albert Hunter put titanium tetrachloride and

sodium together at heat. In 1934 Wilhelm Justin Kroll separated titanium using calcium. This reactant was later changed to magnesium and produced commercially by DuPont in 1948. (Donachie, 2000; Leyens & Peters, 2006; Lutgering, 2007)

Titanium is a highly sought after metal because it has a specific gravity of 4.85g/cm^3 (Figure 2.23) and a melting point of 1668 ^{o}C. Titanium's specific gravity is lower than steel's 7.8 g/cm^3. The specific gravity of titanium classes it as a light metal (less than 5 g/cm^3) yet it is the heaviest light metal. Titanium has high strength, comparable to high strength steels and nickel based super alloys. (Donachie, 2000; Leyens & Peters, 2006; Wayman & Bringas, 1993)

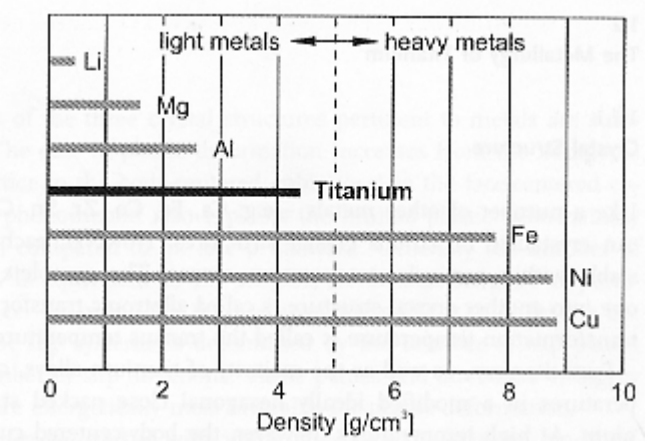

Figure 2.23 Density of various metals (Leyens & Peters, 2006)

Titanium is considered an exotic material due to its limited use. This is primarily due to the extremely high extraction costs. There have been recent developments in reducing titanium from a compound to an element. These are the Cambridge and the Armstrong process. The Cambridge process requires further investigation to determine if cheaper titanium will be produced. The Armstrong process is a process that can produce lower cost titanium. A cost comparison of titanium to aluminium, magnesium and steel can be seen in Figure 2.24 (Crowley, 2003).

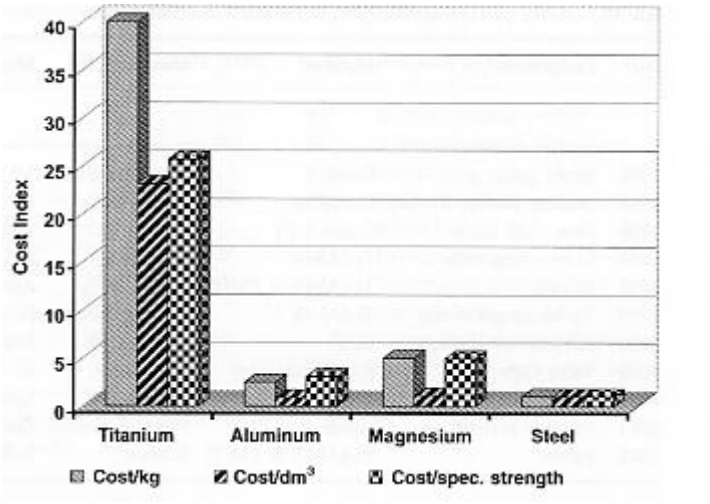

Figure 2.24 Cost comparison of titanium to steel, aluminium and Magnesium (Leyens & Peters, 2006)

Only 5% of all titanium produced is used for metal. 95% of titanium is sold as titanium dioxide to be used as a pigment in paints (Lutgering, 2007). The cost of titanium metal is dictated largely by the aerospace industry as they are the largest titanium metal user. Aerospace titanium usage is not constant and generally has high/low demand cycles. The Kroll process has high capital costs, and these cannot be supported at low demand times. This creates great uncertainty for titanium producers and many American titanium producers have closed due to production becoming uneconomical (Crowley, 2003).

Titanium has a HCP crystal structure at room temperature changing to a BCC crystal structure at temperatures above 882 ^{o}C (Leyens & Peters, 2006). Examples of these crystal structures can be seen in Figure 2.25.(Donachie, 2000; Leyens & Peters, 2006)

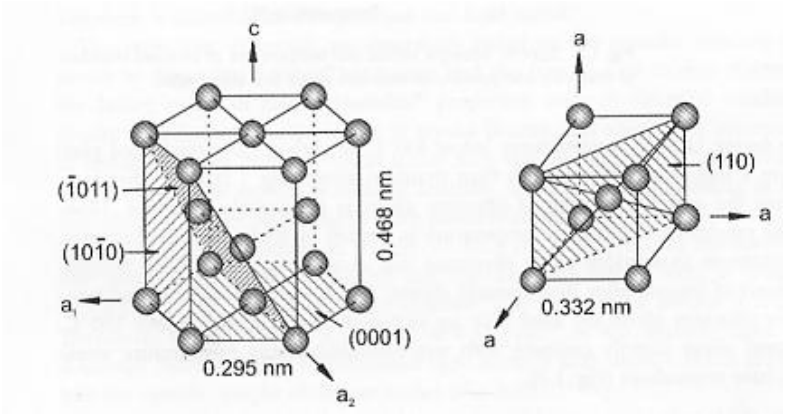

Figure 2.25 HCP and BCC crystal structures

While a TiO_2 layer is advantageous for corrosion resistance, too high oxygen content can make titanium stronger but more brittle. Oxygen diffuses into the metal at temperatures above 600 ^{o}C as an interstitial atom. This creates embrittlement within the metal. The four grades of CP (commercially pure) titanium are differentiated by their different oxygen contents (0.18% (grade1) to 0.40% (grade 4)). Nitrogen has a similar affect to Oxygen although it is not as reactive to titanium. The effects of oxygen, nitrogen and carbon on tensile strength can be seen in Figure 2.26.

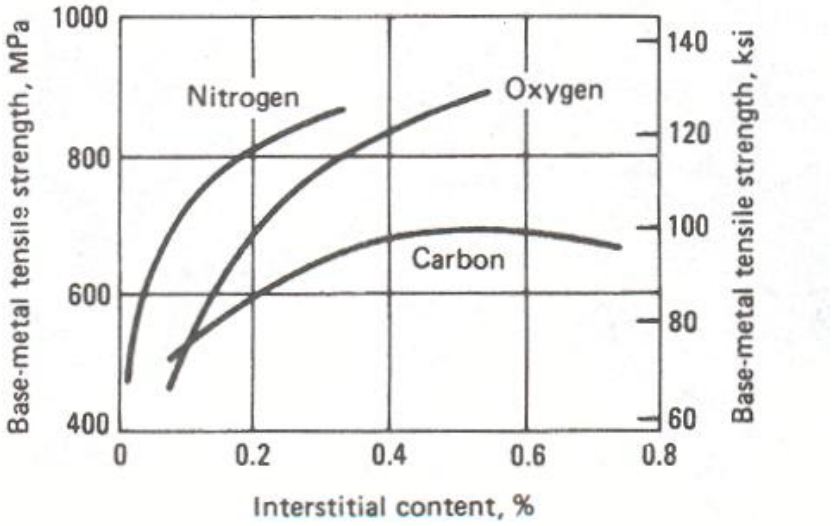

Figure 2.26 The effects of interstitial atoms on the strength of pure titanium (Donachie, 2000)

2.5.3 Titanium Production

Rutile (containing titanium oxide (TiO_2)) is combined with coke and chlorinated in a reactor at 1000 ^oC, then purified. For pigment manufacturers, the purified titanium tetrachloride is oxidised back to TiO_2. For the metal industry, the Kroll process is undertaken. The Kroll process involves reducing titanium tetrachloride in a retort at 800 ^oC to 900 ^oC to produce titanium sponge. The titanium tetrachloride is reduced by magnesium. The unreacted magnesium and magnesium chloride are distilled off, leaving a porous titanium sponge. The titanium sponge is removed from the retort and melted down several times to ensure uniformity and remove inclusions. The Kroll process is a labour intensive, expensive and inefficient. Its batch processing is not suitable for large volumes.(Gerdemann, 2001; Leyens & Peters, 2006)

The Hunter process is similar to the Kroll process but uses sodium instead of magnesium, making it a slightly more inefficient process

The FFC Cambridge process involves pressing TiO_2 into pellets so it becomes a cathode in a 950 ^oC calcium chloride bath. The anode is Graphite. A current is applied and the oxygen in the TiO_2 is ionised, dissolving into the bath. This process can produce titanium with oxygen content down to 60 parts per million (PPM). The advantage of this process is it can begin with a cheaper material, Rutile containing TiO_2. The current difficulty with the FFC Cambridge process is that an inexpensive source of pure TiO_2 is needed to produce titanium with lower impurities. In the Kroll process, chlorination purifies the TiO_2, removing impurities. (Gerdemann, 2001)

The Armstrong process reduces titanium by injecting titanium tetrachloride into a stream of liquid sodium (Figure 2.27). This is a continuous process as opposed to all other processes which are batch processes. A continuous process is much more desirable for the production of metals as it improves product quality, consistency and is more economically efficient. The products of this reaction are titanium powder which meets specifications for commercially pure titanium, and sodium chloride. The sodium chloride is broken down electrolytically for reuse of the

sodium and chloride. The titanium powder is highly suitable for producing powder metallurgy and near-net products. Homogeneous alloys are able to be produced directly by injecting the other alloying elements into the flow along with titanium. Small scale trials have shown consistent blending of all alloying elements. The Armstrong process is believed to reduce final parts production prices by up to 50%.(Crowley, 2003; Leyens & Peters, 2006)

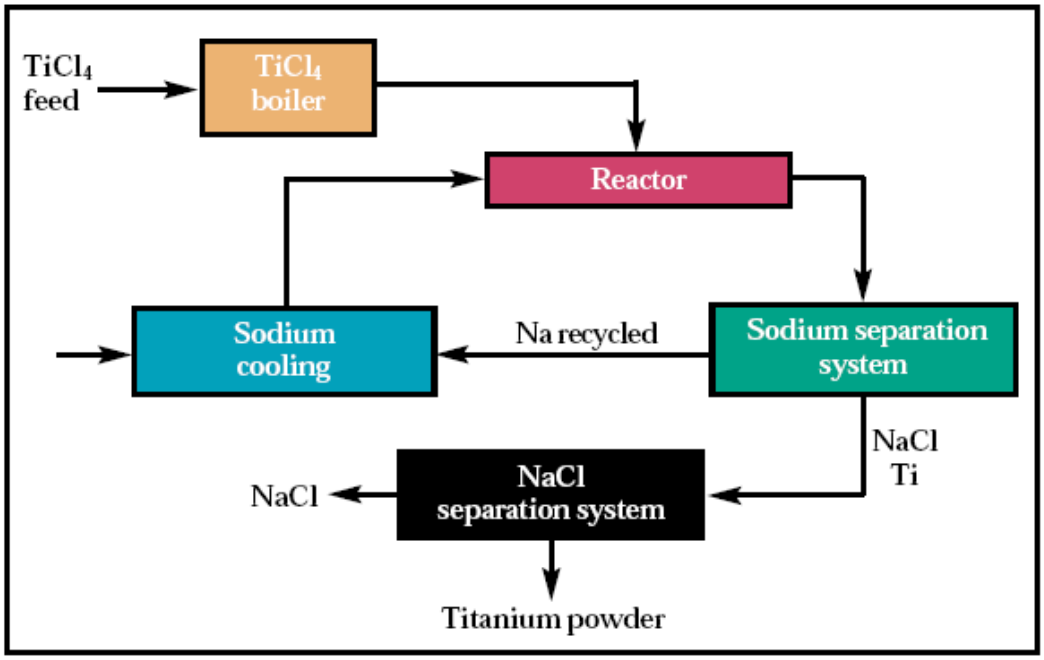

Figure 2.27 An overview of the Armstrong process (Crowley, 2003)

In recent years (2004-2005) there has become a shortage of titanium as recent developments and demand grows for its use in new aeroplanes such as the Boeing 787. The shortage can also be attributed to the reduction in titanium recycling due to globalisation of titanium component production, making it uneconomical to return shavings from manufacturing processes to the material supplier. Titanium alloy engine valves appear to be gaining acceptance within the automotive industry with approximately four million valves produced in 2005. (Lutgering, 2007)

2.5.4 Titanium aluminides

Although there are three different phases of titanium aluminide, this research will focus primarily on the Gamma (γ-TiAl) titanium aluminides. Properties of γ-TiAl that make them particularly attractive are: high melting point of 1460 ^{o}C, low density (3.9-4.2kg/cm^{3}), high elastic modulus, high diffusion co-efficient, good resistance to oxidation and corrosion and lower tendencies to combust in comparison to titanium. (Leyens & Peters, 2006)

The binary phase diagram for TiAl has long been debated due to differing amounts of impurities. There are two different phases of TiAl, one with one phase and the other with two phases. γ-TiAl has only the one phase and has an aluminium composition of 50-56 at.%. Whereas (α2 + γ) TiAl generally has a maximum of 48 at.% aluminium. The phase diagram seen in Figure 2.28 shows these TiAl regions. Selection of different solidification paths allows different microstructures to be created. The γ-TiAl phase has a tetragonal structure (Figure 2.29). Titanium aluminides retain this tetragonal structure up to melting point. (Gerling, Clemens, & Schimansky, 2004; Leyens & Peters, 2006; Polmear, 2006)

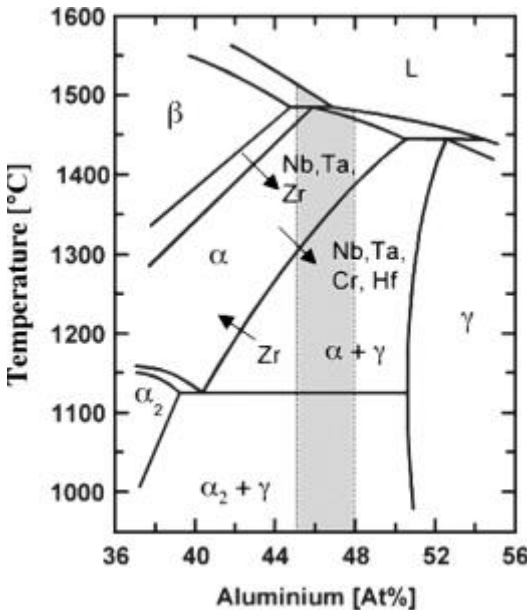

Figure 2.28 The binary phase diagram with the engineering γ-TiAl alloy area highlighted. The diagram also shows how phase boundaries shift by addition of alloying elements. (Gerling, Clemens, & Schimansky, 2004)

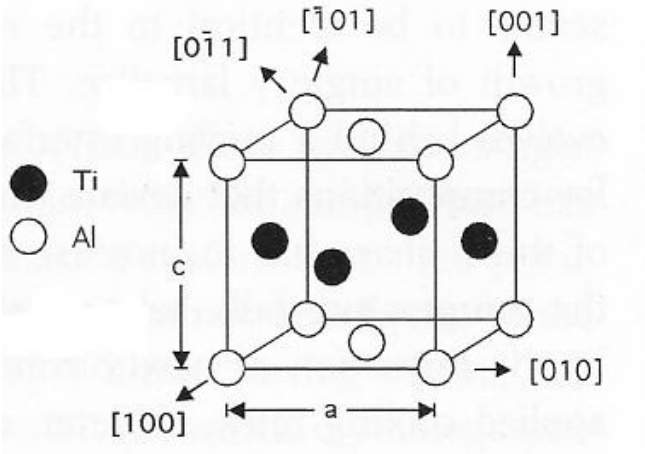

Figure 2.29 γ-TiAl tetrahedral phase structure (Leyens & Peters, 2006)

Table 1 is a comparison of some mechanical properties between conventional titanium alloys, α_2- and γ- TiAl alloys and superalloys.

Property	Ti-based alloys	Ti_3Al-based α_2 alloys	TiAl-based γ alloys	superalloys
Density (g/cm^3)	4.5	4.1–4.7	3.7–3.9	8.3
RT modulus (GPa)	96–115	120–145	160–176	206
RT Yield strength (MPa)	380–1115	700–990	400–630	250–1310*
RT Tensile strength (MPa)	480–1200	800–1140	450–700	620–1620*
Highest temperature with high creep strength (°C)	600	750	1000	1090
Temperature of oxidation (°C)	600	650	900–1000	1090
Ductility (%) at RT	10–20	2–7	1–3	3–5
Ductility (%) at high T	High	10–20	10–90	10–20
Structure	hcp/bcc	DO19	$L1_0$	Fcc/$L1_2$

Table 1. Comparison of γ- and α_2- TiAl alloys to Ti based alloys and superalloys (Kassner & Perez-Prado, 2004)

2.5.5 Alloying

These are guidelines for the mechanical properties of γ-TiAl regarding alloy composition from 'Titanium – a technical guide' (Donachie, 2000)

- Decreasing aluminium content increases strength but lowers ductility and oxidation resistance
- Chrome (Cr), Manganese (Mn) and Vanadium (V) in up to 2 at.% per element have been found to increase ductility.
- Niobium (Nb) of 1-2 at.% is required for oxidation resistance
- Boron (B) in 0.2-2 at.% acts as a grain refining coagulant and for stabilising the microstructure at high temperatures.

While according to the 'Encyclopaedia of materials, parts and finishes' (Schwartz, 2002), the following classification can be used to predict TiAl alloy properties.

Alloy Class	***Compositions (at.%)***
Single Phase (γ)[a]:	Ti-(50-52)Al-(1-2)X_2
Two Phase ($\alpha_2 + \gamma$)[b]:	Ti-(44-49)Al-(1-3)X_1-(1-4)X_2-(0.1-1)X_3

[a] **X2** = W, Nb, Ta

[b] **X1** = V, Mn, Cr; **X2** = Nb, Ta, W, Mo; **X3** = Si, C, B, N, P, Se, Te, Ni, Mo, Fe

From the above classification, the following generalisations apply.

- **X1** elements increase ductility in the two phase alloys (allowing up to twice the ductility)
- **X1** and **X2** elements strengthen the alloy through solid solution strengthening – Cr most, Mn least
- **X1** elements reduce oxidation resistance
- **X2** elements do not increase ductility but they do improve oxidation resistance
- **X3** – C and N_2 improve creep; Si, B, Ni and Fe decrease the melt viscosity and Si may improve oxidation resistance and room temp ductility.

(Polmear, 2006) has a slightly different approach to classifying how alloying elements affect TiAl properties. They are as follows:

- Cr, V, Mn, and Si: improve ductility but decrease oxidation resistance
- Nb, Ta, Mo and W: enhance oxidation resistance
- Si, C and N: in small amounts increase creep resistance

TiAl Metal Matrix Composites (MMC) may be able to improve upon some of TiAl's shortcomings in the future. A TiAl Matrix with 7 vol.% TiB was investment cast to create a missile fin. The TiAl MMC fin had half the density of stainless steel and was stronger at operating temperatures. (Donachie, 2000; Schwartz, 2002)

2.5.6 Mechanical properties

The Hall-Petch equation (1) is used to describe the relation between yield stress and grain size.

$$\sigma = \sigma_o + K_y D^{-1/2} \qquad (1)$$

Where:

σ is the yield stress

σ_o is a material constant for the starting stress for dislocation movement (or the resistance of the lattice to dislocation motion)

K_y is the strengthening coefficient (a constant unique to each material)

D is grain diameter

Using the Hall-Petch equation and results from previous studies, a value for σ_o of 133MPa was found. This low σ_o value means the $K_yD^{-1/2}$ term has the greatest influence (about 70%) on the strength of TiAl alloys. This therefore means the strength of TiAl alloys is mainly determined by microstructure, making grain refinement important to achieving high strength alloys. (Leyens & Peters, 2006)

Deformation at low temperatures is mostly due to slip, although slip movement is severely restricted. At higher temperatures twinning also occurs, permitting higher ductility. (Polmear, 2006)

Titanium aluminides have good strength, particularly when specific strengths are compared to steels and nickel-based alloys. Figure 2.30 compares the different titanium aluminides and the high strength nickel based alloys.

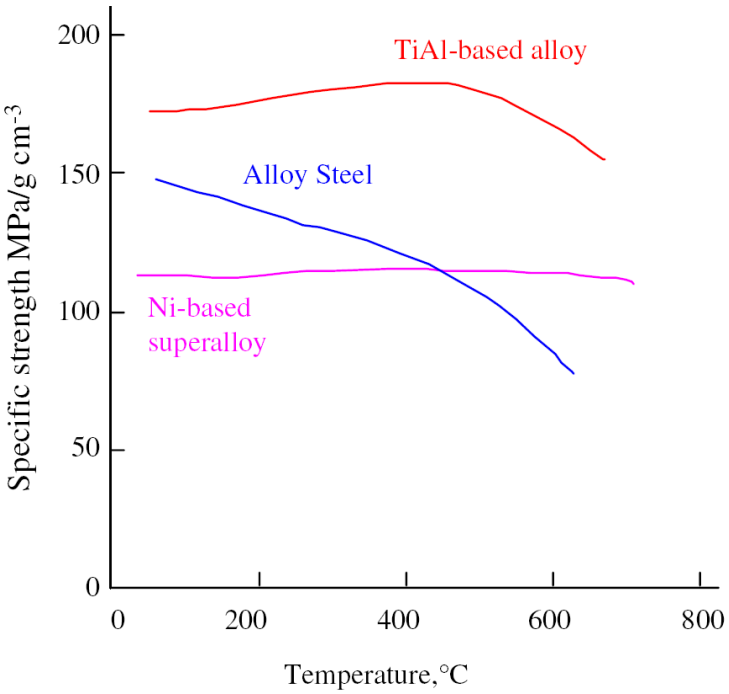

Figure 2.30 Comparisons of TiAl alloys to steel and Ni-based superalloy from 0 ^{o}C to 800 ^{o}C. (Wu, 2006)

Figure 2.31 shows the strength of TiAl alloys stays constant until a temperature between 700 ^{o}C and 800 ^{o}C is reached, whereby ductility increases and the yield stress decreases.

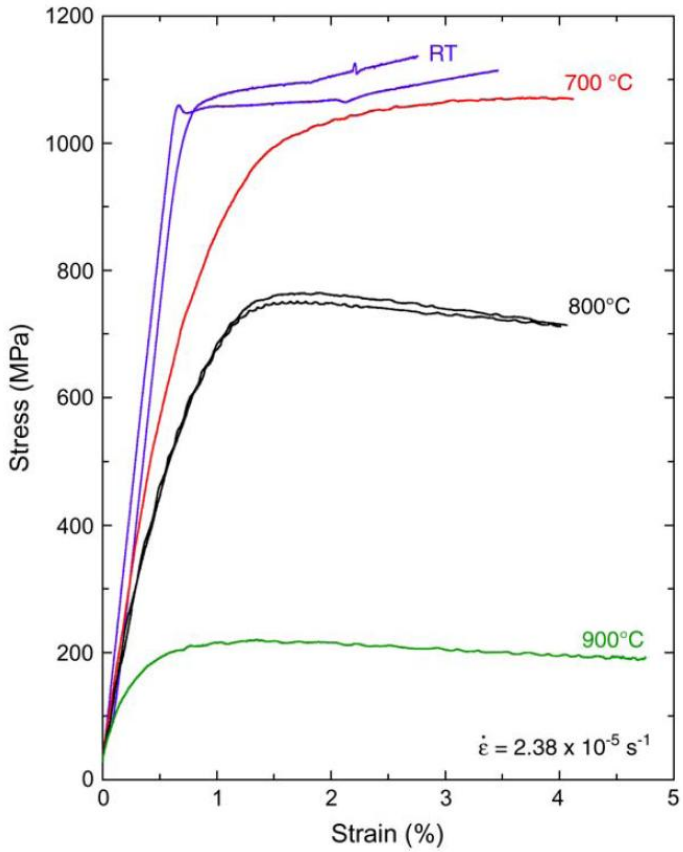

Figure 2.31 A stress-strain graph for Ti45Al8Nb0.5(B,C) TiAl alloy (Wu, 2006)

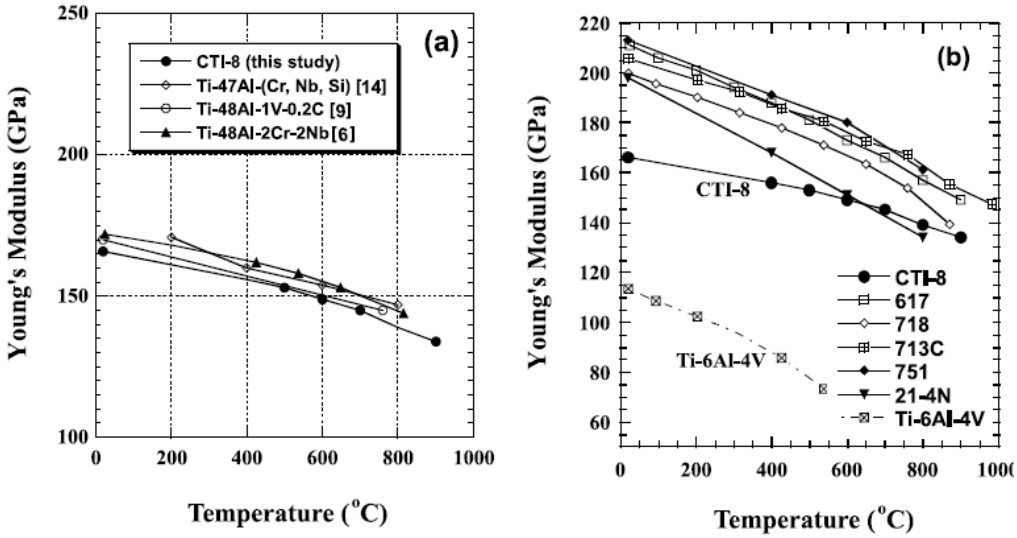

Figure 2.32 The stiffness of TiAl alloys (a) and TiAl alloys compared to other high strength metals (b) (Zhang, Reddy, & Deevi, 2001).

(Zhang, Reddy, & Deevi, 2001) have found the stiffness of TiAl alloys is not too dissimilar from other high strength Metals (Figure 2.32). The stiffness is larger

than the titanium alloy Ti-6Al-4V, showing the increase in aluminium content improves the young's modulus value.

Ductility of TiAl is very low at room temperatures making it a very brittle metal (Table 1, Figure 2.33). The low ductility makes processing and fabrication very difficult as the TiAl acts in a very brittle manner. At elevated temperatures, the ductility of TiAl increases, particularly once the temperature exceeds 600 ^{o}C. (Donachie, 2000; Polmear, 2006)

Controlling the microstructure of a TiAl component is vital to increasing ductility. Lamellar structures in TiAl of alternating γ and α_2 plates provides the best ductility (Wu, 2006). Approximately 30% α_2 appears to be the best ratio of $\alpha_{2:}$ γ to obtain the maximum ductility (Smallman & Bishop, 1999).

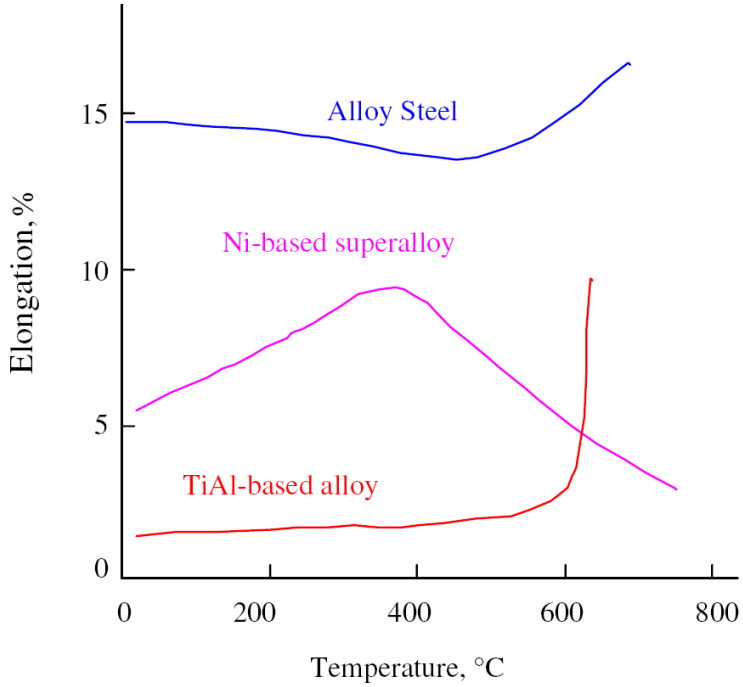

Figure 2.33 Ductility of alloy steel, Ni-based super alloy and a TiAl based alloy (Wu, 2006)

Titanium aluminides have low fracture toughness and thus low tolerance to damage (Donachie, 2000; Leyens & Peters, 2006). TiAl alloys generally have fracture toughness values ranging from 5 to 25MPam$^{1/2}$ which are values which are slightly higher than ceramics but well below titanium alloys. For a material to be considered structural, a lower limit of 25MPam$^{1/2}$ is required. (Wu, 2006)

Toughness is defined as the energy a material can absorb before rupture and is calculated by the area under the stress-strain graph. TiAl has a very low toughness due to its very low ductility as seen in Figure 2.31. The low ductility means the strain axis is very short, lowering the amount of energy TiAl can absorb dramatically.

Fatigue properties of TiAl alloys show that in the event there are no sharp defects, an excellent fatigue resistance is achieved. The excellent fatigue resistance can be seen by the endurance ratio higher than 80% of the ultimate tensile strength of the alloy. Changing the surface and internal properties can change the fatigue strength (Henaf & Gloanec, 2005).

Fatigue crack growth thresholds have been found to be in the range from 6 to 10MPam$^{1/2}$ by (Djanarthany, Viala, & Bouix, 2001).

2.5.7 Thermal Properties

The Thermal Conductivity of four different TiAl alloys can be seen in Figure 2.34 (a). The TiAl alloy tested was the CTI-8, with a composition of Ti-47Al-4(N, W, B). The thermal conductivities of the TiAl alloy were compared to other steel alloys and titanium alloys in Figure 2.34 (b). The thermal conductivity of the TiAl alloy was similar to the conductivity of many of the other alloys, except for the titanium alloy Ti-6Al-4V, which was about half the thermal conductivity. (Zhang, Reddy, & Deevi, 2001)

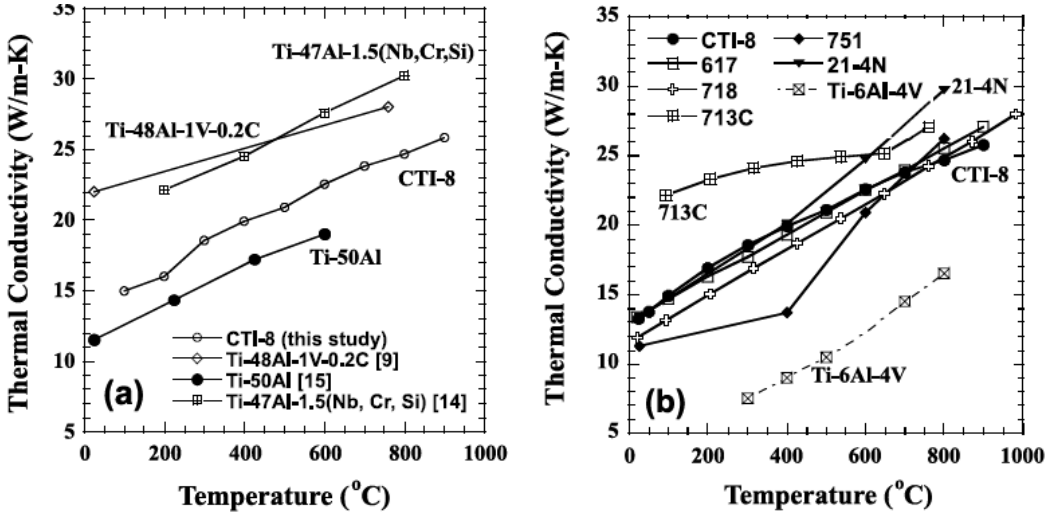

Figure 2.34 Comparisons of CTI-8 (TiAl alloy) with other TiAl alloys (a) and other high strength metals and titanium alloys(b) (Zhang, Reddy, & Deevi, 2001).

The melting point of TiAl alloys is approximately 1460 °C depending on microstructure and alloying constituents (Leyens & Peters, 2006).

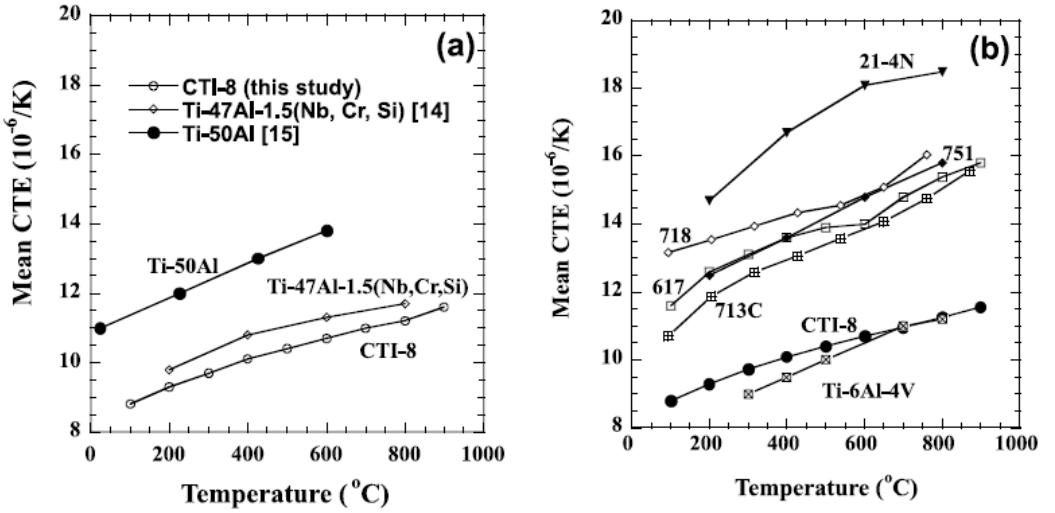

Figure 2.35 Coefficient of thermal expansion of various TiAl alloys (a). CTI-8 is a TiAl alloy. The coefficient of thermal expansion of the TiAl alloy is also compared to other metals (b). (Zhang, Reddy, & Deevi, 2001)

(Zhang, Reddy, & Deevi, 2001) have found the coefficient of thermal expansion of TiAl alloys is less than other high strength alloys (Figure 2.35). A low thermal expansion coefficient is beneficial because it allows better sealing between

components over increasing temperatures. These values were very similar to those found by (Djanarthany, Viala, & Bouix, 2001).

The creep behaviour of TiAl alloys depends strongly on the alloys microstructure and the alloy composition. Fully Laminar microstructures demonstrate the highest creep resistance, the lowest minimum creep rate and the best primary creep behaviour meaning this microstructure has the longest times to attain a certain strain. This property can be clearly seen in Figure 2.36. (Kassner & Perez-Prado, 2004)

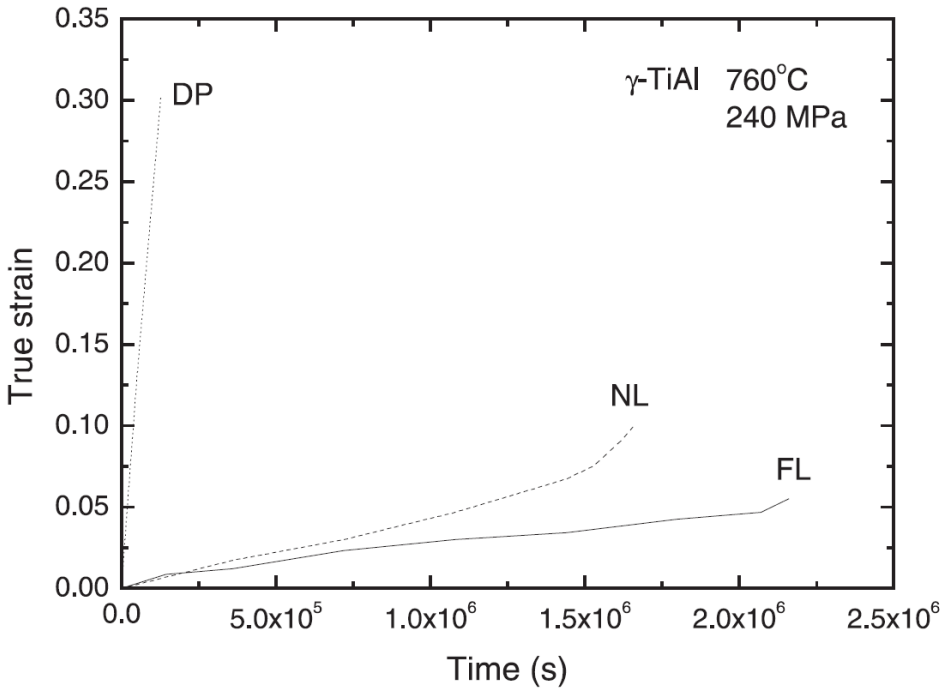

Figure 2.36 Creep curves at 760 ^{o}C and 240MPa for three different microstructures, Fully Laminar (FL), Nearly Laminar (NL) and Duplex (DP). The alloy is Ti-48Al. (Kassner & Perez-Prado, 2004)

2.5.8 Physical properties

γ-TiAl alloys have Densities of 3.9-4.2kg/cm^3. This is approximately 49% the density of steel, making titanium an excellent lightweight substitution for steel and other high strength, high density metals (Leyens & Peters, 2006).

The cost of titanium compared to other metals can be seen in Figure 2.24. It is clearly shown that the cost of titanium is substantially greater than that of other common metals. This is due to the processing costs as discussed under the heading Titanium Production. While the cost of Aluminium is not as much as titanium, it is still greater than that of steel. (Donachie, 2000)

Due to the high costs associated with TiAl alloy elements, cheaper processing and manufacturing methods are being developed which are near net shape (NNS). NNS components are very close to final shape and therefore there is only very minimal material wastage. These processes include powder metallurgy (PM), metal injection moulding and Laser RP

TiAl alloys are very corrosion resistant at low temperatures but at temperatures above 600 ^{o}C the oxide layer becomes brittle due to oxygen. This brittle layer can cause premature fracture damage in fatigue. The Oxide layer that forms below 600 ^{o}C is alumina (Al_2O_3), which is different to titanium alloys. Titanium alloys have greater oxidation resistance but not to as high temperatures. Improving the oxidation temperature at high temperatures through the use of surface coatings is currently under investigation. (Djanarthany, Viala, & Bouix, 2001)

The Human body is in a very susceptible to unfamiliar metals and therefore introducing implants within the body can produce unwanted effects within the body including death. Titanium is a bioactive material that can have body tissue actively bond to it, creating a strong bond. Ti-6Al-4V is generally used. The γ-TiAl alloy Ti–45Al–2W–0.6Si–0.7B shows promising attributes such as producing lower concentrations of Al and Ti ions while in a solution resembling body fluids. The TiAl alloys also had low passive current densities. The passive current densities are lower than for Ti-6Al-4V, a very common implant material, but the TiAl alloy has yet to undergo full testing (Escudero, Munoz-Morris, Garcia-Alonso, & Fernandez-Escalante, 2004).

TiAl wear properties are generally not acceptable as seen in Figure 2.37 and Figure 2.38. Thin hard coatings of nitrides or carbides can be prepared by physical

(PVD) and chemical (CVD) vapour deposition. Titanium Nitrate (TiN) is the most widely used coating for PVD while titanium aluminide nitrate (TiAlN) is used for demanding surfaces. (Boonruanga, Thongtema, McNallanb, & Thongtem, 2004; Schwartz, 2002)

Tribological tests were performed on many coatings. They were: CrN, TiAlN, TiAlCN, TiCN, TiCN+C, TiN+C, TiB2 and WC and molybdenum coatings. The coatings were tested for load capacity, adhesion power, abrasion force, hardness and fatigue strength. Of all of the coatings TiAlN gave the best results (Schwartz, 2002).

Coatings can also be applied to obtain greater oxidation resistance. These include: aluminizing, metal-chromium-aluminium-yttrium overlay coatings and silicides/ceramics.

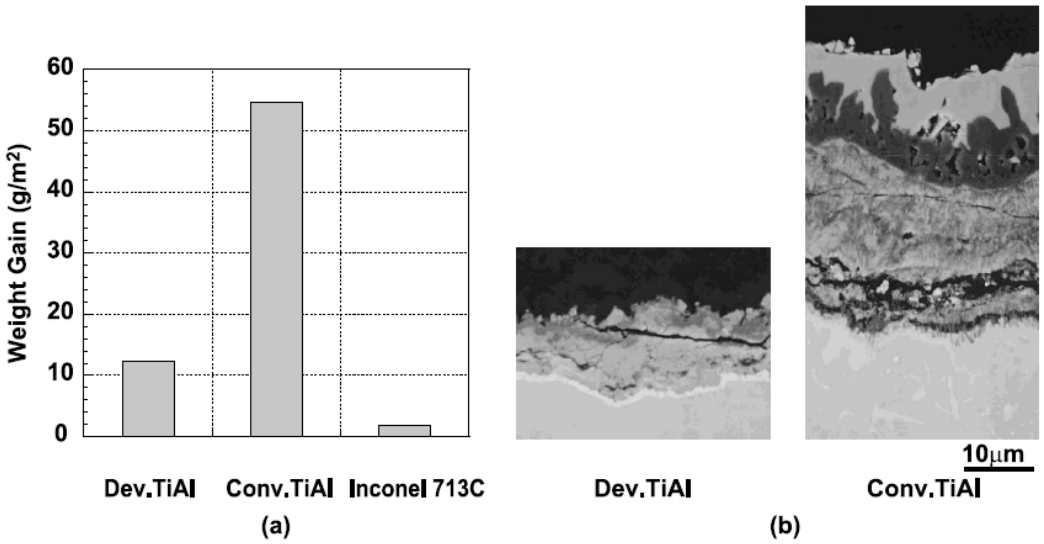

Figure 2.37 Results from testing a TiAl alloy for use as a turbocharger turbine at 850 ^{o}C for 500hrs in normal atmosphere. (a) is the weight gained by the turbines, and (b) is backscattered images of cross sections through the surfaces. Dev. TiAl is the TiAl alloy developed by Mitsubishi heavy industries, Conv. TiAl is a conventional TiAl alloy and Inconel 713C is a nickel based super alloy that has conventionally been used. (T. Tetsui, 2002)

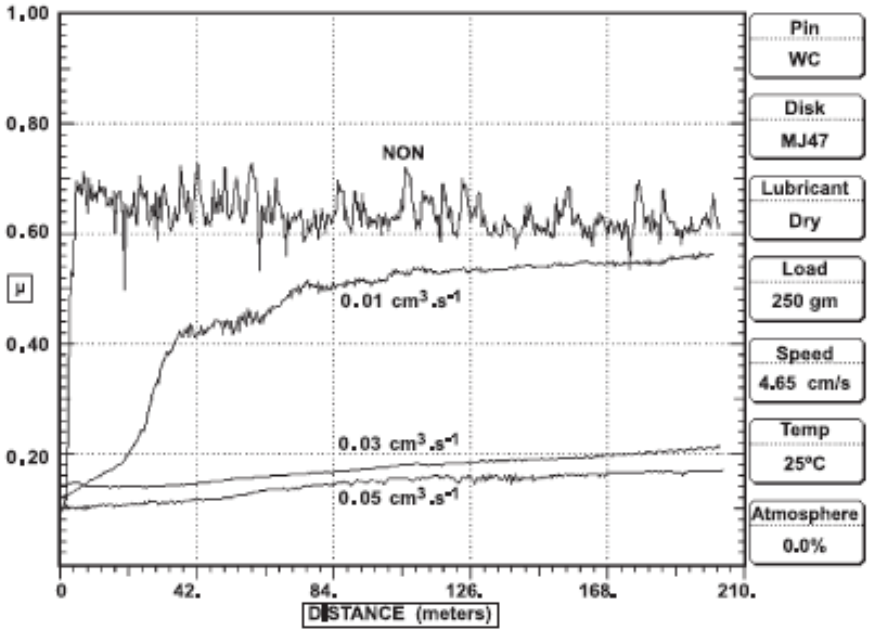

Figure 2.38 Nitriding and carburising affects of a TiAl alloy with changing nitriding and carburising rates. The value is for coefficient of friction (Boonruanga, Thongtema, McNallanb, & Thongtem, 2004)

Titanium burns when it is ignited at high temperatures and can burn in air, carbon dioxide and nitrogen atmospheres. Once ignited, titanium will burn very fiercely and is difficult to extinguish. It can only be extinguished by smothering with sand or salt. Materials such as foils, powder and dust are greater risk of combusting due to their greater surface areas. This combustibility is due to titanium's low thermal conductivity and the high heat of formation for TiO_2.

TiAl alloys have less of a risk of combusting as there is less titanium and the thermal conductivity is increased over titanium alloys (Djanarthany, Viala, & Bouix, 2001).

2.5.9 Processing/manufacturing

TiAl alloys can be processed in many of the conventional methods with slight modifications.

Casting of TiAl alloys is currently used in the aerospace industry as it allows large complex parts to be produced with minimal processing and material wastage.

Some castings may require HIP'ing (Hot Isostatic Pressing) to increase the part density if pores are present. Melting and casting of TiAl alloys can be difficult due to thermal stresses creating cracking, although this depends on the casting method used. A fully lamellar microstructure is commonly found for cast TiAl alloys (T. Tetsui, 2002).

Forging of titanium landing gear and diffusion bonding of turbine blades has also recently been introduced. Forging of TiAl components requires high temperatures to enable suitable ductility to be reached. The increased temperatures add to the difficulty and cost of producing forgings. (Polmear, 2006)

Powder metallurgy (PM) has not yet been used for large scale production of TiAl components. PM has an advantage over casting because it can be used to create fine grained, texture free materials with equiaxed grains and a homogeneous microstructure with substantial reductions in the amount of wasted material. PM requires HIP'ing to increase the component density. This can be done during sintering or after. (Djanarthany, Viala, & Bouix, 2001; Leyens & Peters, 2006)

TiAl alloys can be welded in an inert atmosphere but machining is difficult due to its very low ductility. Much research has been conducted into manufacturing processes of TiAl and new processes are constantly being developed.

For applications requiring high wear resistance, coatings can be applied although the coatings are costly to apply. Coatings can also be applied to increase the oxidation resistance.

2.5.10 Current Automotive applications

Current TiAl mainstream automotive applications are limited to Mitsubishi's use of γ-TiAl for turbocharger rotors. The rotor can be seen in Figure 2.39. The rotor is manufactured using the LEVICAST method developed by Daido Steel Co. Ltd. LEVICAST has advantages over other casting methods in that it minimizes casting defects and impurities. The casting has a fully lamellar microstructure which is carefully maintained during HIP'ing. (Baur, Wortberg, & Clemens,

2003; Froes, Friedrich, Kiese, & Bergoint, 2004; Schauerte, 2003; T. Tetsui, 2002)

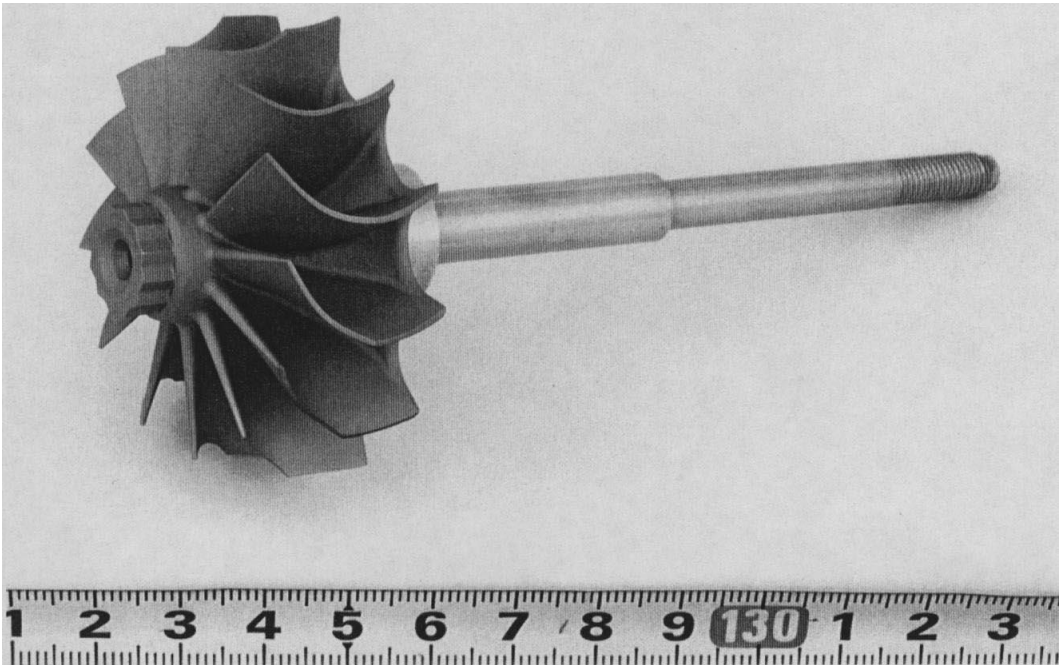

Figure 2.39 The Mitsubishi turbocharger rotor made from γ-TiAl (Tetsui, 1999)

The advantages of a TiAl turbocharger rotor can be seen in Figure 2.40. To increase the supercharging pressure from 0 to 50kPa takes 0.2s shorter time, meaning a vehicle with a TiAl turbocharger rotor will get more power due to boost pressures increasing faster than conventional metal rotors. This advantage is due to the decreased rotating mass of the rotor, allowing it to spin up faster. (Djanarthany, Viala, & Bouix, 2001; T. Tetsui, 2002)

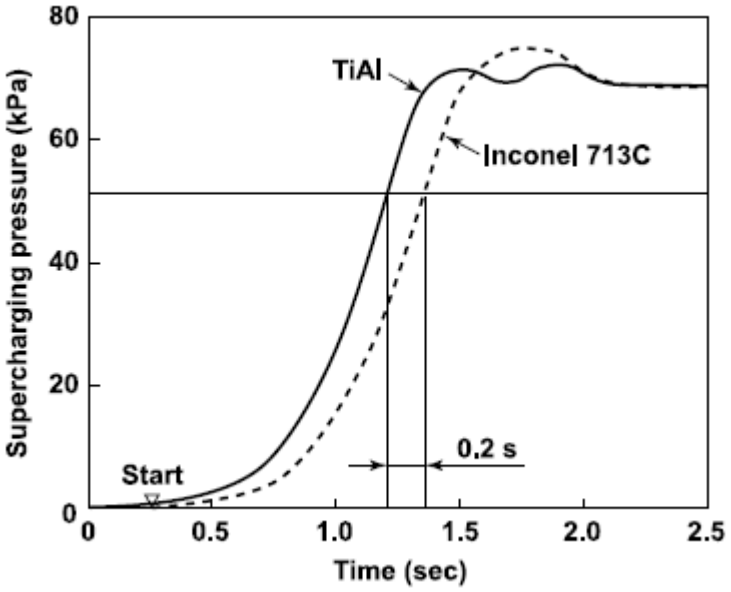

Figure 2.40 Comparison of the advantages of a TiAl turbocharger rotor (T. Tetsui, 2002)

An important consideration for safety is burst tip speed (Figure 2.41). The burst tip speed is the velocity of the tip of the rotor when failure occurs. Testing undertaken by Mitsubishi Heavy Industries Ltd, shows the burst tip speed of a TiAl rotor is greater than 600m/s and that during testing none of the TiAl tips ever burst. The TiAl rotor was compared to the Inconel713C (most commonly used for turbochargers) and MAR-M247 (used for race engines). This greater burst tip speed allows increasing of turbocharger size and greater aerodynamic efficiency as the rotor design can be further optimised by minimising the weight further, decreasing burst tip speed. (T. Tetsui, 2002)

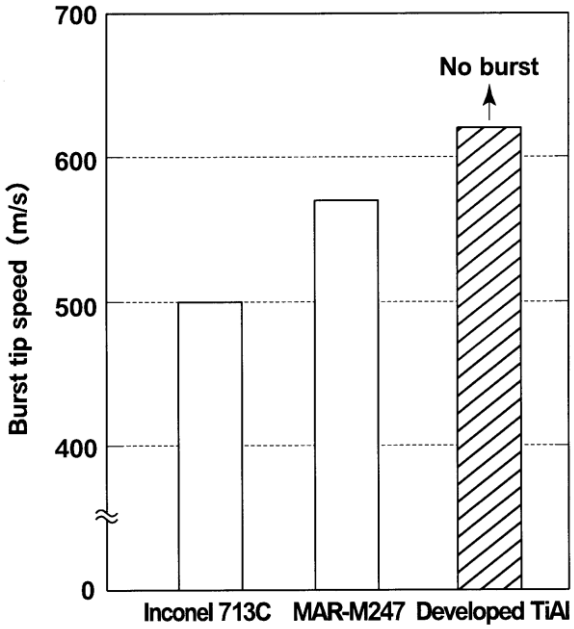

Figure 2.41 Comparisons of the burst tip speed for commonly used turbocharger rotors (T. Tetsui, 2002)

The other TiAl use in the automotive industry is for valves in race cars and motorbikes. Formula 1 racing cars were using TiAl valves at the turn of the century but TiAl valves were banned due to their high costs being a disadvantage to teams with lower funds. TiAl valves and fasteners are still used on MotoGP motorbikes and NASCAR teams are looking to use this technology. TiAl valves that have been produced have been manufactured by casting or thermomechanical forming but casting produces too much waste to be cost effective and thermomechanical forming must be performed at temperatures of ~1100 ^{o}C making it inefficient. The TiAl valves that have been produced are successful in terms of performance but are too costly to implement. An example of the benefits TiAl alloys bring for use in the valve train is seen in Figure 2.42 where there is a 1000RPM increase in engine speed before valve bounce, a major restriction on maximum engine speed. (Baur, Wortberg, & Clemens, 2003; Dowling, Donlon, & Allison, 1994; Froes, Friedrich, Kiese, & Bergoint, 2004; Gebauer, 2006; Knippscheer & Frommeyer, 1999; Knippscheer et al., 2000; Schauerte, 2003; Tetsui, 1999; Winkler, 2000; Wu, 2006)

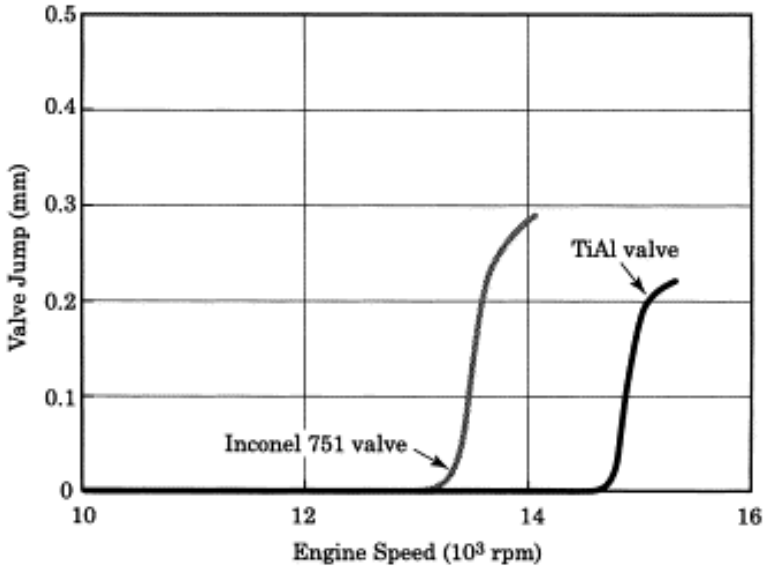

Figure 2.42 Graph showing the 1000RPM increase before valve jump occurs when using a TiAl valve (Tetsui, 1999)

(Eylona, Kellera, & Jones, 1998) with help from GM and FORD successfully manufactured and tested over 800 permanent mould cast TiAl valves. The valves were tested over 50,000km with no valve damage and an average of 2% fuel savings. The only inhibiting factor is the high cost.

Other TiAl valves have been produced using thermomechanical forming by extruding a rod and then hot bulging of one end followed by quasi-static die forging. All processes were performed at temperatures between 1100 ^{o}C and 1300 ^{o}C. The valves were tested for over 100,000km without failure. At 140,000km testing, wear at the top of the valve stem was observed but was not of great concern. The valves were coated before trialling to enhance wear resistance.

From 1998, for 5 years, half of all Toyota Altezza's had Powder Metallurgy (PM) TiAl intake valves. The PM TiAl valves weighed 27g as opposed to the previous steel valves weighing 44.6g. The PM valves proved to be successful in their application. The reduction in valve mass allowed the valve spring mass to be reduced by 17%. While (Faller & Froes, 2001) believed casting is the way to manufacture valves, the large material wastage makes PM valves an attractive solution to the high prices.

Chapter 3 Ultracommuter Chassis design

3.1 Introduction

A vehicle chassis design is very complex, requiring the integration of multiple components, cost considerations and meeting of performance goals using available materials to obtain an optimal design.

Aspects of this chassis design requiring particular consideration were occupant safety, chassis stiffness, how the suspension would be mounted due to material selection, where and how the batteries would be mounted, occupant ergonomics and suspension, chassis and body shell interaction.

A chassis design similar to conventional cars would be beneficial as consumers can react unfavourably to changes to convention, particularly if the design lacks refinement and reliability (Happian-Smith, 2001). The chassis design for this BEV would be different to a conventional car due to the chosen materials physical and mechanical characteristics and the desire to exploit the numerous advantages 'in-wheel' motor driven BEV's have over conventional internal combustion vehicles.

Advantages of an 'in-wheel' motor driven BEV include motors inside the wheel, therefore more space within the body shell and flexibility in the mounting position of the batteries. By using 'in-wheel' motors and batteries, the space occupied by propulsion reduces from 304 litres (engine minus ancillaries and fuel tank only) to 110L (batteries and motor controllers). That is a decrease from 7% to 2.6% of the total volume available beneath the **Ultra**commuter body shell (Appendix 1).

3.2 Previous concept

A Honeycomb panel BEV chassis was designed and constructed in 2006. The chassis proved to be exceptionally light, weighing only 59.6kg. The chassis consisted of interlocking honeycomb panels that were water jet cut to the correct shape from CAD files. The panels were bonded together. The 2006 chassis can be seen in Figure 3.1.

Figure 3.1 The 2006 NZeco chassis

The chassis was based around using two ‘in-wheel’ motors, a battery pack, Mazda MX-5 suspension and steering and a bodyshell shape from *Hybrid*Auto. The chassis consists of front, middle and rear compartments with suspension wishbones attached through mounts to the sides of the front and rear compartments. The chassis never had any propulsion system attached so its performance was unknown.

For 2007 there were changes to the components used within the vehicle. These included custom suspension based on the Lotus Elise, Lotus steering components and Thunder-Sky Li-ion batteries. The 2006 chassis was analysed for its suitability for use in 2007 and Table 2 was collated to display its advantages and disadvantages.

Strengths	**Weaknesses**
Very stiff design	Not enough space within the chassis
Load bearing beams front and rear	Not integrated to the bodyshell
Impact absorbing beams front and rear	Poor suspension and steering design
Central tunnel for strength	Poor workmanship
Lightweight (under 60kg)	Poor occupant ergonomics (dash too far away and too low)
	No provision for roll hoop attachment
	The suspension did not fit completely within the bodyshell

Table 2 Assessment of the 2006 chassis

To implement the required changes to the 2006 chassis would be difficult and time consuming.

3.3 Chassis selection

The research undertaken into chassis designs allowed a decision to be made on how the 2007 **Ultra**commuter chassis would be constructed. The main priority in the chassis design was its requirement to be lightweight. There were also limits on available skilled labour and expenditure. These main factors contributed to the decision to design a new aluminium honeycomb sandwich panel chassis. The design would be similar to a space frame in that it was a complete assembly mounted below a bodyshell, but it would not be constructed from metal tubing.

The aluminium honeycomb chassis has advantages in that it does not require skilled labour to assemble, the material and processing costs are minimal and the design allows a lightweight design without the need for in-depth finite element analysis and mathematical modelling.

Therefore to successfully prove the concept of BEV's in 2007 a new, more refined version of the 2006 chassis was designed and built.

3.4 Material selection

Aluminium honeycomb sandwich panel was chosen as the chassis material because it has high stiffness, is lightweight with a density of only 7% of aluminium, high corrosion resistance and low cost (Ayres Composites Panels Pty Ltd, 2006).

The honeycomb panel consists of an aluminium honeycomb core sandwiched by two aluminium facings. The honeycomb is a repeating hexagonal structure resembling the appearance of bees wax inside a beehive. The aluminium facing sheets are bonded to the honeycomb core as shown in Figure 3.2.

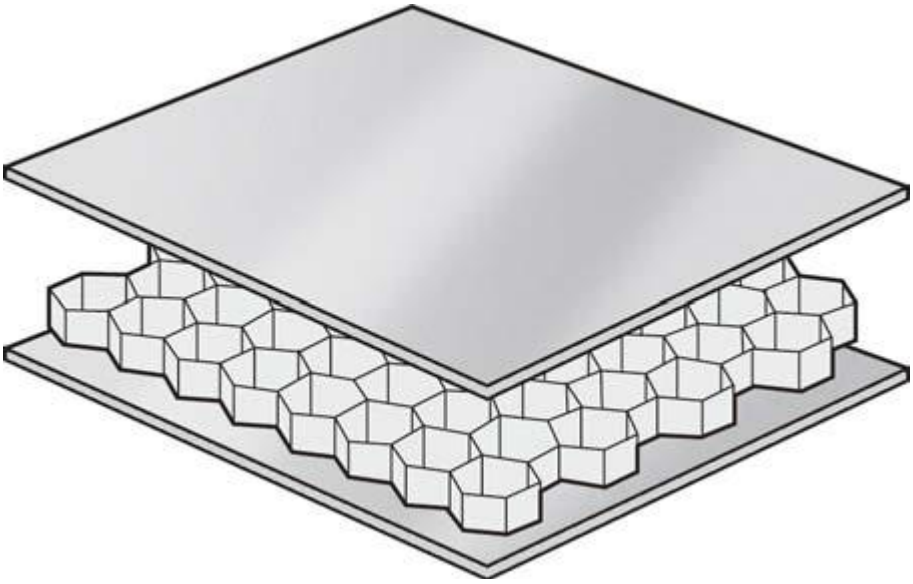

Figure 3.2 An exploded view of aluminium honeycomb (Ayres Composite, 2007)

$$I_x = \frac{bh^3}{12} \quad (2)$$

- I_x is the second moment of inertia about the x-axis
- b is the beam width
- h is the height of the beam

$$\sigma = \frac{My}{I_x} \quad (3)$$

- σ is the normal stress in a beam due to bending
- M is the bending moment
- y is the perpendicular distance to the centre axis

Sandwich structures are well known to be strong and stiff with low weight due to their high second moment of area 'I' (2). The main advantage with sandwich structures is an increased thickness, with very minimal weight addition. The high

second moment of area values are due to the larger ‘h’ value which is the thickness of the beam. As the ‘h’ is cubed, it has a much larger influence on the second moment of area than the width ‘b’. The larger second moment of area makes the stresses at the upper and lower surfaces smaller due to the Euler-Bernoulli beam equation (3) therefore a larger moment can be applied to the beam before it fails.

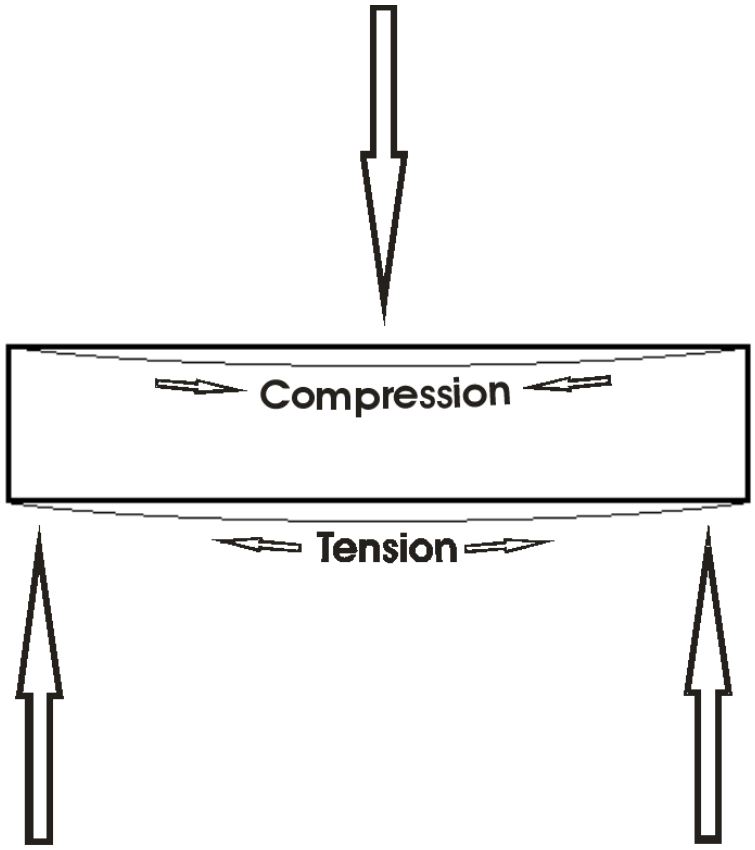

Figure 3.3 A beam under bending indicating where compression and tension occurs in face materials

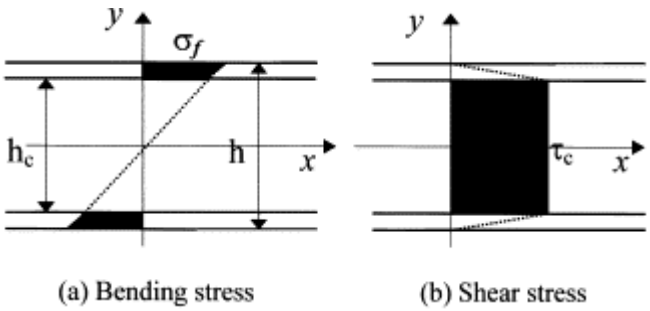

Figure 3.4 Stress distributions in aluminium honeycomb sandwich panel under bending (Kee Paik, Thayamballi, & Sung Kim, 1999)

Sandwich panels work under the same principal as 'I' Beams. An object that is under bending forces has the largest stress concentrations on the upper and lower surfaces of the object as demonstrated in Figure 3.3. The stress distribution within a sandwich panel is shown in Figure 3.4 when subjected to bending. The figure clearly indicates the bending forces are carried within the facing material. Using (2), doubling the thickness of the material results in an 800% load carrying capacity increases because the stresses now carried by the upper and lower surfaces are lower. Experimentation of this theory was undertaken by (McBeath, 2000) and his results (Figure 3.5) are slightly below the calculated values but are none the less representative. Therefore if a very low density core material is used the stiffness will greatly increase but the mass will increase relatively less. This is the principal how 'I beams' function and are thus utilised in the building industry for decreasing mass and material use.

	Solid material	*Core thickness t*	*Core thickness 3t*
Thickness	t	2t	4t
Stiffness	1.0	7.0	37.0
Flexural strength	1.0	3.5	9.2
Weight	1.0	1.03	1.06

Figure 3.5 Results from experimentation of beam stiffness with changing core thicknesses. A honeycomb core was used. (McBeath, 2000)

The core material acts to keep the two facings apart and is able to transfer forces between them. This requires core materials to be strong in shear and compression.

The bond between the facings and core material must be strong or the sandwich panel will fail.

Honeycombs have excellent energy absorbing properties (McBeath, 2000). This is demonstrated by the use of 50mm thick Ayrlite® panels in the Australian V8 Supercars ™ (Ayres Composite, 2007). Ayrlite® is used inside the door panels to protect drivers from side impacts (Figure 3.6).

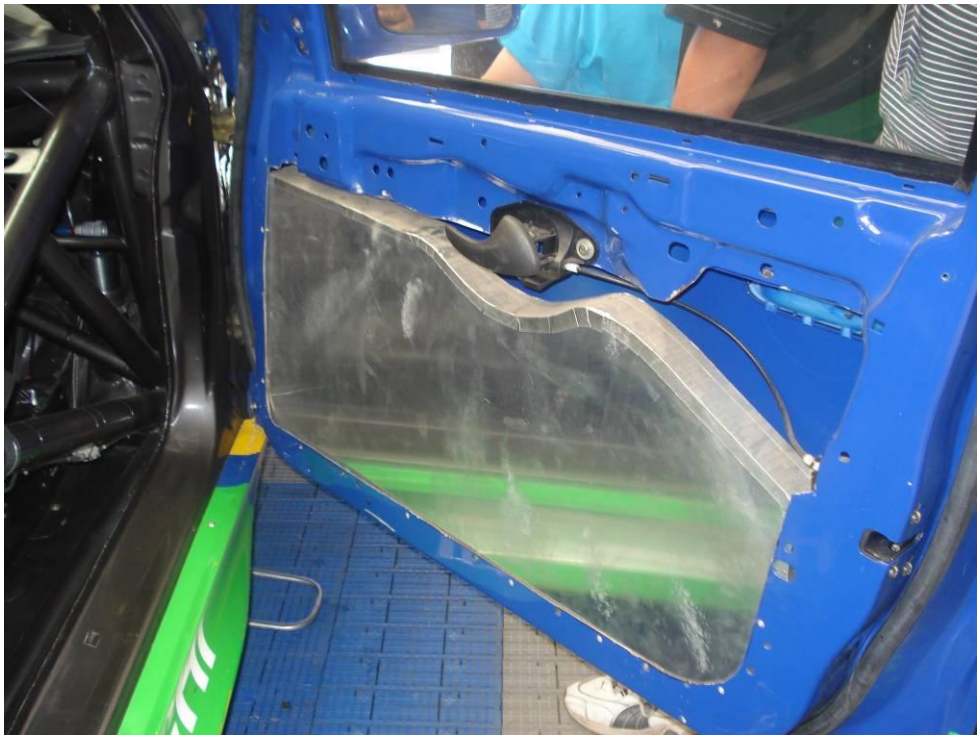

Figure 3.6 Ayres 2022 Aluminium honeycomb used for side impact protection in the Australian V8 Supercars™ (Ayres, 2008).

The aluminium honeycomb sandwich panel for the **Ultra**commuter chassis is the Ayrlite® 2022, available in sheets 2400mm x 1200mm with a thickness of 20mm. The sandwich panel was supplied by Ayres Composite Panels Pty Ltd in Perth, Australia. The Facings are 0.5mm thick 5052/5251 aluminium sheet and the honeycomb core consists of 19mm deep, strain hardened 6.35mm cell size aluminium honeycomb. Ayrlite® is non-combustible and corrosion resistant and therefore is used a great deal in the marine industry for lightweight walls and panelling (Ayres Composite, 2007).

3.5 Specifications and constraints

Constraints on the chassis design are factors that are out of the control of the chassis design. Specifications are targets for the chassis design.

The chassis design must meet these criteria.

- Fit completely within the bodyshell
- Use Lotus suspension placement
- Steering rack placement
- Occupant position
- Fit one battery pack
- Meet the LVVTA regulations

The chassis is designed to these specifications.

- Ability to withstand minimum and maximum temperatures of -20 ^{o}C and 50 ^{o}C respectively
- Ability to withstand humidity's of 0-100%
- Suitable for driving on all sealed road conditions
- To be designed to be as stiff as possible
- Lightweight ~60kg
- Low COM
- Close to 50-50 weight distribution
- Have a useful life of at least 5 years
- Must be Ergonomic
- Designed to maximise available space
- Cost

Detailed specifications

All aspects of the chassis, suspension and steering must meet the relative LVVTA regulations to enable the car to be driven on the road.

The rear suspension design is from a Louts Elise, adapted to take ‘in-wheel’ electric motors. Using ‘in-wheel’ electric motors creates increased loadings on the rear suspension components compared to a conventional power train. The ‘in-wheel’ motors must create a reaction torque for the torque they are producing to enable the vehicle to move. Conventionally this meant the torque is provided by the motor, through drive shafts with reaction forces acting through the motor mounts to counter the torque to move the vehicle. With in wheel motors, the suspension has to transfer these reaction forces through the wishbones; thereby the suspension mounts must be able to withstand this increased loading through the suspension mounts. This increased loading requires lower link tubes to be used to link both sides lower wishbone mounts together. The link tubes work in the same manner as a strut brace. The link tubes are used to directly transfer forces from one mount to the opposing side mount.

The suspension mounting points are from a Lotus Elise chassis. To maintain correct geometry during suspension movement and prevent fouling, the location of the suspension mounting points needed to be maintained on the **Ultra**commuter chassis.

Forces are transmitted from the suspension to the chassis at all times, even when at rest. Therefore the suspension attachment points must be strong as failure could be catastrophic, particularly if failure were to occur at high speeds.

All suspension components must clear the chassis at all times. If any component, including tyres, were to foul on the chassis, the chassis or suspension components may become damaged and fail.

The Steering geometry must be designed to minimise bump steer and other unwanted geometry changes. To minimise weight the steering system will be manually operated.

The aerodynamically efficient body shell design was obtained from *Hybrid*Auto in Australia (Figure 3.7). The body shell was designed to fit over a Lotus Elise

chassis. To maintain the aerodynamics of the body shell, no components were to protrude past the body shell extremities, excluding tyres.

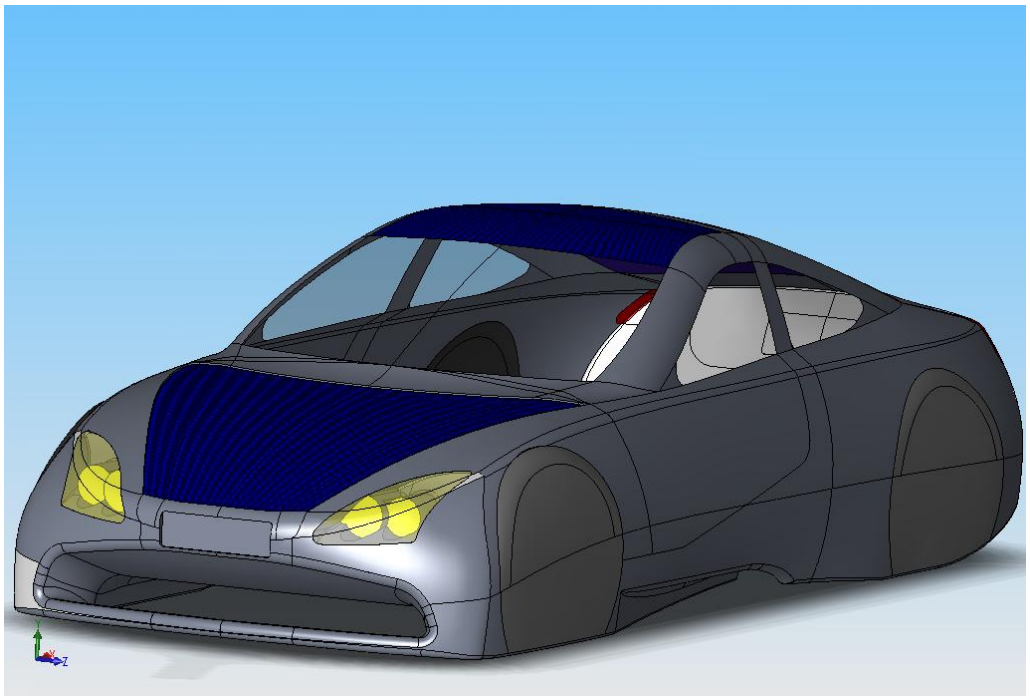

Figure 3.7 The *Hybrid*Auto bodyshell

Batteries are the single largest mass within the vehicle, so their placement is important as it greatly affects the COM and the weight distribution. The COM is the central point where if the car were to be supported there, the car would balance. For vehicle dynamic handling the COM needs to be located as low as possible. A low COM decreases the amount vehicle body roll. Ideally weight distribution in a vehicle is 50:50, and such a weight distribution enhances a vehicles dynamic performance as all tyres get the similar amounts of grip. Thus, at entry to a corner, the front will not tend to understeer as much as a vehicle with weight distributed towards the front.

A 16kWh battery pack was mounted in the vehicle. Easy access to the batteries was required to enable them to be quickly and easily replaced.

The chassis performance must not be affected by moisture, be able to withstand temperatures ranging from -20 ^{o}C to 50 ^{o}C and humidity's of 0% to 100%. The

vehicle will be driven primarily on sealed roads. The chassis must withstand being driven on short unsealed patches of road.

The **Ultra**commuter raced the World Solar Challenge in October 2007 so it had to be designed to withstand driving the 3000km from Darwin to Adelaide. The temperatures in Darwin can reach 40+ ^{o}C in October with humidity's of up to 100%. The highway is a two lane road with many road trains. The surface is relatively smooth and flat.

The **Ultra**commuter will be driven on a variety of roads, from smooth motorways to gravel. The **Ultra**commuter is not intended to be driven on unsealed roads but this must be considered for events such as road works where fresh tar seal results in loose stones. Due to the landscape in New Zealand, roads have numerous hills, as well as irregularities such as pot holes. The chassis would need to withstand the forces from the suspension that these roads create.

Occupant location within the vehicle is determined by the body shell and the available space. The occupant must be able to get in and out of the car unaided and ergonomics within the cockpit must be similar to a conventional car. The chassis design must maximise available space.

The chassis design and construction must fall within the allotted $5000 budget.

3.6 Design

3.6.1 Safety

The **Ultra**commuter is to be driven on public roads therefore it is required to meet local regulations to ensure it is safe for the vehicle occupants and other road users. In New Zealand the Low Volume Vehicle Technical Association (LVVTA), established by car clubs and associations around New Zealand, is the regulatory body allowing custom built and modified vehicles to operate on public roads provided they meet the required safety regulations. These regulations allow custom built and modified vehicles to be driven on the road without expensive crash testing, enabling cars to be constructed without significant financial cost.

Vehicle safety can be either passive or active in nature. Passive safety is operational at all times and therefore requires no inputs to operate. Passive safety devices include crumple zones, seatbelts and dash padding. Examples of the energy absorbing properties of steel and aluminium as a function of mass can be seen in Figure 3.8. Active safety devices are not always working and require a signal generated from sensors to activate. Active safety devices include Anti-lock braking systems (ABS), air bags and electronic stability control. It is well known that there is increasing demand for increased occupant safety; thereby more safety systems are being incorporated into vehicles to meet his demand.

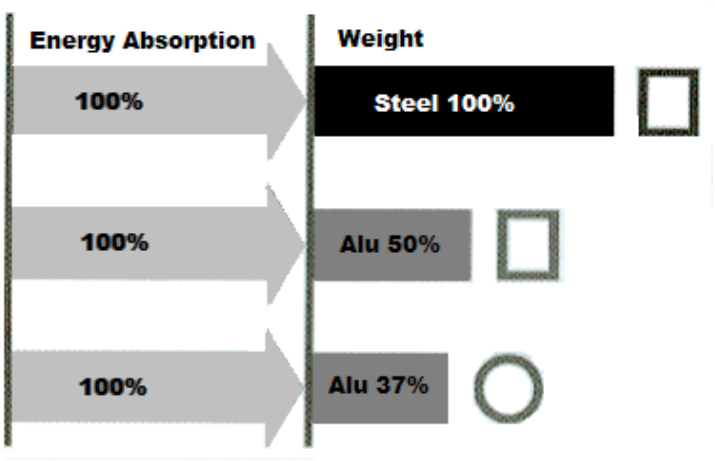

Figure 3.8 Energy absorption of different cross sectional structures as a function of weight (Braess & Seiffert, 2005).

Safety devices incorporated into the **Ultra**commuter chassis design consist primarily of passive safety devices due to the vehicles experimental nature. Passive safety devices are cheaper and simpler to install than active safety systems. Active safety systems would not be present on this car due to their high costs, installation difficulties and their added weight.

It is well known that new car buyers are demanding safer vehicles with lower emissions. Safety features include the addition of air bags (driver, passenger and side), stability control, ABS, electronic brake force distribution and many other new safety features. The addition of these features creates more weight within the vehicle, and in many circumstances has resulted in the addition of these features

negating any weight decrease in the chassis or body. An example of this is the Lotus Elise. To be able to sell the Elise in the United States of America the Federal Elise had to meet the crash testing and emissions standards. To meet these standards, the Federal Elise gained 65kg (Figure 3.9). 13kg of the 65kg is for A/C, which while not mandatory, is expected of vehicles sold in the USA. This is an increase in weight of 7.8% from the base model Lotus Elise S2. (Jost, October 2004)

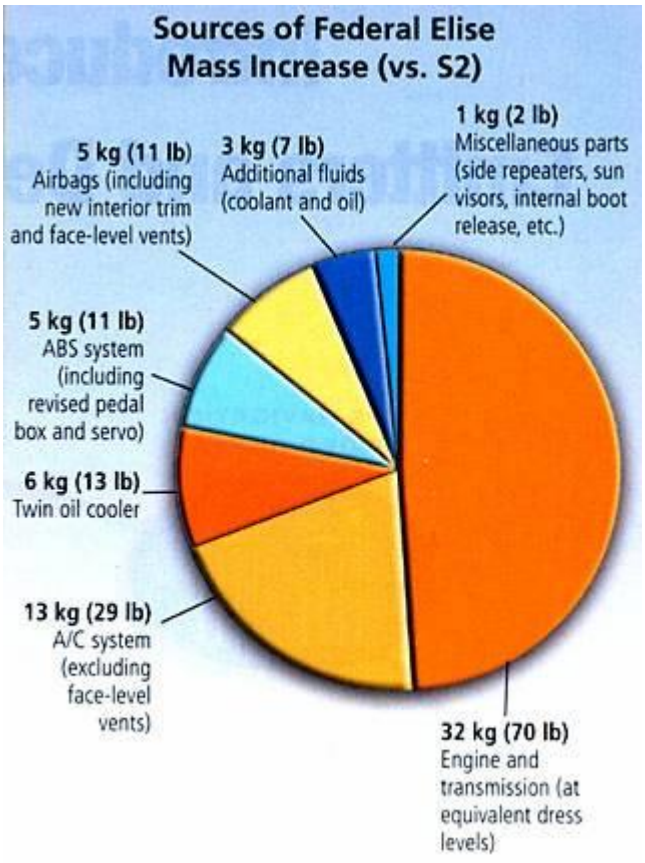

Figure 3.9 Sources of weight increase for the Lotus Elise Federal (Jost, October 2004)

3.6.2 Computer Aided Drawing

SolidWorks, a 3D Solid modelling program, was used to design the **Ultra**commuter chassis. Using 3D CAD software to develop a vehicle allows faster development times than 2D drawing and constructing prototypes. The use of CAD allows fewer prototypes to be built, as the fit and function of components

can be determined in the CAD model. If prototypes are built they are generally constructed using Rapid Prototyping (RP) techniques or CNC machining directly from the CAD models. 3D CAD packages allow the chassis to be completely designed and tested virtually. This virtual testing meant the chassis could be designed faster, more accurately and simultaneously with the rest of the car (concurrent engineering).

CAD allows the chassis to be integrated with other components very early in the design process. The fit and design of components can be optimised prior to any manufacturing of components begins. This process creates significant reductions in the cost and time for development of a vehicle. Ford motor company used 90% less prototypes during the development of the FORD GT through greater use of CAD and FEA (Ford Motor Company, 2003).

Holden (GM) reduced development time for the latest Monaro (Figure 3.10) substantially through greater use of CAD and their new Virtual Reality Design Studio. Development of niche cars from design freeze generally takes about 3 years. Holden took just 22 months to develop the Monaro. It took only 1 year to produce the first running concept car. The development process also allows substantial savings in cost. (Alias Systems Corp, 2004; Newton, 2001, , 2005)

Figure 3.10 The 2005 CV8 Holden VZ Monaro (Kodack, 2005)

Use of CAD is allowing small reductions in chassis mass to be achieved. A chassis design for the mass consumer market with substantial weight loss will require a radical new chassis design and use of lighter materials. CAE is a tool which can be utilised to create this mass reduction. Through the use of Computer Aided Drawing (CAD) allowing the transferring of ideas around the world instantly via the internet and allowing complex stress analysis in components and assemblies through the use of finite element analysis (FEA) it can be achieved.

The 3D CAD drawing techniques used during the chassis development were different to the 2006 design. A new CAD concept of ‘drawing in context’ meant file sizes were smaller, there were fewer update errors which were easier to correct and SolidWorks was more stable. The chassis context sketch can be seen in Figure 3.11.From these sketches, extrusions were easily created. While it took time to become accustomed to this new technique it resulted in faster drawing and better understandings of the finer details of CAD design.

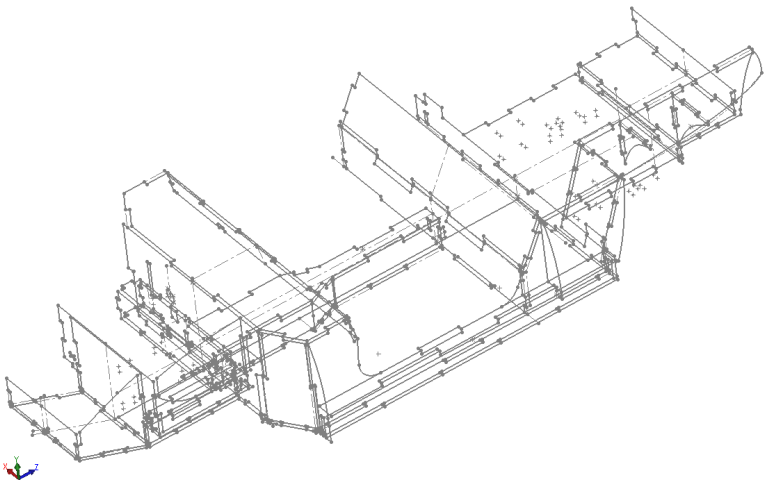

Figure 3.11 The final chassis context sketches

3.6.3 FEA Analysis

FEA entails the use of computers to calculate answers to complex mathematical equations. The complex mathematical equations are derived from a 3D model whereby a ‘mesh’ (Figure 3.12) of the model is created. From the mesh, variables are obtained which are input into mathematical equations to solve for the

unknown values. The mathematical equations results can be for impact loading, static loading, fatigue, vibration, heat transfer, fluid dynamics and electromagnetism.

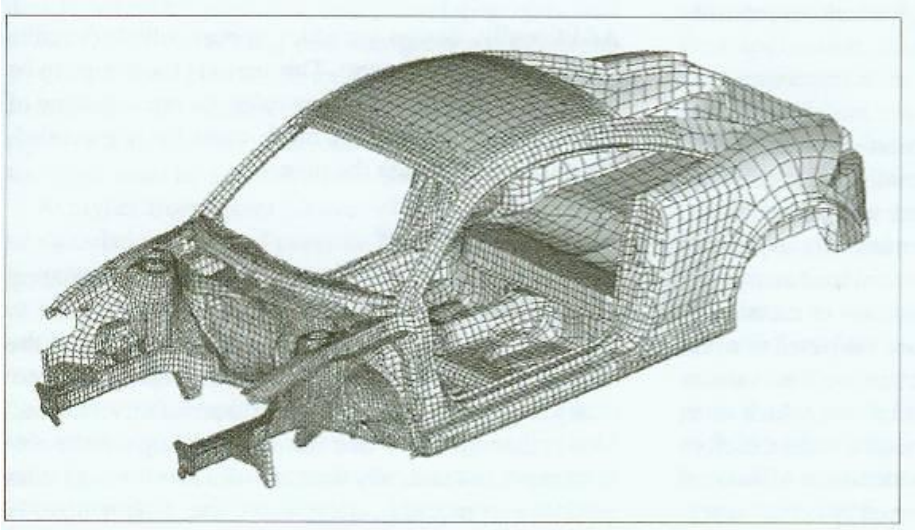

Figure 3.12 A mesh crated on a 3D CAD model for Finite Element Analysis (Braess & Seiffert, 2005)

The outputs or results from FEA analysis are typically graphs or images. Graphs simply show the data along axes, whereas the images utilise different colours or shades to represent different loading conditions within the component. Typically for static load analysis, areas of high stress are represented by red and low stress areas are blue with the differing shades and colours in between. This output of differing shades or colours makes FEA results very easy to understand, but it must be used with caution to ensure the applied design scenario is correct. An image of FEA analysis of a frontal impact can be seen in Figure 3.13.

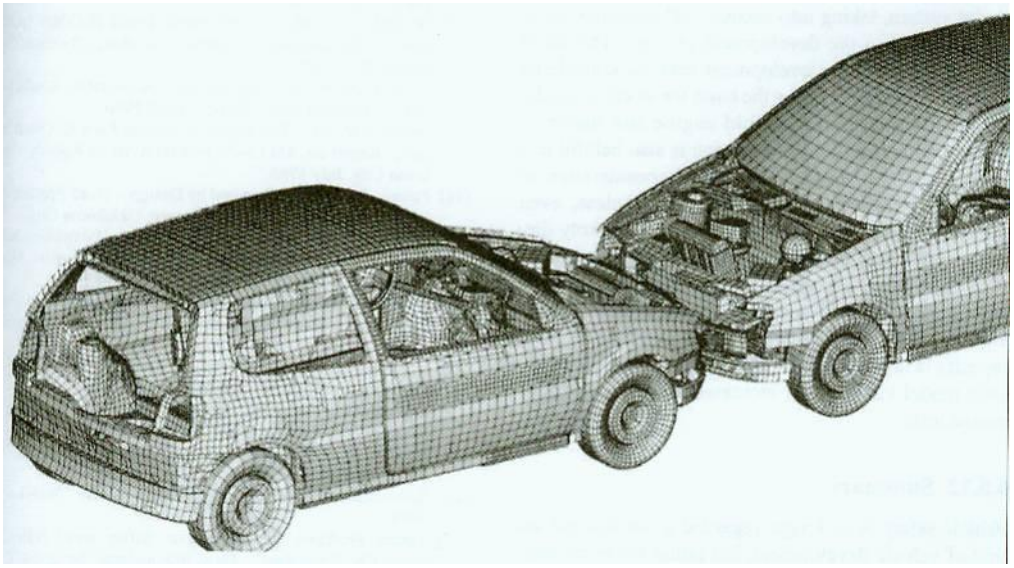

Figure 3.13 Computer simulation of a head on collision (Braess & Seiffert, 2005)

Chassis design has been extended to its limit through the use of FEA by optimising material properties and minimising material dimensions. By optimising the chassis design the amount of material used has been reduced.

Finite Element analysis (FEA) was performed on the chassis designs as they were developed. For static FEA, as was performed on the **Ultra**commuter chassis designs, the material, applied restraints and loads and a 3D model are required. The material defines the models properties and this is used to calculate the stresses and strains within the model. The Complex calculations require significant computer power, so depending on the specifications of the computer used, FEA analysis could take up to 8 minutes to complete, and therefore at times multiple computers were used. The time to calculate largely depends on the complexity of the model, the required numerical accuracy and the performance of the computer used. The mesh can take over 5 times as long to create than the stress analysis. The chassis mesh can be seen in Figure 3.14. It is very fine as this was the only way the mesh was able to be created due to its complex nature.

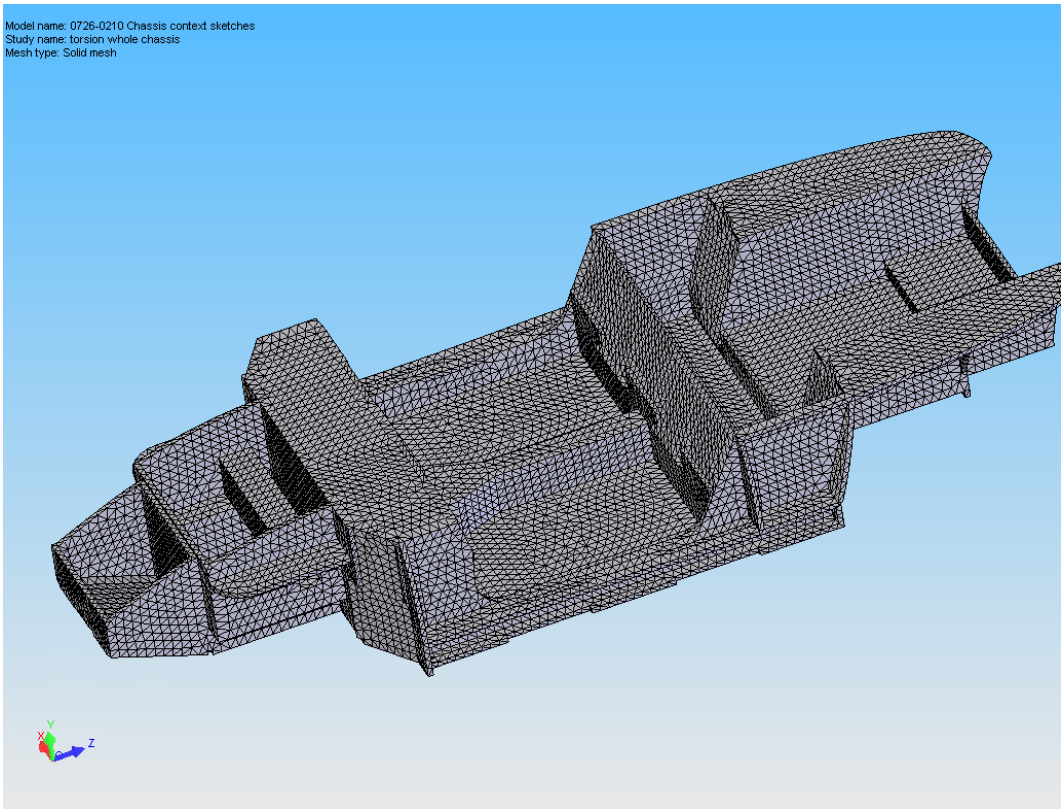

Figure 3.14 An FEA mesh of the Ultracommuter chassis

The FEA analysis was performed by modelling the aluminium honeycomb as solid aluminium with solid instead of bonded joints. This meant the loads applied in the analysis were different to the loads the chassis would actually be subjected to. The analysis for the chassis involved identifying areas of high stress for the model and identifying if this area would be weak or not due to the loading and direction of load on the joint as different joints can handle different sized loads. The CAD model of the chassis required many hours of static FEA analysis. After the analysis had run, small changes were made to the design to minimise stress concentrations.

The two main static loading scenarios analysed were torsion and bending, with a small amount of static analysis undertaken on frontal forces. Torsion analysis was performed by applying loads upwards to the panels where the suspension was attached. The opposing end of the car would then have all panels having suspension attached restrained. This simulates a vehicle with occupants going around a corner at high speed and one front corner of the chassis having to carry a

larger amount of force as the momentum of the vehicle is changed. Bending analysis was performed by restraining either end of the chassis and applying an upwards force at the other end, or restraining both ends of the car and applying forces within the middle of the chassis to simulate the forces the masses of occupants and batteries would create.

3.6.4 Design

To create the best ride handling and comfort, a chassis needs to be very stiff and strong and this can be difficult when there is no top to the chassis as it reduces the chassis's second moment of area and therefore significantly affects the chassis stiffness. There was no top for the **Ultra**commuter chassis due to the honeycomb not being suitable for curved areas, thus the chassis was designed from the outset to be topless. A roll hoop was to be used to support the bodyshell and increase the chassis stiffness. The body shell's low roof meant there was little space for the honeycomb to fit, and the bodyshell had continuous 3D curves which the honeycomb could not fit to. An example of how the rigidity of a vehicle can change with the removal of the roof is research undertaken by (Masini, Taraborrelli, Pivetti, & Feraboli, 2004) where it was found removal of the roof of the Lamborghini Murciélago coupe reduced torsional stiffness by 50%.

The constraints and specifications had to be adhered to create a successfully integrated, high performance chassis. Creating a well integrated chassis within these limits was the main research and development area of this project.

As there are currently no vehicle chassis constructed primarily from honeycomb, inspiration and design ideas were gained from composite chassis cars such as the McLaren F1, Lamborghini Murciélago and Koenigsegg CCR Supercars and aluminium chassis cars such as the Lotus Elise and Strathcarron. Much research was also conducted into the design and construction methods of many vehicles chassis and their latest advancements (Asnafi, Langstedt, Anderson, Ostergren, & Hakansson, 2000; Bak, Bartlett, & Hars, 1995; Brylawski & Lovins, 1999; Cole & Sherman, 1995; Corum, Battiste, Ruggles, & Ren, 2001; Cramer, Taggart, & Inc, 2002; Feraboli & Masini, 2004; GSV, 2005; Inagaki & Tanaka, 2002; Miller,

1996; Saito, Iwatsuki, Yasunaga, & Andoh, 2000; Tamaki, 1999; Yokota et al., 2002)

Suspension

Forces are transmitted from the suspension to the chassis from static and dynamic impacts. Therefore the suspension attachment points must be capable of preventing catastrophic failure, particularly at high speeds. Increased loading is placed on the suspension mounting points when hard braking and cornering occur simultaneously.

At rest, due to the static weight of the car, the front and rear shock absorber mounts will have 1230N and 1770N of force acting on them respectively. This force is from the static weight of the car. Vehicle manufacturers include a factor of safety of 2.5 - 3.0 to account for the increased forces under dynamic loading (Happian-Smith, 2001).

For the **Ultra**commuter, load paths were created to transfer forces from the suspension as directly as possible to minimise chassis flex. A front strut brace was attached between the two front shock mounts, which stiffens the front of the chassis by creating direct load paths between the two shock absorber mounts (Figure 3.15). This minimises chassis flex as the forces are being transferred through the strut brace, not through the chassis. Strut braces were also placed across the rear upper wishbone mounts. The rear shock mount utilised the roll hoop as a strut brace.

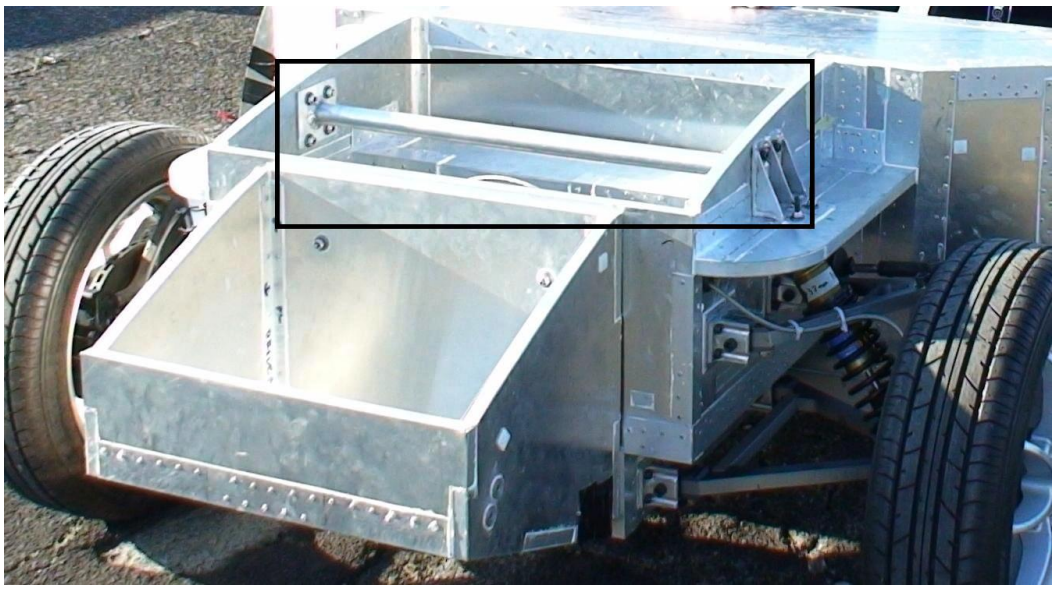

Figure 3.15 The front strut brace connecting the two front shock absorbers

Sufficient clearance between the suspension mount and other parts of the chassis was essential to enable bolts to be inserted and nuts tightened. The suspension needed to clear the chassis at all times. At the rear of the chassis, the floor had to be raised 20mm to prevent the lower wishbones impacting on the chassis in the event the suspension was fully compressed. The front corner of the cockpit was required to be angled to allow for clearance of the wheel during cornering. The angle creates a stronger design as it makes a smoother load path, front to rear. Occupant safety increases in the event of a frontal impact because the tyre will get deflected outwards, away from the occupant.

The final rear shock absorber placement was not finalised until all of the rear suspension had been attached to the chassis. This was due to tight clearances between the wheel and suspension components. Leaving this mount until after initial assembly meant there would be no problems of components fouling.

Steering

To keep the correct steering geometry the steering rack must be correctly placed. This is due to the front wheels travelling along different radius curves. This can be seen in Figure 3.16 by the different angles the front wheels are turning during the

turn. These differences in angle are called Ackermann geometry. If the front wheels do not have the correct geometry, such as both wheels turn at the same angle one tyre will scuff, wasting energy and wearing tyres prematurely. The geometry of the steering was modified by moving the steering rack fore and aft until the correct geometry was obtained.

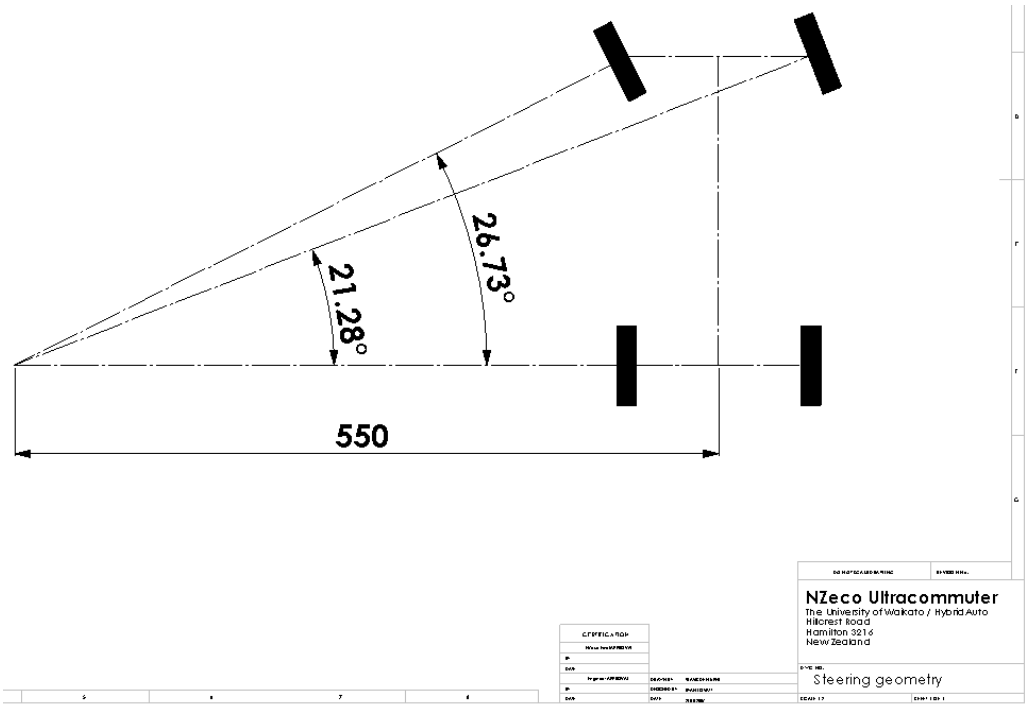

Figure 3.16 Ackermann steering geometry

To avoid bump steer the inboard pivot points were placed in line with the top wishbone pivot (Figure 3.17). This prevented the steering geometry changing as the wishbones move up or down. This is only true when driving in a straight line, not during cornering.

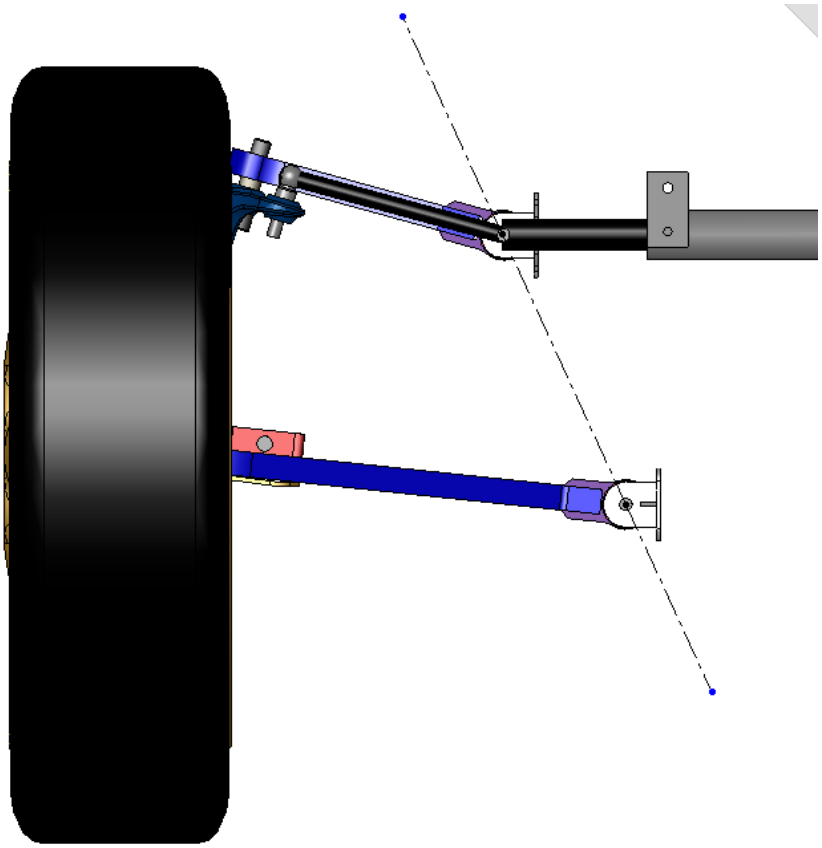

Figure 3.17 Steering pivot points

The steering column placement needed to be correct so the steering wheel would be central to the driver and within easy reach while the angle between either of the two universal joints did not exceed 30^{o}. The steering column required a “dog leg” in between it and the steering rack for safety. If the occupant were to contact on the steering wheel from an impact, the steering column would move sideways and not be rigid due to the dog leg thus preventing injury.

Bodyshell

The aerodynamic body shell envelopes the entire car including under body. This meant the chassis had to be designed to very tight tolerances to ensure that all available space was used yet no part of the chassis or suspension protruded beyond the body shell. The body shell curves upwards towards the rear of the vehicle and in order to accommodate the lower rear suspension components and mounting points the rear of the chassis had to be sloped like the bodyshell or stepped.

Another issue was the minimal occupant head room, whereby the occupant fore and aft position was predetermined. Limited available headroom meant the vehicle occupants had to be placed towards the centre of the vehicle (Figure 3.18). The roof height increased towards the highest point at the middle of the bodyshell. The ergonomics of the occupants within the vehicle was affected by their position. The egress of the occupant was also a contributing factor as many lightweight vehicles tend to have high sides to achieve a stiff chassis. The occupant has to step over the side of the car making entry and egress difficult. With the **Ultra**commuter bodyshell design incorporating a roof that dictated entry and egress ergonomics, the sides of the chassis had to be lower than comparative lightweight chassis'.

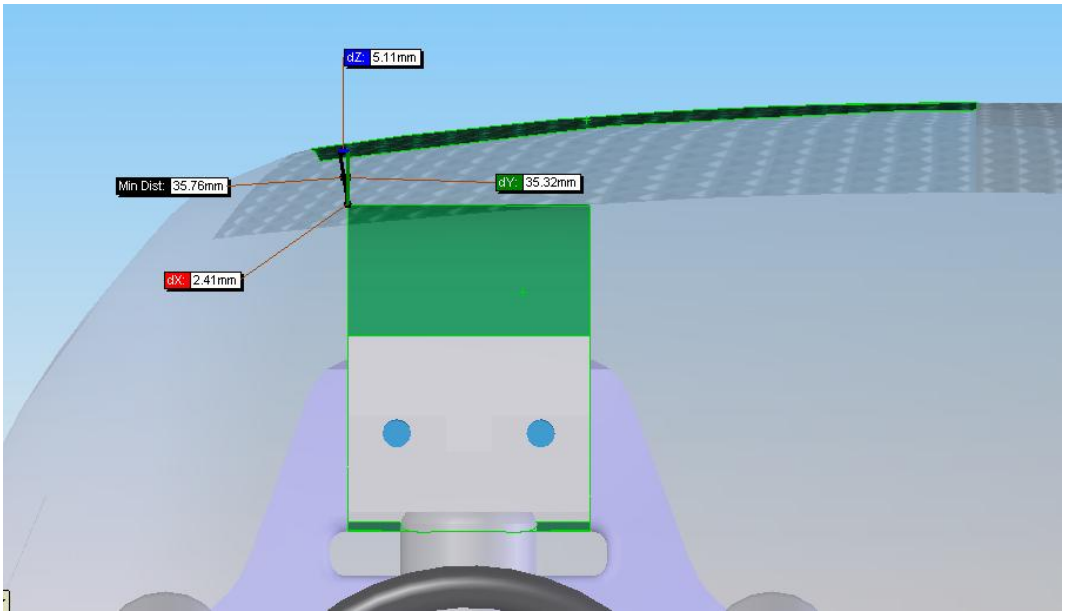

Figure 3.18 An Illustration of the limited occupant headroom in the Ultracommuter.

Batteries

The batteries used for the car were not confirmed until quite late in the chassis design therefore the chassis could not be accurately analysed early on in the design process. Batteries size, weight and placement had to be estimated until the batteries were finalised. For the benefit of weight distribution, placing the batteries near the front of the vehicle would result in improved handling and performance but this had to be weighed up against the need to place the batteries near the rear of the car so they were close to the motor controllers and motors. Therefore there would be no need for long high voltage cables which could become hazardous in the event of an accident and also reduced electrical power losses. The batteries had to be exchanged so easy access was required. As the batteries were the single largest mass onboard the car, it is beneficial to get them mounted as low as possible as this makes the car more stable during cornering by lowering the centre of mass.

Ergonomics

With the occupant position fore and aft constrained along with the suspension mounting points, the firewall and frontal chassis design needed to incorporate as much length for the occupant as possible (Figure 3.19). Using the human model in the CAD design, the cockpit was able to be extended to maximise available space for the occupant while retaining room for the lower suspension wishbones.

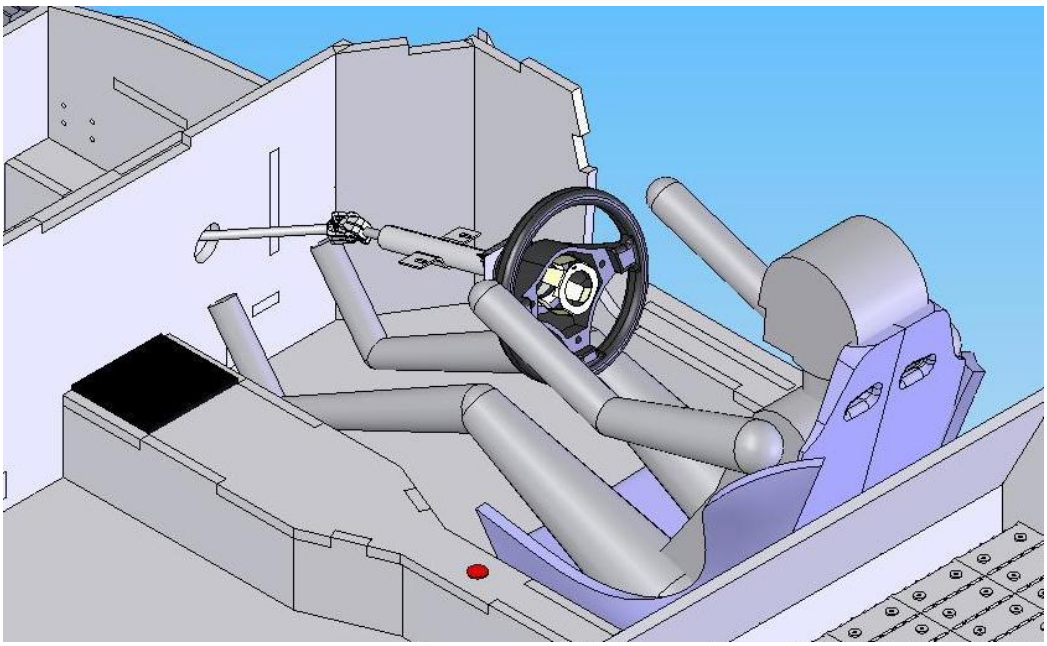

Figure 3.19 The Human model in the cockpit with their feet very close to firewall.

General

While flat floors can be advantageous for increasing free space within the cockpit, (Masini, Taraborrelli, Pivetti, & Feraboli, 2004) found that to increase the stiffness of a topless vehicle the central tunnel and side beams needed to be increased in size compared to a roofed vehicle to get comparable torsional stiffness. The central tunnel also serves as a place to mount switches and monitoring equipment. The side beams of the Murciélago coupe were reinforced to increase stiffness and act to create better front-to-rear flow of energy (Figure 3.20) (Masini, Taraborrelli, Pivetti, & Feraboli, 2004). Early in the design, beams were included along the side of the chassis. An increase of 7% torsional rigidity was gained for an insignificant increase in weight.

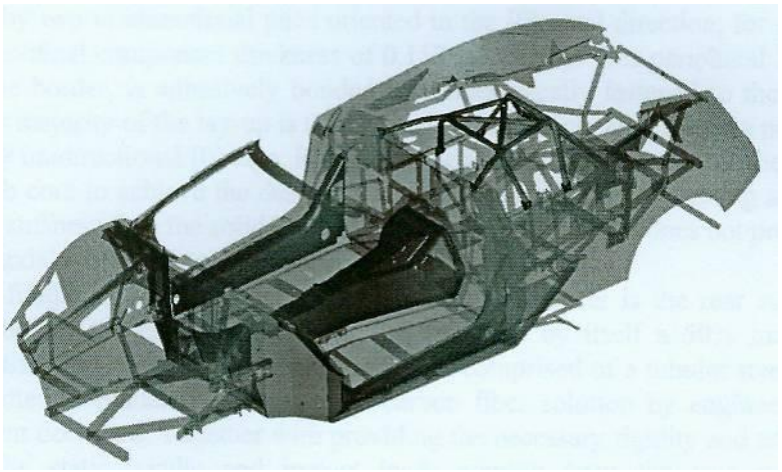

Figure 3.20 The Lamborghini Murciélago coupe. Darkened areas indicate the areas where reinforcement was required to stiffen the coupe. (Masini, Taraborrelli, Pivetti, & Feraboli, 2004)

The **Ultra**commuter chassis was designed using an interlocking technique. This technique uses finger and butt joints commonly used in carpentry to strengthen corner joints. This technique resulted in a 3D jigsaw type construction that was strong and stiff. The loading of the box combing and butt joints are varied due to their different configurations. Box combing was the most common joint used in the chassis as it is the strongest. This is due to the interlocking nature and its ability to transfer forces effectively.

Due to there being no roof structure, a roll hoop was incorporated into the design. It is designed to protect occupants in the event of a roll over. The roll hoop also transfers forces between the rear of the cockpit and the rear suspension. This is ideal due to the inherent weakness of the chassis as it steps upwards behind the batteries. The roll hoop takes forces from the rear shock absorber and transfers them to the cockpit, or if the front half of the body shell is on, through the windscreen support to the dashboard. The dashboard is a structural component of the car and is designed to transfer torsional and bending forces back through the car.

Designing for a low COM was not difficult as the low body height dictated that the majority of components must be mounted low. The lower the mass of components, the lower the COM, creating a stable car that is less prone to body roll. A low COM creates less body roll because the distance from the road to the COM results in a lower roll moment.

Lateral loading can be determined by using (4) (Happian-Smith, 2001). This equation gives the condition that the resultant of the centripetal force and the weight of the vehicle passes outside the inner wheel contact patch (Happian-Smith, 2001).

$$\frac{MV^2}{R}h = Mg\frac{t}{2} \qquad \textbf{(}4\text{)}$$

V = velocity

R = Radius of the bend

t = track width = 1.4m

h = height of COM = 0.512m

Simplifying (4) gives (5).

$$\text{Lateral Acceleration} = \frac{V^2}{R} = \frac{gt}{2h} = \frac{g*1.4}{2*.512} = 1.37g \qquad (5)$$

Therefore, with a track of 1.4m and a COM height of 0.512m (conventional cars are approximately 0.52m (Happian-Smith, 2001)), a theoretical maximum lateral acceleration before roll over occurs is 1.37g, which is slightly lower than a conventional cars average of 1.42g. This is primarily due to the reduced track of the **Ultra**commuter as the COM is very similar to a conventional car. The limiting factor is that tyres can only withstand maximum side forces of maximum of approximately 0.75g (Happian-Smith, 2001).

Beams were placed at the front of the chassis near the front suspension to increase stiffness and give more support to the honeycomb (Figure 3.21). The beam also acts as a crumple zone in the event of a frontal impact. While it is not ideal to have integral beams because if there were an impact, the chassis would be very hard to repair, it would be easier and more accurate on this prototype vehicle to make a new chassis than try to repair the damage. The beams also transfer closer to the central tunnel than if the beams were not used, which aids in transferring of forces.

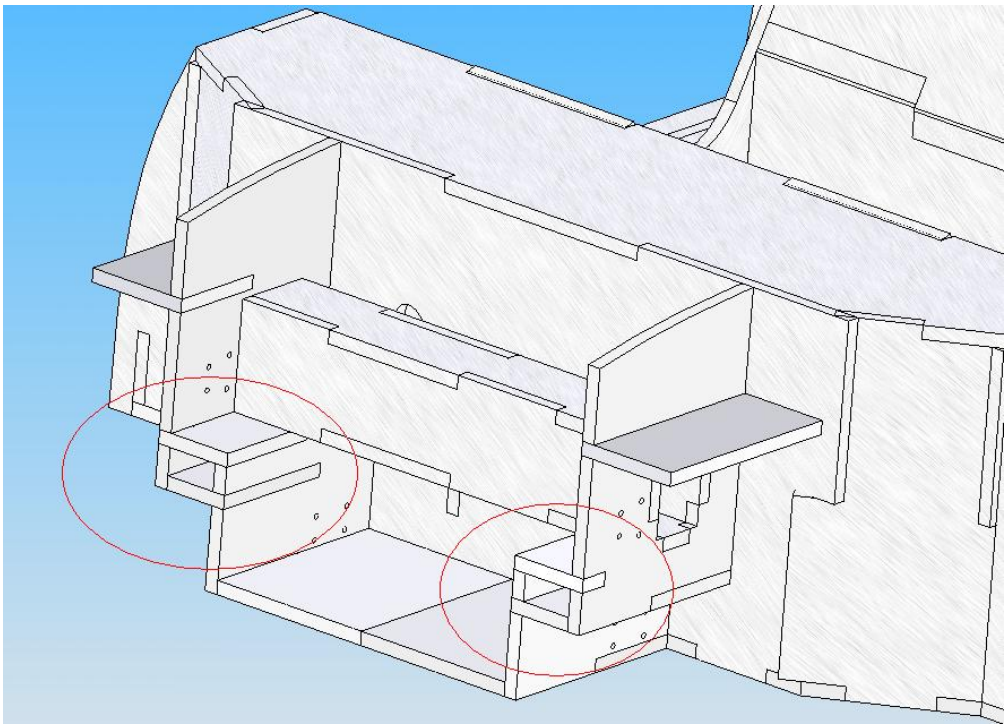

Figure 3.21 A sectioned view of the front of the Ultracommuter chassis showing the inbuilt frontal beams.

The bending forces on the **Ultra**commuter chassis were found to be comparable to a conventional car (Figure 3.22, Figure 3.23). The main differences are the increased forces from rear seat passengers, although this could be compared to the batteries; and there being no engine or transmission forces at the front of the chassis. The maximum shear forces the chassis would be subjected to were calculated (Figure 3.24) and compared conventional cars (Figure 3.25). As can be seen in the figures, the maximum shear force in the **Ultra**commuter is less than half that of a conventional car.

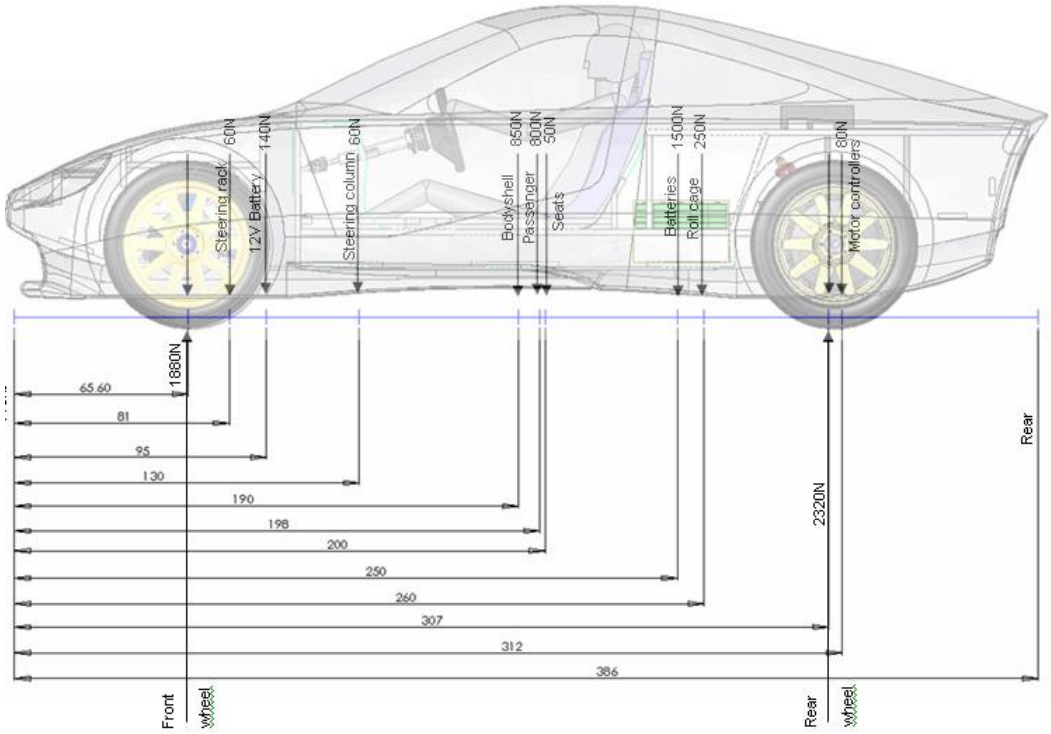

Figure 3.22 The Ultracommuter bending force diagram

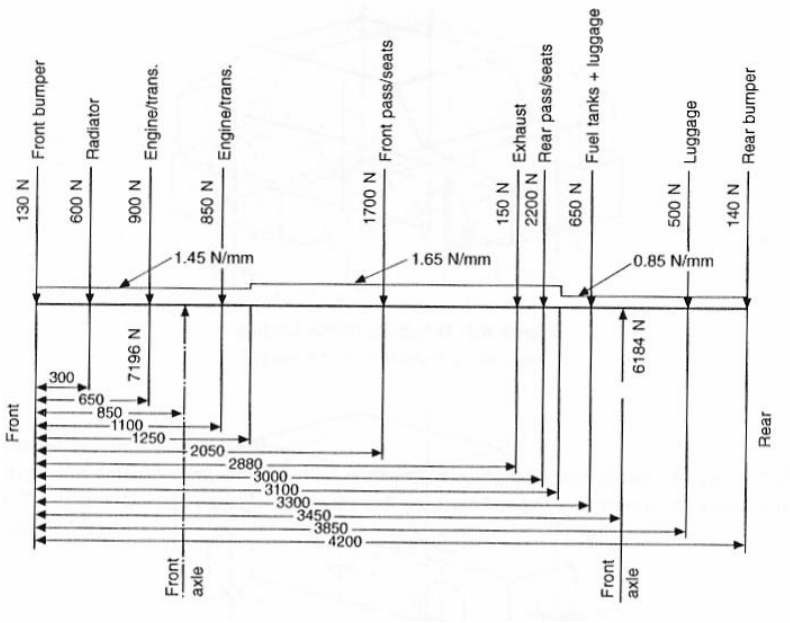

Figure 3.23 Bending force diagram for a passenger vehicle (Happian-Smith, 2001)

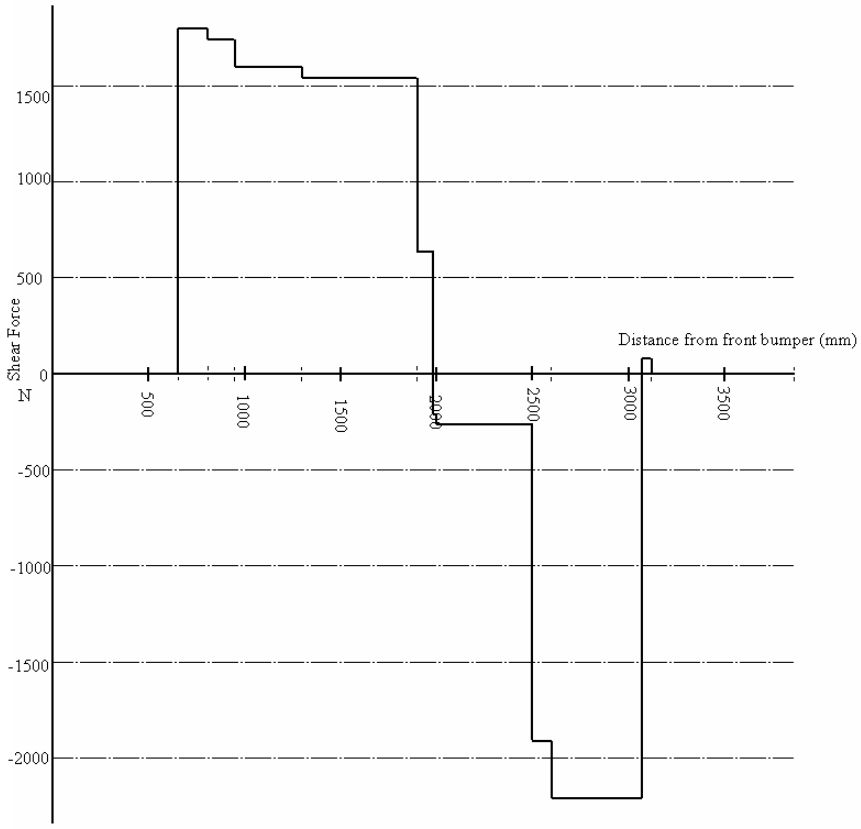

Figure 3.24 Ultracommuter Shear force diagram

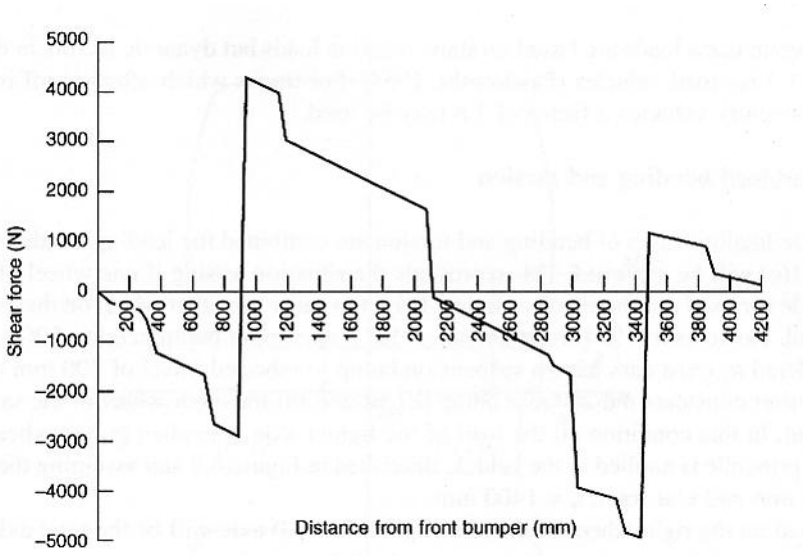

Figure 3.25 Passenger car shear force diagrams (Happian-Smith, 2001)

The chassis was designed as if it were to go into low volume production; therefore it had to be designed to be low cost, simple, strong and good quality. Finding this balance has proved to be difficult.

Developments

Developments began by deciding to use different components from the 2006 Chassis seen in Figure 3.1. With the 2006 Chassis as a basis, the new chassis is designed with more room and ease of manufacture.

Developments continued with most changes aimed at extending the chassis to the bodyshell. The chassis seen in Figure 3.26 and Figure 3.27 were the earliest developments. It includes reversed rear top wishbone mounts to bring the pivot points closer to the chassis, a large flat boot, a central console and an angled dash. The reversed rear suspension mounts were rejected due to the honeycomb being weakened by the required holes. The Large flat boot was an improvement over the 2006 chassis which had very little luggage space. The central console was added for further stiffening. The Angled dash was later reversed as it was considered safer for the occupants in the case of impact.

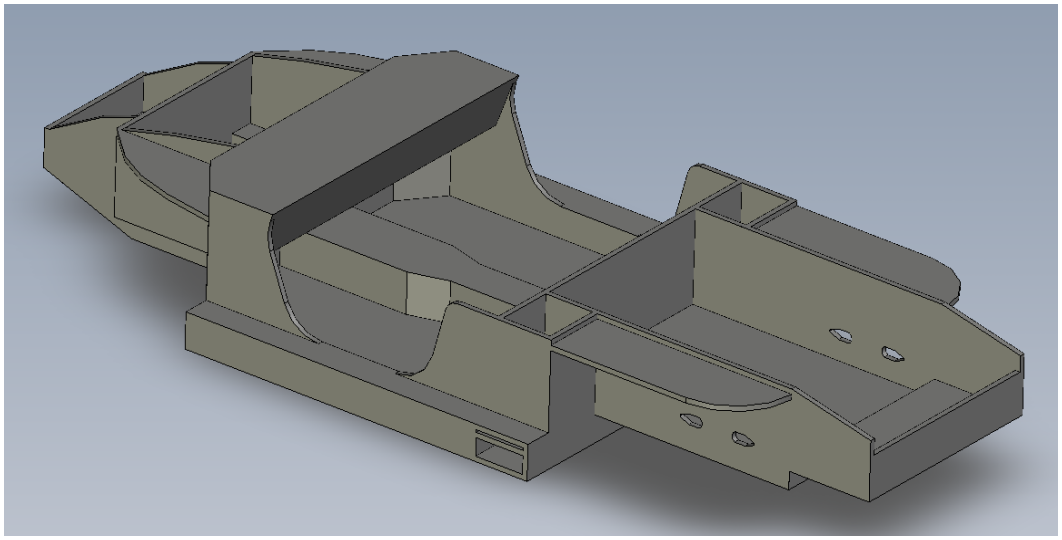

Figure 3.26 The Ultracommuter chassis - 8 Feb 07

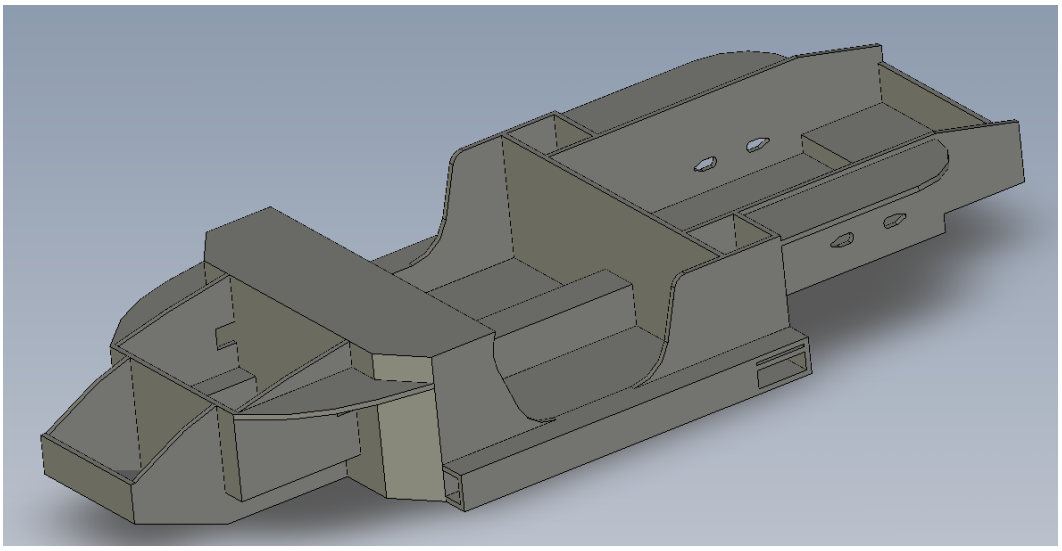

Figure 3.27 The Ultracommuter chassis - 8 Feb 07

The next developments involved creating enough space in the car to house the batteries. The batteries were placed behind the driver, but their layout and placement has varied as different positions were investigated. In Figure 3.28 the batteries are installed behind the driver, but access to them is restricted by the beam placed behind the dividing wall. There was also a design concept where the batteries could be exchanged through a hole in the bottom of the car, but this was not adopted because of the added complexities it brought into the chassis design. The steering rack was chosen, and thus a beam was created in front of the dash to house it. The dash slope has been reversed from previous designs. There are

hollow vertical beams behind and to the side of the driver. These were designed to aid front-to-rear flow, but they used space ineffectively and in later designs were removed and the batteries moved further forward.

An investigation into using a double skin on the bottom of the chassis to house the batteries was undertaken but due to the low headroom available, it was found there would not be sufficient room for an average human to be seated comfortably. Creating a double skin on the bottom of the chassis would significantly improve stiffness increasing the I-value of the base of the chassis. The COM would also be lowered.

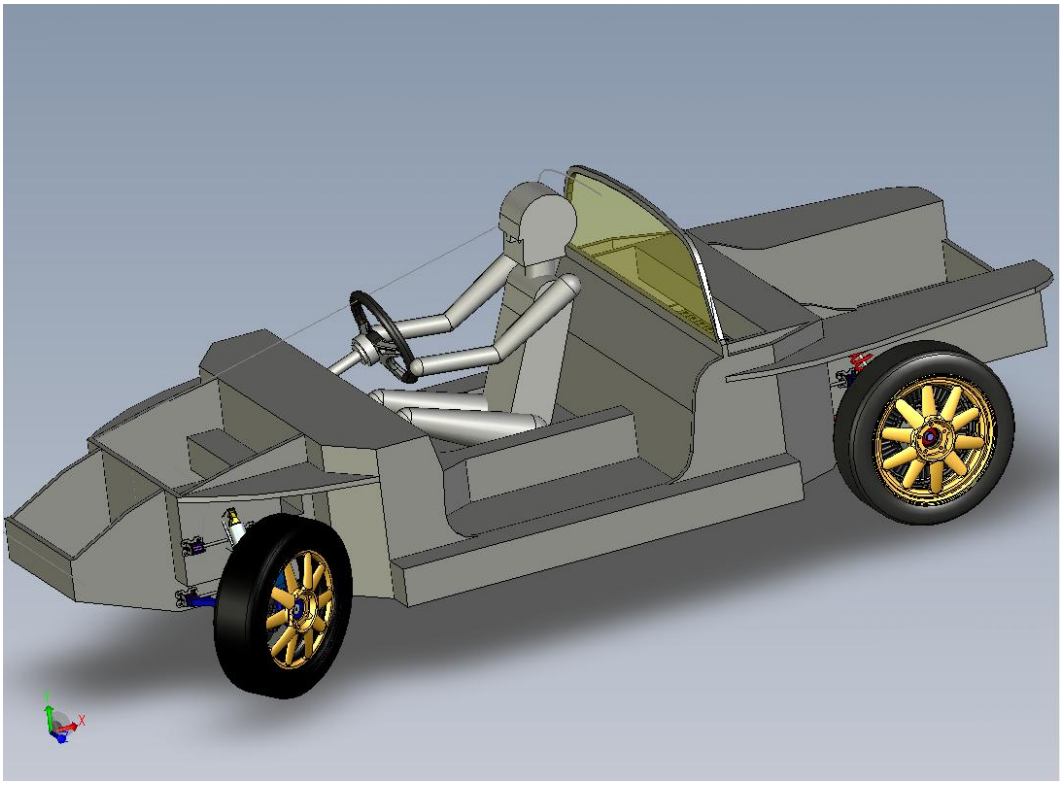

Figure 3.28 Chassis version 15 Feb 07– drawn as a solid model

3.6.5 The Final Design

The final chassis design consists of four main areas, the front, cockpit, battery compartment and the rear. The chassis design is simple and uses space effectively (Figure 3.29).

There are 118mm x 80mm beams running forward from the front firewall and 140mm x 80mm beams running down the sides of the cockpit. The sides are 140mm high, permitting relatively easy egress. The side beams provide the strength through the centre of the chassis as the doors are non-structural, therefore the side beams are designed to provide strength and safety protection. The floor is constructed from aluminium honeycomb panels and can also absorb impact energy, unlike steel bodied cars where the floor is not used for this. The centre console houses monitoring equipment and switches and also stiffens the chassis. The suspension and steering mount holes were cut accurately during waterjet cutting of the aluminium honeycomb to ensure correct geometry.

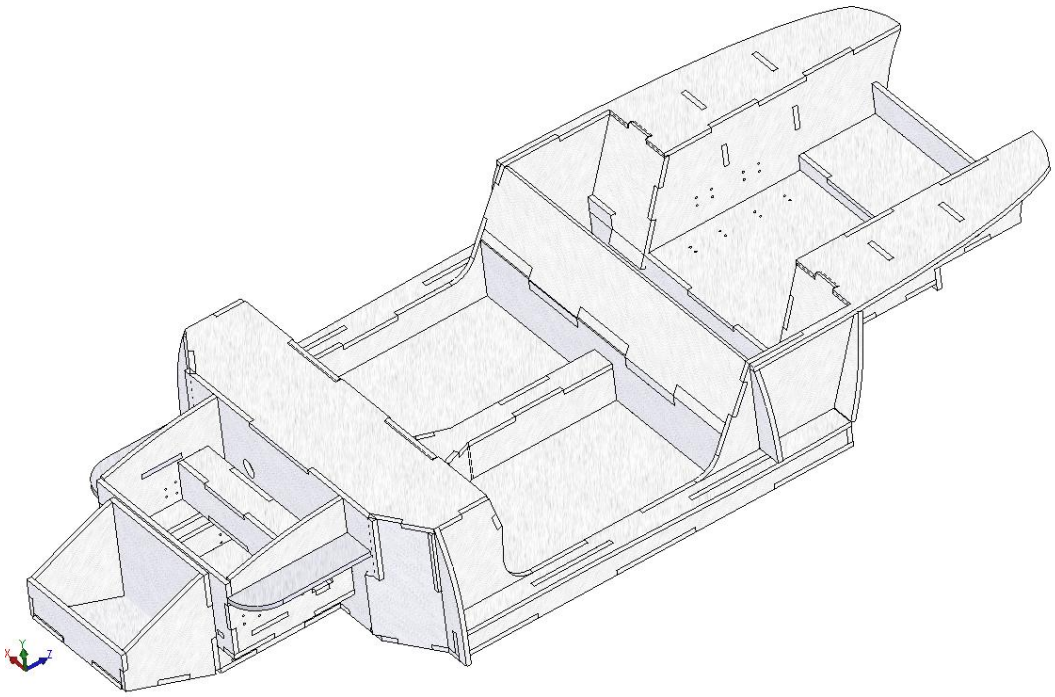

Figure 3.29 The final Ultracommuter chassis

The batteries were placed behind the driver at floor level. The batteries can be seen just behind and below the driver in Figure 3.30. The battery placement kept weight low and as far forward as possible.

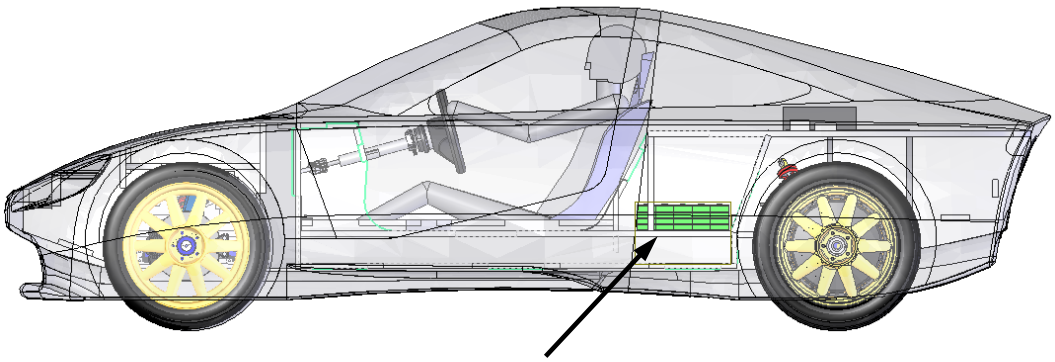

Figure 3.30 Final battery and driver placement

The COM of the **Ultra**commuter was positioned near the centre of the occupant Figure 3.31, creating a 45:55 (front:rear) weight distribution. The COM height is similar to a conventional car. The final driver position is a compromise between headroom, leg room and battery positioning and is shown in Figure 3.30.

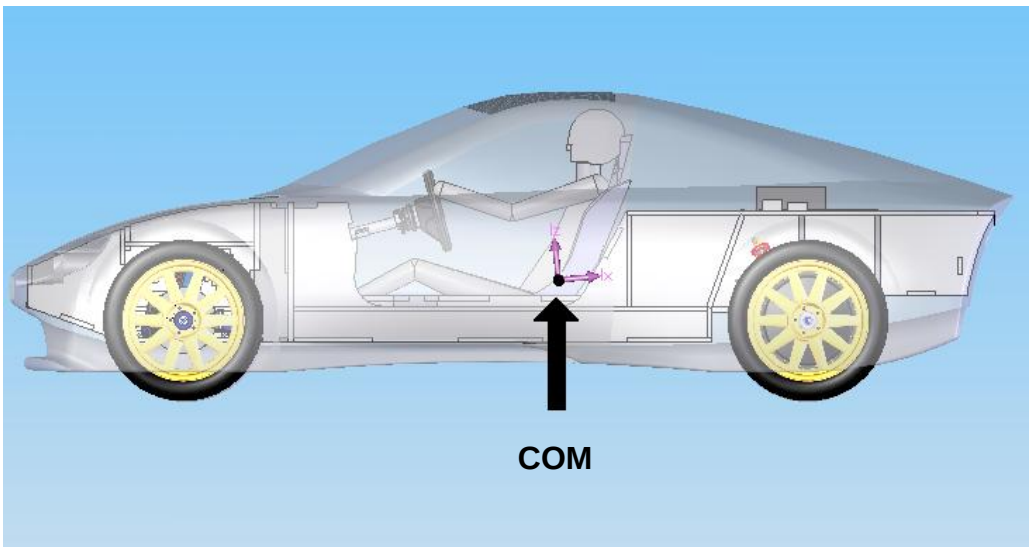

Figure 3.31 COM of the Ultracommuter

The front crumple zone consists of a 390mm high x 380mm long x 535mm wide box that can be filled with an absorbent material such as high density foam to absorb energy in a frontal impact. The box is itself an impact energy absorber as it is constructed from aluminium honeycomb.

A tubular box constructed from aluminium honeycomb was designed into the chassis to house the steering rack. The box was created as there were no mounting

points to mount the steering rack. It also creates a direct load path joining the sides.

The rear suspension lower wishbone mounts are situated 20mm below the bottom of the chassis to avoid the chassis fouling the suspension or bodyshell (Figure 3.32). Aluminium honeycomb is used for the spacers with a longer ‘top hat’ going through both layers of aluminium honeycomb.

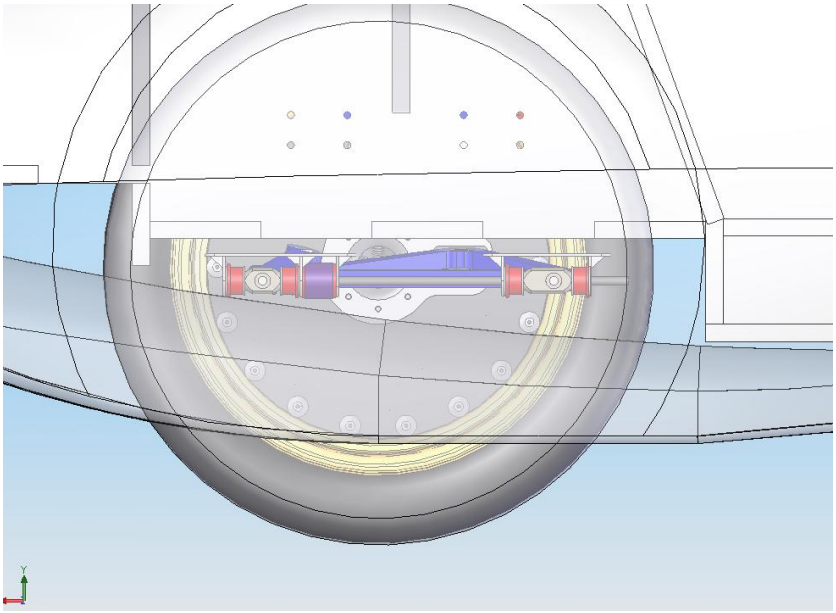

Figure 3.32 Rear suspension lower wishbone suspension mounting

The rear shock absorber is mounted into a corner of the chassis and is directly connected to the roll hoop to transfer the shock absorber loads.

Chapter 4 Manufacture

4.1 Introduction

The manufacture of the chassis needed to be simple to minimise the required labour skills and as low cost as possible due to the limited funds available. The aluminium honeycomb panels were cut to shape using a CNC waterjet cutter. The panels were then assembled, bonded and riveted in place.

The many parts of the chassis were drawn as 2D shapes nested within a flat sheet the size of the aluminium honeycomb. This process was relatively straightforward due to the chassis being drawn in context. The individual parts were placed onto 6 sheets of honeycomb and the resulting 2D figure could be converted to a drawing and the required file formats for the waterjet cutting.

4.2 Water jet cutting

An automated process was used to cut the aluminium honeycomb as it is more efficient than cutting the aluminium honeycomb manually. An automated process can also produce the required accuracy allowing the numerous parts to fit together after the removal of burrs. The process has a faster production line than manually cutting the parts due to the large part count and the accuracy required. It also eliminates the tendency for errors occurring when manual processes are used, reducing material wastage. The cut aluminium honeycomb sheets returned virtually scratch free. It would have been very difficult to achieve this manually.

Waterjet cutting was chosen to cut the honeycomb as opposed to laser cutting or CNC milling due to the varying cross material thickness as the honeycomb panel was cut.

The water jet cutter had an accuracy of ±0.1mm and was located at Aquacut2000 Ltd in Auckland. 2D CAD files (Figure 4.1, Figure 4.2) were provided with the chassis part patterns and subsequently programmed into the machine using CAM

software to control the movements of the cutter. The water jet cutting proved to be accurate and with the finished parts requiring minimal finishing (Figure 4.3).

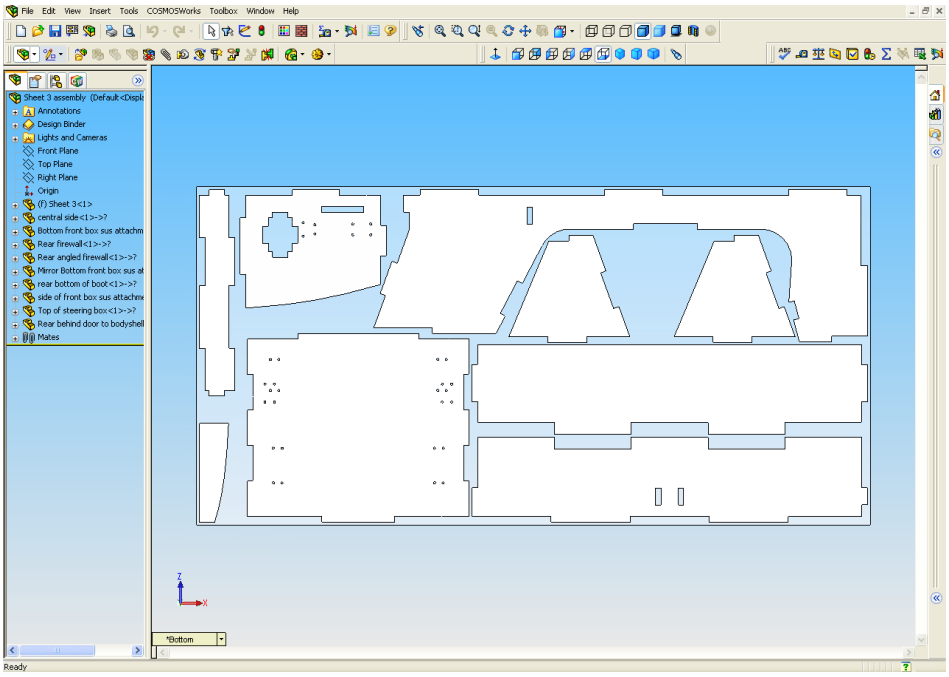

Figure 4.1 Chassis parts placed onto a sheet

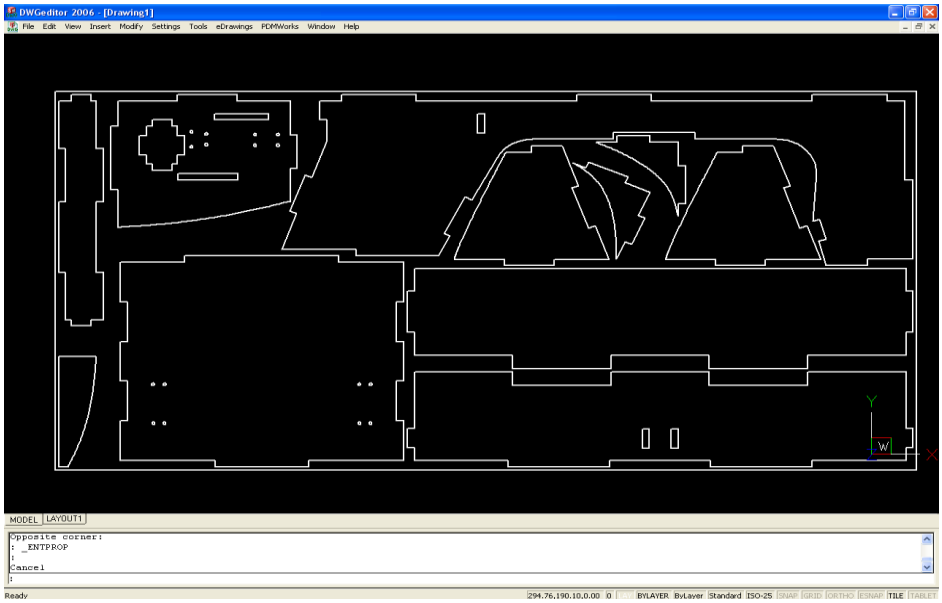

Figure 4.2 Chassis parts converted to 2D drawing

Figure 4.3 Aluminium honeycomb sandwich panel cut by waterjet

As there were some joints requiring non-perpendicular angled edges, they were created manually using a file or hacksaw.

The aluminium surfaces were prepared for bonding by scouring with 200grit sandpaper to create a surface the adhesive could readily key to. The surfaces were then wiped with acetone to remove contaminants. The aluminium needed to be clean to maximise the achievable bond strength.

4.3 Construction

Riveting

3.2mm Aluminium Steel rivets were used to attach parts to the aluminium honeycomb. The rivets served as fasteners to pull the aluminium honeycomb and the part to be bonded together and to keep them positioned.

Holes for the rivets were predrilled before cleaning to keep swarf and contamination away from the joint. The rivets were attached using a hand riveter or an air driven riveter.

Bonding

HPR25 toughened epoxy adhesive supplied by Adhesive Technologies was used to bond the aluminium together. HPR25 adhesive was designed for bonding aluminium sheets to low density cores, so this adhesive was deemed appropriate for this application. The failure stress under shear loading for the adhesive is given as 15.9MPa when tested to ASTM D1002 (Adhesive Technologies NZ, 2007). The HPR25 adhesive has a working time of 45 minutes with a full cure taking 7 days.

Toughened epoxy has small rubbery inclusions which act to reduce crack propagation and movement. This is a requirement of the adhesive due to the loading environments where small impacts are common and by using toughened epoxy, the adhesive will flex small amounts but not crack.

The thickness of the adhesive layer can affect the bond strength. From Figure 4.4, the general adhesive thickness for best shear strength is less than 0.6mm. This was accomplished by securing components using rivets.

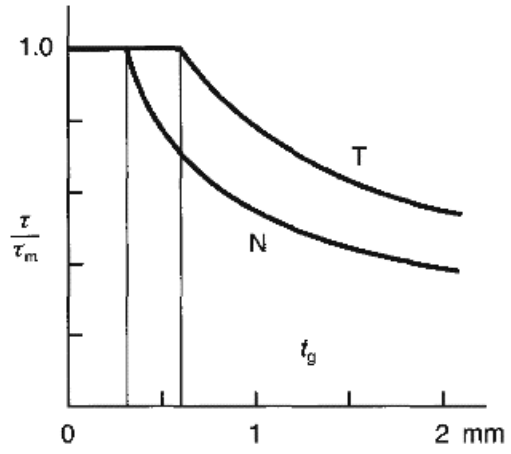

Figure 4.4 The effect of glue thickness on shear strength of adhesive (N=non-toughened, T= Toughened) (Dwight, 1998)

Surface pretreatment	Adhesive	Cure conditions	Lap-shear (psi)	strength (MPa)
Vapor degrease	EA-9309[b]	60 min [180 °F(82 °C)]	3400	23.43
Aloxite 60 abrade	EA-9309	60 min [180 °F(82 °C)]	5000	34.45
HCl etching with paste for 2 min at RT	EA-9309	60 min [180 °F(82 °C)]	5100	35.14
Vapor degrease	EA-9320[b]	60 min [180 °F(82 °C)]	3090	21.29
Aloxite 60 abrade	EA-9320	60 min [180 °F(82 °C)]	4380	30.18
HCl etching	EA-9320	60 min [180 °F(82 °C)]	5800	39.96
Vapor degrease	EA-9320	7 da at R.T.	2320	15.98
Aloxite 60 abrade	EA-9320	7 da at R.T.	4100	28.25
HCl etching	EA-9320	7 da at R.T.	5620	38.72

[a]All joints fabricated with 0.125 in (3.18 mm) 6061–T6 aluminum.
[b]Both adhesives are products of Hysol and are two-part epoxies formulated for high-strength applications demanding flexibility without the need for special heat-curing. EA–9309 has a T-peel of 42 pli (7355.3 N/m), whereas EA–9320 has a floating drum peel of 55 pli (9632 N/m)

Figure 4.5 Bond strength of adhesive joints after changing the surface pre-treatments (Dwight, 1998).

Bonding of aluminium requires a strong bond between the adhesive and the aluminium oxide. Aluminium oxide forms nearly instantaneously on exposed aluminium. Adhesives do not bond with metal atoms (Minford, 1993). The aluminium oxide layer can be removed or changed to improve bond strength to another compound through the use of etching. Etching was unsuitable for use in the chassis due to the time required, variety of chemicals and the unsuitability with the honeycomb. Abrading with sandpaper produced satisfactory results and can be confirmed by other research performed (figure 4.5) (Aloxite 60 Abrade is a synthetic aluminium abrasive sandpaper). (Minford, 1993)

The use of adhesives has meant joints are stronger because there is a larger surface area for bonding. This creates larger surfaces to transfer forces and leads to uniform stress distribution (Braess & Seiffert, 2005). Material can be of a lighter gauge as there is no welding which can weaken joints because of the heat affected zone (Braess & Seiffert, 2005) and thus must be compensated for by larger wall thickness material (Wan, 1998-2000). Less than 4kg of adhesive was used in the construction of the chassis. Glue usage was minimised to decrease chassis mass.

The outside and inside of right angle joints were reinforced using extruded equal angle aluminium (20mm x 1.6mm and 30mm x 1.6mm). Non-perpendicular joints were reinforced with aluminium sheet folded to the correct angle. Flat butt joints were reinforced with 40mm x 3mm flat bar. All of the reinforcement was riveted and bonded to the aluminium honeycomb panel.

4.4 Finishing

Extruded aluminium bar was placed along exposed edges of the honeycomb to protect the exposed core from debris and to cover sharp edges. They also support the two facings and ensured they did not delaminate from the core or the edges. The edging prevented damage from localised loading on the edges as the aluminium honeycomb panels had reduced load carrying capacity near its edges.

The edging used was 19.05mm x 2.64mm aluminium bar with the edges sanded off to reduce the width to below 19mm. The core was cut away from near the edge so the bar could fit between the faces with no distortion to the faces.

Bracing was placed across areas where weaknesses were identified. These key areas were between the top rear wishbone mounts to stiffen and strengthen the rear suspension, particularly since there would be more forces generated through the suspension due to the ‘in-wheel’ motor. A brace was also placed across the front of the chassis between the two shock mounts to stiffen the chassis and transfer loadings.

4.5 Top-hats

Tophats were used in the honeycomb for attaching load bearing components. The use of tophats meant the load being applied to the chassis would be distributed over a large area. They also incorporate their own crush tube, required for attaching components to areas with hollow or minimal transverse load carrying capacity to prevent the loaded surface from buckling (Figure 4.6).

Figure 4.6 Tophats installed onto the chassis

Tophats have been used as an attachment method for the chassis as standard bolts will crush the honeycomb core as the bolt is tightened. The tophats are glued into position and they distribute the point load from the bolt across a larger area, resulting in a lower stress concentrations and a lower chance of honeycomb failure.

The ‘top-hat’s were machined from aluminium that, according to (Camanho & Matthews, 2000) is more suitable for inserts than steel especially when the ‘top-hat’ has a small wall thickness. This is due to adhesive failure occurring before carbon fibre reinforced plastic laminate failure when a thick stiff insert is used because the loading mechanism for the adhesive changes from compression, for which adhesive is strong, to tension for which it is weak. The added benefit of aluminium is they are lighter than steel ones.

‘Top-hat’s were bonded to the honeycomb sandwich and a torque of 25Nm was applied by placing a bolt through the centre. The ‘top-hat’s were compression tested to ensure they would be able to withstand the forces they would experience

when in use. The ‘top-hat’ was subjected to 1700N before the honeycomb began to deform and the ‘top-hat’ delaminated. As there are four ‘top-hat’s per suspension mount, that means combined, they can withstand 6800N, or 693kg before failure. This is has proved to be sufficient strength for the suspension mountings.

4.6 Chassis testing

Testing of the chassis began with slow driving around the university car park (Figure 4.7). Initial speeds were kept low so the chassis and suspension could be checked while the car was in motion. Applied loads can be significantly different to static loads therefore this was a very important check. The low speeds also meant if there were to be any failures there would be less damage to the car and lower chances of driver injury. During the initial testing noises were heard coming from the front of the car. At first it was believed the noise was coming from the suspension mounts, but it later became clear the problem was in fact the chassis failing due to insufficient reinforcement along the aluminium honeycomb joints near the lower mounts. The damaged aluminium honeycomb was replaced and the front of the chassis was reinforced. The honeycomb had pulled away due to the large forces exerted on the suspension during braking and insufficient reinforcing near the suspension mount.

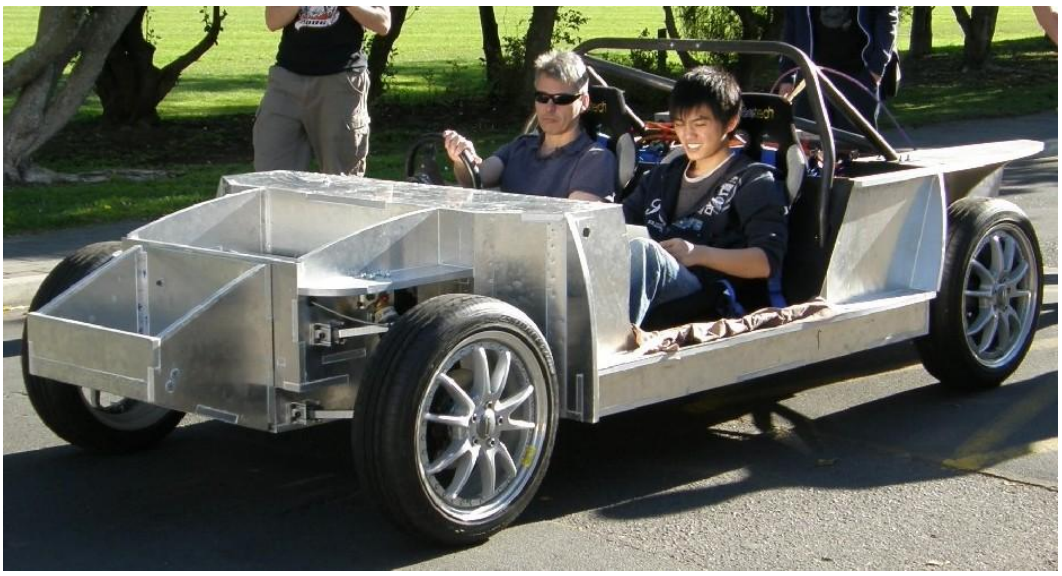

Figure 4.7 The first test drive of the car

The front wheels rubbed on the chassis during tight turning, but this was not significant and the area where the rubbing occurred was already reinforced with more aluminium. This did not present any problems during the WSC.

After the chassis was repaired, further testing was conducted at higher speeds (up to 75km/hr). Tests were also conducted through chicanes to test the chassis and suspension. After each short run, the chassis was inspected for any sign of failure but none was detected. The chassis performed well and proved to be stiff and strong enough.

Chapter 5 Economics

As part of this project, a budget was required to be adhered too as limited funds were available. For most items, sponsorship was first sought to lower the cost to the team. Many companies were willing to support the cause and gave us free-of-charge or discounted items. It was difficult to stick to the budget at times and restrict spending to what was required. A budget for the chassis design and construction can be seen below in Table 3.

Item	Supplier	Quantity	Cost	Total cost	Discount?
Aluminium honeycomb	Ayres composite panels	6	$375.00	$2,250.00	Yes
Rivets (box)	MSL	2	$30.00	$60.00	No
Waterjet cutting	Aquacut2000	1	$1,933.26	$1,933.26	No
Freight	DHL	1	$400.00	$400.00	No
Adhesive (4Kg)	Adhesive technologies	1	$120.00	$120.00	Yes
Aluminium flat bar	Ullrich aluinium	6	$12.00	$72.00	Yes
Aluminium angle	Ullrich aluminium	12	$14.00	$168.00	Yes
Top hats	Page Macrae Engineering	350	$0.00	$0.00	Yes
			Total	$5,003.26	

Table 3 Budget for Ultracommuter chassis

A brief timeline of the chassis design, construction and testing is presented below.

Chassis design began	-December 2006
Received Hybrid auto Suspension CAD	-1 February 2007
Drawings sent to waterjet cutters	-29 March 2007
Cut honeycomb collected	-19 April 2007
Chassis fully assembled	-12 June 2007
First test drive	-30 September 2007
Unveiling	-12 September 2007
Shipped to Australia	-21 September 2007
WSC	-21-28 October 2007

Chapter 6 Titanium aluminide properties for automotive applications

In relation to the automotive industry the most important properties of titanium alloys are their high strength to density ratio and corrosion resistance (Froes, Friedrich, Kiese, & Bergoint, 2004). The major challenge facing increased titanium use is the high raw material and processing costs. Applications for TiAl have been found with some large automobile manufacturers proving their reliability and technical viability however the factor preventing their use in mainstream automobiles is cost.

Producing near net shape (NNS) parts for TiAl components are preferred to material removal or shaping processes due to the high costs of titanium and processing difficulties. NNS produces less waste material because the component shape is close to the finished shape, only requiring minimal machining to get the component to fit within the required tolerances. TiAl components are difficult to process because of their very low ductility (~1%) and low fracture strength causing components to become damaged. TiAl is also difficult to machine, causing tools to wear fast due to increased cutting forces and higher interface temperatures. This can be minimised by high speed machining (up to 100,000rev/min) or slow machining. Grinding appears to be the best suited machining process with low tool wear rates (Mantle & Aspinwall, 2001).

Hot isostatic pressing (HIP) is a commonly used process to increase powder compact density and reduce porosity. HIP involves taking the compact (or component with a plasma coating) and applying pressure at high temperatures. The pressure is applied uniformly and equally to all surfaces. The compacts are usually placed inside a capsule with powder packed around it. Heat and pressure are then applied to the outside of the capsule which plastically deforms, transferring the heat and pressure to the surface of the component through the powder. HIP temperatures are generally ~1000 ^{o}C although this temperature varies depending on the desired microstructure. Successful forging of a HIP

compacted powder at 850 ^{o}C (lower than usual for TiAl) was performed by (Gerling, Schimansky, & Clemens, 2003) while retaining a very fine microstructure.

6.1 Manufacturing processes

The following processes are all NNS processes.

Powder Metallurgy (PM) involves taking powdered titanium and aluminium and placing it into a mould of the desired shape. The powder is then uniaxially pressed into shape inside the mould. This compacted powder is called a 'green' compact. It is called 'green' because it can only just hold itself together but has no mechanical strength. The green compact of TiAl is then reactive sintered. Reactive sintering involves heating the compact to a temperature above the melting point for titanium but below the melting point of aluminium. This creates molten aluminium, which flows between the titanium creating a nearly 100% dense product. Isostatic pressure can also be applied during this process, allowing the density to increase further. Disadvantages of PM are the component density will not be linear throughout the component and complex parts are unable to be produced. The outside faces of the component will be more dense due to the pressure acting on them but the middle of the component will not be as dense. PM parts cannot be complex shapes as there is a need to apply force to compact the powder and create the green compact while still allowing the compact to be taken out of the mould. Advantages of PM include very small amounts of machining, minimal scrap material, low cost and are suitable for mid-high production runs. PM was used to produce titanium valves for the Toyota Altezza (Froes, Friedrich, Kiese, & Bergoint, 2004).

Powder/metal injection moulding is similar to plastic injection moulding. The metal powder is mixed with a binder which is then injected into the die. This 'green' compact is then removed from the die and heated to remove the binder. The compact is then sintered to consolidate the powder. Metal injection moulding is able to produce components having properties similar to wrought materials with excellent dimensional accuracy. Metal injection moulding allows complex shaped

high volume components to be produced although components are generally below 250grams. (Gerling & Schimansky, 2002), produced a component using metal injection moulding that had a porosity of 3.8% after sintering with porosity reducing to 0.4% after a HIP treatment. A yield strength of 410MPa was achieved with 0.6% elongation.

Laser forming/sintering of TiAl components allows components to be produced directly from powder, resulting in time and cost savings. Laser forming involves utilising a laser to melt and consolidate powder to produce a prototype component. The component can be formed directly from a computer model. Microstructures of laser formed components are generally of fine, fully lamellar nature with tensile properties similar to extrusions and PM components. Laser forming is a useful Rapid Prototyping (RP) technique as it allows fast prototype manufacturing while having the same properties as the final product (Moll & McTiernan, 2000).

Coatings may be required to protect TiAl components from wear due to its low wear resistance. Nitriding and carburizing have been successfully used. Plasma nitriding of TiAl improved the wear resistance by up to a factor of ten and lowered the coefficient of friction by a third while reducing coefficient of friction fluctuation (Rastkar & Bell, 2002). (Tetsui, 1999) found carburizing or nitriding was sufficient to prevent wear of TiAl valves. Coatings of TiAlN are applied to machining tools in demanding situations due to its excellent wear resistance and hardness (Boonruanga, Thongtema, McNallanb, & Thongtem, 2004; Schwartz, 2002). The thickness of the coating has a large affect on wear life. TiN (titanium nitrate) coating on high speed steel was found to have an optimum coating thickness of 2-3μm for planning and 6μm for turning tools (Posti & Nieminen, 1989).

Plasma spraying involves introducing powder metal into a plasma jet, whereby the powder is propelled towards a substrate at extremely high temperatures and velocities. The powder (melted) splats onto the substrate and solidifies very quickly. The rapid solidification creates a very fine lamellar microstructure (~90nm). Slow traversing of the substrate by the plasma spray creates larger

grains due to the impacted material temperature not decreasing as fast due to hot splats landing near. (Khor, Murakoshi, Takahashi, & Sano, 1995) found increasing secondary gas pressure can result in lower porosity and reduction in unmelted particles. The increased pressure means molten droplets travel faster onto the substrate, spreading further than at the lower velocities. The samples they created were subjected to a HIP process after plasma spraying. The HIP process increased the hardness while decreasing the porosity. TiAlN can be produced by plasma spraying, simply by using nitrogen as the plasma gas. The nitrogen plasma gas reacts with the TiAl as it goes through the plasma jet.

LPPS (low pressure plasma spraying) is an alternative to conventional plasma spraying. Plasma spraying in atmospheric pressures cannot produce dense layers and is not suitable for formation of TiAl which consists of oxidizable elements. LPPS prevents oxidation of sprayed particles while having the flexibility to allow composite layers to be produced with a reactive gas (RLPPS) such as nitrogen. Fine γ grains are produced from this process. (K. Honda, Hirose, & Kobayashi, 1997) found TiAl plate had a hardness range of 241-175Hv across the temperature range of room temperature to 900 ^{o}C. Sprayed TiAl had Hv of 589 with 400Hv at 800 ^{o}C, dropping to 275Hv at 900 ^{o}C. This increased hardness over the plate is attributed to the fine grain size the LPPS sample has. The samples tensile strength of 400MPa is slightly higher than TiAl plate. Elongation of the plate and the LPPS sample was 1%. LPPS samples annealed for over 24hours had unchanged hardness values up to 700 ^{o}C, with the hardness decreasing to 350Hv at 900 ^{o}C. The annealed samples had a comparable tensile stress of 405MPa. (K. Honda, Hirose, & Kobayashi, 1997)

Electron beam and GTAW (Gas Tungsten Arc Welding) welding has been proven successful for joining and fixing Ti-48Al-2Cr-2Nb castings. Welding was performed in an inert atmosphere at elevated temperatures. The weld tensile properties are improved on the base material at room temperature. The fracture strengths and creep are similar to the base material. (Bartolotta, Barret, Kelly, & Smashey, 1997)

6.2 Areas for TiAl application

Due to TiAl properties, the areas within an automobile which would benefit from its use are areas which would benefit from weight reduction and increased strength at high temperatures. Such areas include the suspension system and 'in-wheel' electric motors to reduce unsprung and rotating mass and inside internal combustion engines and driveline to reduce rotating and reciprocating masses.

Reducing unsprung mass in a vehicle improves the handling because the suspension is able to change direction faster due to lower masses and therefore lower suspension momentum. The lower unsprung mass allows the wheel to stay in contact with the ground therefore providing more grip. Components attached to the suspension such as brakes and wheels are considered part of the suspension system and therefore they would also benefit the unsprung mass by reduced mass.

Reducing the mass of rotating and reciprocating components can result in reduced fuel/energy consumption and improved performance. Rotating or reciprocating masses are considered as anything which reciprocates or rotates from the engine to the wheels including brake rotors and drive shaft. Reduced fuel/energy consumption can be realized if rotating masses are lightened, as less energy is required to increase or decrease the components speed.

6.3 Specific Applications

Brakes

Braking components that may be suited to be constructed from TiAl are brake rotors.

Brake rotors made from TiAl would produce multiple benefits. A TiAl rotor would have approximately half the weight of current cast iron rotors which would decrease unsprung and rotating masses. TiAl is suited to this application because it has the excellent high temperature strength that is required. However a TiAl brake rotor would require a protective coating due to TiAl's weak Tribological properties. Nitriding of the surface would create a suitable hard wearing surface.

The brake rotor could be manufactured using PM with HIP processing to increase density and lower porosity. The ‘green’ compact die would be complicated but would be manageable. If large metal injection moulding products (up to 4kg) were able to be produced, this process would be recommended.

Titanium rotors are currently produced by Red Devil Brakes. They use Ti-6Al-4V titanium alloy that is investment cast. A ceramic composite coating is applied over the titanium alloy to produce a wear resistant surface and to absorb the heat energy as titanium alloys have low thermal conductivity, allowing the rotor inner material to run cooler. The Ceramic composite coating does not gas. A gaseous layer that forms on cast-iron brake discs at high temperatures can reduce the co-efficient of friction between the brake pads and rotor causing brake fade. They also claim the titanium coated brake discs provide increased stopping power, reducing braking distances of a C5 Corvette from 125ft to 85-90ft from 60mph (Ultra Lite Brakes and Components, 2008).

Tests conducted on several titanium alloys and composites found friction coefficients were within the typical range for brake materials (0.35–0.55) and some showed excellent resistance to fade, a phenomenon in which braking effectiveness decreases as temperature rises. The thermally spray-coated Ti disc exhibited the least wear and merits further attention as a lightweight, corrosion-resistant brake rotor material. The thermally coated brake disc referred to is one produced by Red Devil Brakes (Blau, Jolly, Qu, Peter, & Blue, 2007).

Brake calliper pistons and brake pad backing plates would benefit greatly with the use of a titanium alloy due to their reduced thermal conductivity. This would keep heat away from the brake fluid, preventing it from boiling under harsh braking conditions.

Brake callipers are more suited to being made from aluminium due to its lower mass and excellent thermal conductivity.

Electric motors

TiAl may have applications within ‘in-wheel’ electric motors due to their increased specific strength and stiffness over aluminum. The magnet mountings (backing plates) in AC ‘in-wheel’ motors could be manufactured from PM TiAl, increasing stiffness while decreasing the weight by nearly half. Decreasing mass within an ‘in-wheel’ motor reduces unsprung mass and improves the motors performance by reducing rotating mass, making the motor more responsive to accelerations and decelerations. The increased stiffness would also allow tighter tolerances between rotating motor components allowing a more compact and efficient motor to be produced.

Internal Combustion engines

Applications within an internal combustion engine are suited to TiAl components because of TiAl’s reduced density, high temperature strengths and oxidation resistance. Examples of components that could be produced are valves, high temperature pistons and turbocharger rotors.

Many TiAl valves have been produced (see Current Automotive applications) although only Toyota has mass produced valves for the Altezza. The Toyota Altezza valves were produced using PM (T. Yamaguchi et al., 2000). The PM process is more suited to valve production due to the microstructure produced and the very small waste material produced. Upset forging is not as well suited because of the changing microstructures that develop where the material cross-sectional area decreases. TiAl is suited for use as valves because of its low density and high temperature strength. Lighter valves are beneficial because they create reduced inertia and friction loss resulting in fuel economy improvements and noise reduction. (T. Yamaguchi et al., 2000) also found there were no significant differences between the different TiAl alloys tested. Coatings would need to be applied to the valve to prevent wear.

Turbocharger rotors made from TiAl are currently being manufactured by Mitsubishi Motors for its Lancer Evolution vehicles. The turbocharger rotors are manufactured using the LEVICAST process. Metal injection moulding would be

suitable for this process as it can accommodate smaller wall thicknesses than casting. The surface finish would be better than from a casting while the parts conform to very tight tolerances requiring less finishing. An example of the intricate metal injection mouldings which can be achieved can be seen in Figure 6.1. The part is a hinge mechanism for a Motorola cellphone. The hinge is constructed from 17-4 PH Stainless Steel.

Figure 6.1 A complex metal injection moulding part for the hinge of a cellphone (PickPM, 2008).

Coatings

Coatings of TiAlN could be applied to products requiring a durable hard wearing surface. The coating could be applied using conventional plasma spraying or low pressure plasma spraying.

Chapter 7 Conclusions and Recommendations

7.1 Conclusions

After the initial failure of the chassis during testing, the **Ultra**commuter chassis proved to be fit for its purpose by successfully driving 1800km during the WSC. The chassis weighed 62 kg while the car had a final weight distribution of 45:55, acceptable for a rear wheel drive vehicle. The chassis came in on budget.

Preplanning of events and the resources required was challenging but it reduced lost time due to material shortages and allowed accurate allocation of time for labour.

TiAl would be an excellent structural material due to its high specific strength and stiffness but the very limited ductility hinders conventional manufacturing processes. TiAl would be highly suitable for valves, brake rotors and turbocharger rotors if suitable powder processes are not too costly.

Widespread use of titanium is not anticipated unless a new extraction process such as the Anderson process can create large amounts of titanium at significantly lower costs.

7.2 Recommendations

The long term performance of the chassis, particularly with regards to the adhesive fatigue and the effect of vibrations will need to be assessed. Lifting points to lift the chassis are required as it is very difficult to lift it currently.

If the **Ultra**commuter chassis were to be redesigned, it would be beneficial to tie the dash into the centre console by extending the dash down. Aluminium extrusion channel could be used on the edges of the honeycomb (obtained from Nalco, part No. U8029). This edging would be tidier and would be more structurally sound as there would not be any chance of the facings delaminating.

A thinner equal angle extrusion for honeycomb joints could also be used to decrease weight.

Production of automotive TiAl components would be highly beneficial to the automotive and titanium industries. The use of TiAl allows greater efficiencies and reduced fuel consumption.

Further research into TiAl applications within ‘in-wheel’ electric motors would be beneficial as they would bring many benefits due to their high specific stiffness and strength.

References

Adhesive Technologies NZ, L. (2007). *HPR 25 Toughened Epoxy Adhesive*.

Alexander, D. (October 2007). *High-Performance Handling Handbook*. Wisconsin: Motorbooks International.

Alias Systems Corp. (2004). Holden's Monaro Coupe Wins Australia's Heart. Retrieved 23 March, 2007, from http://cad.digitalmedianet.com/articles/viewarticle.jsp?id=28020

Asnafi, N., Langstedt, G., Anderson, C. H., Ostergren, N., & Hakansson, T. (2000). A new lightweight metal-composite-metal panel for applications in the automotive and other industries. *Thin-walled structures, 36*, 289-310.

Audi. (8 December 2006). Award for innovative TT body concept. Retrieved December, 2007, from http://audi.co.za/news/archive.php?articleID=904

Audi. (22 January 2007). Audi R8: the design. Retrieved November, 2007, from http://www.carbodydesign.com/archive/2007/01/22-audi-r8-design/?page=3

Audi. (2003). Latest-generation Audi Space Frame Advances Design, Safety and Performance Standards. Retrieved 12 January, 2008, from http://www.media.audiusa.com/article_display.cfm?article_id=8994

Audi AG. (2002). The New Audi A8: A New Sporting Dimension in the Luxury Segment. Retrieved 13 December, 2007, from http://www.audiworld.com/news/02/a8launch/content.shtml

Ayres, C. (2008). In R. Lovatt (Ed.).

Ayres Composite, P. (2007). Welcome. Retrieved November, 2006, from http://www.ayrescom.com/

Ayres Composites Panels Pty Ltd. (2006). *Ayrlite 2022 Datasheet*.

Bak, D. J., Bartlett, N., & Hars, A. (1995, 22 May 1995). CAD, CAM, and CAE: Formula one's favoured team. *Design news*, 70-72.

Bartolotta, P., Barret, J., Kelly, T., & Smashey, R. (1997). The use of cast Ti-48Al-2Cr-2Nb in jet engines. *JOM, 49*(5), 4pp.

Baur, H., Wortberg, D. B., & Clemens, H. (2003). *Titanium aluminides for automotive applications.* Paper presented at the Gamma Titanium Aluminides 2003, San Diego.

Birch, S. (2000). Automotive dieting Automotive Engineering International Online.

Blau, P. J., Jolly, B. C., Qu, J., Peter, W. H., & Blue, C. A. (2007). Tribological investigation of titanium-based materials for brakes. *Wear, 263*, 1202-1211.

Boonruanga, C., Thongtema, T., McNallanb, M., & Thongtem, S. (2004). Effect of nitridation and carburisation of gamma-TiAl alloys on wear resistance. *Materials letters, 58*, 3175-3181.

Braess, H.-H., & Seiffert, U. (2005). *Handbook of automotive engineering*. Warrendale, Pennsylvania: SAE International.

Bryant, E. (2006). Paris Motor Show: Audi R8 cutaways. Retrieved 15 January, 2008, from http://www.autoblog.com/2006/10/02/paris-motor-show-audi-r8-cutaways/

Bryant, E. (2008). Detroit 2008: Corvette ZR1 chassis display. Retrieved 21 January, 2008, from http://www.autoblog.com/2008/01/14/detroit-2008-corvette-zr1-chassis-display/

Brylawski, M., & Lovins, A. (1999). Advanced composites: The car is at the crossroads. *SAMPE Journal, 35*(2), 25-36.

Callister, W. D. (2003). *Materials science and engineering. An introduction*. New Jersey: John Wiley and sons, inc.

Camanho, P. P., & Matthews, F. L. (2000). Bonded metallic inserts for bolted joints in composite laminates. *Proc Instn Mech Engrs, 24*(L), 33-40.

Chrysler, L. (2007). RAM 2500 Hydroformed ladder frame. Retrieved January, 2008, from http://www.dodge.com/en/2007/ram_2500/durability/structural_strength/

Cole, G. S., & Sherman, A. M. (1995). Lightweight materials for automotive applications. *Materials characterisation, 35*, 3-9.

Corum, J. M., Battiste, R. L., Ruggles, M. B., & Ren, W. (2001). Durability-based design criteria for a chopped-glass-fibre automotive structural composite. *Composites science and technology, 61*, 1083-1095.

Cramer, D. R., Taggart, D. F., & Inc, H. (2002). *Design and manufacture of an affordable advanced-composite automotive body structure.* Paper presented at the Proceedings from The 19th international battery, hybrid and fuel cell electric vehicle symposium and exhibition.

Crowley, G. (2003). How to Extract LOW-COST TITANIUM. *Advanced Materials & Processes, 161*(11), 25-27.

Djanarthany, S., Viala, J.-C., & Bouix, J. (2001). An overview of monolithic titanium aluminides based on Ti3Al and TiAl. *Materials Chemistry and Physics, 72*, 301-319.

Donachie, M. J. (2000). *Titanium: A technical guide*. Ohio: ASM International.

Dowling, W. E. J., Donlon, W. T., & Allison, J. E. (1994). *Development of TiAl-based automotive engine valves.* Paper presented at the Materials Research Society Symposium, Boston, USA.

Dwight, J. (1998). *Aluminium Design and Construction* London: E & F.N Spon.

Engineering, D. A. m. (2007). Characteristics of Aluminium Tailor Welded Blanks for Automotive Panels and Structures. Retrieved 6 January, 2008, from http://www.technet.pnl.gov/dme/manufacturing/characteristics.stm

Escudero, M. L., Munoz-Morris, M. A., Garcia-Alonso, M. C., & Fernandez-Escalante, E. (2004). In vitro evaluation of a γ-TiAl intermetallic for potential endoprothesic applications. *Intermetallics, 12*(3), 253-260.

Eylona, D., Kellera, M. M., & Jones, P. E. (1998). Development of permanent-mold cast TiAl automotive valves. *Intermetallics, 6*(7-8), 703-708.

Faller, K., & Froes, F. H. (2001). The use of titanium in family automobiles: current trends. *JOM, 53*(4), 27-28.

Feraboli, P., & Masini, A. (2004). Development of carbon/epoxy structural components for a high performance vehicle. *Composites, Part B, 35*, 323-330.

Ford Motor, C. (2005). Ford Mustang GT (2005) - Old School Muscle. Retrieved 27 December, 2007, from http://www.modernracer.com/features/carcutawayfordmustanggt.html

Ford Motor Company. (2003). FORD GT GOES DIGITAL ON RACE TO RECORD DEVELOPMENT TIME. Retrieved 11 January, 2008, from http://media.ford.com/newsroom/release_display_foriframe.cfm?release=14806

Froes, F. H., Friedrich, H., Kiese, J., & Bergoint, D. (2004). Titanium in the family automobile: the cost challenge. *Journal of Materials, 56*(2), 40-44.

Gebauer, K. (2006). Performance, tolerance and cost of TiAl passenger car valves. *Intermetallics, 14*(4), 355-360.

Gerdemann, S. J. (2001). Titanium process technologies. *Advanced Materials & Processes, 159*(7), 41-43.

Gerling, R., Clemens, H., & Schimansky, F. P. (2004). Powder Metallurgical Processing of Intermetallic Gamma Titanium Aluminides. *Advanced Engineering Materials, 6*(1-2), 23-38.

Gerling, R., & Schimansky, F.-P. (2002). Prospects for metal injection moulding using a gamma titanium aluminide based alloy powder. *Materials science and Engineering A, 329-331*, 45-49.

Gerling, R., Schimansky, F. P., & Clemens, H. (2003). *Powder production techniques and PM processing routes for gamma titanium aluminides.* Paper presented at the Gamma titanium aluminides 2003 symposium, San Diego.

GSV. (2005). Producing cool cars. *Automotive design and production, December*.

Gupta, N. S. (2006, 31 March 2006). An overhaul for Auto Street *The Economic Times*.

Happian-Smith, J. (2001). *An introduction to modern vehicle design*. Oxford: Butterworth Heinemann.

Henaf, G., & Gloanec, A.-L. (2005). Fatigue properties of TiAl alloys. *Intermetallics, 13*, 543-558.

Honda. Honda NSX. Retrieved 20 January, 2008, from http://www.noelwatson.com/blog/content/binary/HondaNSX.pdf

Honda, K., Hirose, A., & Kobayashi, K. (1997). Properties of titanium-aluminide layer formed by low pressure plasma spraying. *Materials science and Engineering A, 222*, 212-220.

Inagaki, S., & Tanaka, Y. (2002). Development of rally car for world rally championship. *Mitsubishi motors technical review, 14*, 63-65.

Jaguar, U. S. A. (2007). Jaguar XJ Introduction - Aluminium Construction. Retrieved January, 2008, from http://www.jaguarusa.com/us/en/xj/highlights/highlights/introduction.htm

Jost, K. (October 2004). The company hopes the re-engineered Elise can out-manoeuvre its competition by showing the importance of performance through light weight. Retrieved 20 Dec, 2006, from http://www.sandsmuseum.com/cars/elise/information/technical/aeoct04/aeoct04.html

Kassner, M., & Perez-Prado, M.-T. (2004). *Fundamentals of Creep in Metals and Alloys*. Oxford: Elsevier.

Kee Paik, J., Thayamballi, A. K., & Sung Kim, G. (1999). The strength characteristics of aluminium honeycomb sandwich panels. *Thin-Walled Structures, 35*(3), 205-231.

Khor, K. A., Murakoshi, Y., Takahashi, M., & Sano, T. (1995). Plasma spraying of titanium aluminide coatings: process parameters and microstructure. *Journal of materials processing technology, 48*, 413-419.

Kinsey, B., Viswanathan, V., & Cao, J. (2001). Forming of Aluminium Tailor Welded Blanks. *Journal of Materials & Manufacturing, 110*(5), 673-679.

Knippscheer, S., & Frommeyer, G. (1999). Intermetallic TiAl(Cr,Mo,Si) alloys for lightweight engine parts: Structure, properties, and applications. *Advanced Engineering Materials, 1*(3-4), 187-191.

Knippscheer, S., Frommeyer, G., Baur, H., Joos, R., Lohmann, M., Berg, O., et al. (2000). *TiAl Automotive valves - Fabrication and properties*. Weinheim: Wiley-VCH.

Kodack, A. (2005). 2004 VZ Monaro Retrieved 15 January, 2008, from http://www.topspeed.com/cars/holden/2004-vz-monaro-ar537.html

Koenigsegg. (2006). Koenigsegg engineering - Chassis: Koenigsegg.

Koenigsegg. (2007). Retrieved 14 Jan, 2008, from http://www.koenigsegg.com/thecars/ccx.asp?ccx=3

Koganti, R. (2005). Re-Engineering A LEGEND. *Manufacturing Engineering, 135*(3), 101.

Land Transport Safety Authority of NZ. (2001). Land Transport Rule Frontal Impact 2001 Rule 32006/1. Retrieved 16 June, 2007, from http://www.landtransport.govt.nz/rules/frontal-impact-2001.html#232

Leyens, C., & Peters, M. (2006). *Titanium and Titanium Alloys: Fundamentals and Applications*: Wiley-VCH.

Lutgering, G. (2007). *Titanium* (second ed.). New York: Springer.

Mantle, A. L., & Aspinwall, D. K. (2001). Surface integrity of a high speed milled gamma titanium aluminide. *Journal of Materials Processing Technology, 118*, 143-150.

Masini, A., Taraborrelli, L., Pivetti, A., & Feraboli, P. (2004). *Development of carbon/epoxy structural components for a topless high performance vehicle*.

McBeath, S. (2000). *Competition car composites: a practical handbook*. Sparkford, Nr Yeovil, Somerset: Haynes Publishers.

Miller, B. (1996, Dec 1996). Front end bodes well for composites. *Plastics world, 54*, 12.

Mills, A. (2002). Carbon car comes of age. *Materials world, 10*(9), 20-22.

Minford, J. D. (1993). *Handbook of Aluminium Bonding Technology and Data*. New York: Marcell Dekker.

Moll, J. H., & McTiernan, B. J. (2000). PM TiAl alloys: the sky's the limit. *Metal powder report, 55*(1), 18-22.

Newton, B. (2001). Holden delivers its cyber-age baby. Retrieved 15 December, 2007, from http://www1.autotrader.com.au/mellor/MELLOR.NSF/story2/2AA87A45919CBEFCCA256AE1008022DA

Newton, B. (2005, 07 September 2005). Monaro makes a getaway. *The Age*.

Peters, M., Kumpfert, J., Ward, C. H., & Leyens, C. (2003). Titanium Alloys for Aerospace Applications. *Advanced Engineering Materials, 5*(6), 419-427.

PickPM. (2008). Mobile Phone Flip Slider & Hinge Barrel case study. Retrieved 2 February, 2008, from http://www.pickpm.com/casestudy/case_study.asp?locarr=4

Pistonheads. (2001). STRATHCARRON It's all over. Another chapter in British motoring closes as liquidators are called in. Retrieved 22 March, 2007, from http://www.pistonheads.com/doc.asp?c=47&i=2923

Polmear, I. J. (2006). *Light alloys: metallurgy of the light metals* (4th ed.). Auckland: Arnold.

Porsche Engineering. (2005). Steel vs. Aluminium: Hood. Retrieved 11 December, 2008, from http://www.ussautomotive.com/auto/steelvsal/hood.htm

Porsche Engineering Services, I. (1998). *Ultra Light Auto Steel Body Phase 2 findings*.

Posti, E., & Nieminen, I. (1989). Coating thickness effects on the life of titanium nitride PVD coated tools. *Materials & Manufacturing Processes, 4*(2), 239-252.

Ramsden, D. (2006). Spaceframe propels Ford GT. *Modern Casting, 96*(2), 26-29.

Rastkar, A. R., & Bell, T. (2002). Tribological performance of plasma nitrided gamma based titanium aluminides. *Wear, 253*, 1121-1131.

restorations, S. S. (2007). HISTORY of the 300SL. Retrieved Dec, 2006, from http://www.silverstarrestorations.com/300SL.htm

Reynolds Metals Company and Ogihara America Corporation. (2007). Design and Manufacturing Engineering.

s.r.o., P. (2007). Prostorový hliníkový rám ASF. Retrieved 21 January, 2008, from http://www.picsearch.com/info.cgi?q=audi%20a8%20asf&id=SfiOwJEzSn3VhfqdEtmrYAJY9V4-m2vSaBS3r20Y-c0&start=21

Saito, M., Iwatsuki, S., Yasunaga, K., & Andoh, K. (2000). Development of aluminium body for the most fuel efficient vehicle. *JSAE Review, 21*, 511-516.

Schauerte, O. (2003). Titanium in automotive production. *Advanced Engineering Materials, 5*(6), 411-418.

Schlendorf, D. W. (2002). Alcoa and the Aluminium Auto. Retrieved 8 January, 2008, from http://www.alcoa.com/global/en/news/whats_new/2002/audi.asp

Schwartz, M. M. (2002). *Encyclopaedia of Materials, Parts, and Finishes*: CRC Press.

Smallman, R. E., & Bishop, R. J. (1999). *Modern physical metallurgy & materials engineering* (6th ed.). Auckland: Butterworth Heinmann.

Spain, R. (2003). *GT40: An Individual History and Race Record*. Minnesota: MBI Publishing Company.

Stasik, M. C., & Wagoner, R. H. (1997). Forming of Tailor-Welded Aluminium Blanks. *Int. J. Form. Technol.*

Tamaki, Y. (1999). Research into achieving a lightweight vehicle body utilizing structure optimising analysis: aim for a lightweight and high and rigid vehicle body. *JSAE review, 20*, 555-561.

Team, T. W. B. P. (1995). Tailor Welded Blank Design and Manufacturing Manual Retrieved 6 January, 2008, from http://www.a-sp.org/publications.htm

Tetsui. (1999). Gamma Ti aluminides for non-aerospace applications. *Current Opinion in Solid State and Materials Science 4*(3), 243-248.

Tetsui, T. (2002). Development of a TiAl turbocharger for passenger vehicles. *Materials Science and Engineering A,*, 329-331.

Toyota. (2007). Life Cycle Analysis Retrieved 2008, 11 January, from http://www.toyota.co.nz/AboutUs/The+Environment/Product+-+Life+Cycle.htm

Toyota, N. Z. (2007). Camry Sportivo 4 Dr Sedan 2.4L Auto Engine. Retrieved 2 January, 2008, from http://www.toyota.co.nz/NewVehicles/Models/Passenger/Camry/Sportivo+4+Door+Sedan/2.4L/Auto/Tech+Spec/Engine.htm

Ultra Lite Brakes and Components. (2008). Ceramic coated titanium brake rotors. Retrieved 4 January, 2008, from http://www.reddevilbrakes.com/page/page/903312.htm

Wan, M. (1998-2000). Different Types of Chassis. Retrieved 25 April, 2006, from http://www.autozine.org/technical_school/chassis/tech_chassis.htm#Ladder

Wan, M. (2000). Different types of chassis. Retrieved 18 May, 2006, from http://www.autozine.org/technical_school/chassis/tech_chassis.htm

Wayman, D. M., & Bringas, J. (1993). *The metals red book* (Vol. 2). Alberta: Casti Publishing Inc.

Wilton, P. (2002). *Tomorrows Vehicles* (No. Issue 22). Swindon: Engineering and Physical Sciences Research Council.

Winkler, P. J. (2000). *Materials for transportation technology*. Weinheim: Wiley-VCH.

Wu, X. (2006). Review of alloy and process development of TiAl alloys. *Intermetallics, 14*, 1114-1122.

Yamaguchi, J. (2000). Toyota's new inline four-cylinder engine. Retrieved 11 January, 2008, from http://www.sae.org/automag/techbriefs_07-00/05.htm

Yamaguchi, J., & online, A. e. i. (2007). All in the Vitz family. Retrieved 22 December, 2007, from http://www.motorsportsengineering.org/automag/globalview_01-00/03.htm

Yamaguchi, T., Morishita, H., Furutani, T., Saito, T., Iwasu, S., & Yamada, S. (2000). Development of P/M Titanium Engine Valves. *SAE technical papers, 2000-01-0905*.

Yokota, C., Nakamura, Y., Yada, S., Funatsu, K., Kubo, F., Ohkubo, T., et al. (2002). Development of the 2001 year model civic. *JSAE review, 23*, 387-399.

Zhang, W. J., Reddy, B. V., & Deevi, S. C. (2001). Physical properties of TiAl-Base alloys. *Scripta Materialia, 45*, 645-651.

Appendix 1

The ‘in-wheel’ motors used in the BEV provide many advantages in terms of space savings. A typical internal combustion engine (Toyota 2AZ-FE, 2.4L) with performance figures of 117kW and 218Nm (N. Z. Toyota, 2007) takes up 259 Litres of space (J. Yamaguchi, 2000) excluding all ancillaries and transmission but including a 45L petrol tank which if installed in the BEV, would take up 7% of all available volume under the body shell. For the BEV, 95 L was required for batteries, which can be mounted in many places within the bodyshell and 15L for the motor controllers takes up only 2.6% of total volume.